NASA/CR-2003-211748

Integrated Approach to the Dynamics and Control of Maneuvering Flexible Aircraft

Leonard Meirovitch and Ilhan Tuzcu
Virginia Polytechnic Institute and State University, Blacksburg, Virginia

June 2003

The NASA STI Program Office . . . in Profile

Since its founding, NASA has been dedicated to the advancement of aeronautics and space science. The NASA Scientific and Technical Information (STI) Program Office plays a key part in helping NASA maintain this important role.

The NASA STI Program Office is operated by Langley Research Center, the lead center for NASA's scientific and technical information. The NASA STI Program Office provides access to the NASA STI Database, the largest collection of aeronautical and space science STI in the world. The Program Office is also NASA's institutional mechanism for disseminating the results of its research and development activities. These results are published by NASA in the NASA STI Report Series, which includes the following report types:

- TECHNICAL PUBLICATION. Reports of completed research or a major significant phase of research that present the results of NASA programs and include extensive data or theoretical analysis. Includes compilations of significant scientific and technical data and information deemed to be of continuing reference value. NASA counterpart of peer-reviewed formal professional papers, but having less stringent limitations on manuscript length and extent of graphic presentations.

- TECHNICAL MEMORANDUM. Scientific and technical findings that are preliminary or of specialized interest, e.g., quick release reports, working papers, and bibliographies that contain minimal annotation. Does not contain extensive analysis.

- CONTRACTOR REPORT. Scientific and technical findings by NASA-sponsored contractors and grantees.

- CONFERENCE PUBLICATION. Collected papers from scientific and technical conferences, symposia, seminars, or other meetings sponsored or co-sponsored by NASA.

- SPECIAL PUBLICATION. Scientific, technical, or historical information from NASA programs, projects, and missions, often concerned with subjects having substantial public interest.

- TECHNICAL TRANSLATION. English-language translations of foreign scientific and technical material pertinent to NASA's mission.

Specialized services that complement the STI Program Office's diverse offerings include creating custom thesauri, building customized databases, organizing and publishing research results ... even providing videos.

For more information about the NASA STI Program Office, see the following:

- Access the NASA STI Program Home Page at ***http://www.sti.nasa.gov***

- E-mail your question via the Internet to help@sti.nasa.gov

- Fax your question to the NASA STI Help Desk at (301) 621-0134

- Phone the NASA STI Help Desk at (301) 621-0390

- Write to:
  NASA STI Help Desk
  NASA Center for AeroSpace Information
  7121 Standard Drive
  Hanover, MD 21076-1320

NASA/CR-2003-211748

Integrated Approach to the Dynamics and Control of Maneuvering Flexible Aircraft

Leonard Meirovitch and Ilhan Tuzcu
Virginia Polytechnic Institute and State University, Blacksburg, Virginia

National Aeronautics and
Space Administration

Langley Research Center
Hampton, Virginia 23681-2199

Prepared for Langley Research Center
under Cooperative Agreement NCC1-346

June 2003

Acknowledgments

The authors wish to thank the monitor, Martin R. Waszak, for his steadfast support and useful advice over the whole duration of the project.

Available from:

NASA Center for AeroSpace Information (CASI)
7121 Standard Drive
Hanover, MD 21076-1320
(301) 621-0390

National Technical Information Service (NTIS)
5285 Port Royal Road
Springfield, VA 22161-2171
(703) 605-6000

Preface

The interest lies in a dynamic formulation capable of simulating the flight of flexible aircraft on a computer. Such simulations can speed up the aircraft design process. Moreover they are indispensable to autonomous aerial vehicles, which require autopilots.

Computer simulation of the flight of flexible aircraft is no trivial matter. Indeed, they require a new paradigm, discarding confining assumptions and adopting potent methodology. This work develops such a paradigm, which amounts to treating the aircraft as a single system. To this end, it integrates into a single mathematical formulation the disciplines pertinent to the flight of flexible aircraft, namely, analytical dynamics, structural dynamics, aerodynamics and controls. The unified formulation is based on fundamental principles and incorporates in a natural manner both rigid body motions of the aircraft as a whole and elastic deformations of the flexible components (fuselage, wing and empennage), as well as the aerodynamic, propulsion, gravity and control forces. The aircraft motion is described in terms of three translations (forward motion, sideslip and plunge) and three rotations (roll, pitch and yaw) of a reference frame attached to the undeformed fuselage, and acting as aircraft body axes, and elastic displacements of each of the flexible components relative to corresponding body axes. The equations of motion are expressed in a form ideally suited for efficient computer processing. A perturbation approach permits division of the problem into a nonlinear flight dynamics problem for maneuvering quasi-rigid aircraft and a linear "extended aeroelasticity" problem for the elastic deformations and perturbations in the rigid body translations and rotations, where the solution of the first problem enters as an input into the second problem. The term "extended aeroservoelasticity" refers to a family of problems, each problem characterized by an input from a different aircraft maneuver, with the corresponding equations involving not only both elastic and rigid body variables but also coefficients depending on any given maneuver, and hence coefficients depending generally on time. This is materially different from the common aeroservoelasticity, which involves for the most part elastic variables alone and is not subject to inputs from aircraft maneuvers. The control forces for the flight dynamics problem are obtained by an "inverse" process. On the other hand, the feedback control forces for the extended aeroelasticity problem are derived by means of LQG theory. A numerical example presents time simulations of rigid body perturbations and elastic deformations about 1) a steady level flight and 2) a steady level turn maneuver.

It should be pointed out that sufficient details are provided so as to permit interested parties to replicate the results.

Contents

1. Introduction and Literature Review

This investigation is concerned with a dynamic formulation capable of simulating the flight of flexible aircraft. It integrates seamlessly in a single and consistent mathematical formulation all the necessary material from the pertinent disciplines, namely, analytical dynamics, structural dynamics, aerodynamics and controls. The unified formulation is based on fundamental principles and incorporates in a natural manner both the rigid body motions and the elastic deformations, and the couplings thereof, as well as the aerodynamic, propulsion, control and gravity forces. In essence, the formulation not only unifies flight dynamics and aeroelasticity, traditionally treated as separate disciplines, but, going beyond that, it permits a computer simulation of the response of flying flexible aircraft to external stimuli.

In describing the motion of *rigid bodies* in space, it is convenient to attach a set of axes to the body, where the axes are commonly known as body axes, and express the motions in terms of components along these body axes. It is quite common to describe the motion of rigid bodies in terms of the translation of the origin of the body axes and the rotation of the body axes; the corresponding variables, particularly the rotations, are referred to as quasi-coordinates. If the origin of this reference frame coincides with the mass center of the body, the translations and rotations are independent of each other. Moreover, if the body axes themselves coincide with the principal axes of the body, then the products of inertia are zero, so that the inertia matrix is diagonal.

The situation is more complicated for *flexible bodies*, in which case there are basically two types of reference frames:

i. **Fixed in the undeformed body** - In this case, it is convenient to define the translation of the origin of the reference frame and the rotation of the reference frame as the rigid body translation and rotation of the body, and regard any displacement relative to the reference frame as elastic deformation.

ii. **Moving relative to the undeformed body** - In this case, it is common to choose the reference axes so that the linear momentum and angular momentum vectors due to elastic deformations vanish; axes satisfying these conditions are called *mean axes*. Because the elastic deformations depend in general on time, the mean axes are continuously moving relative to the undeformed body. Of particular interest are mean axes with the origin at the system mass center, because in this case the three types of motion, namely, the translations of the reference frame, the rotations of the reference frame and the deformations measured relative to this frame, are all inertially decoupled. The price to be paid for the use of mean axes is very steep, however, as the constraints defining these axes are not easy to enforce. For this reason, it is common to invoke the use of mean axes to justify inertial decoupling, but without enforcing the constraints.

Whereas proper use of mean axes for flexible bodies in vacuum can produce inertial decoupling, in the case of aircraft any such benefits are questionable, because the equations of motion remain coupled through the aerodynamic forces. Moreover, if one insists on the use of mean axes, then the aerodynamic forces must also be expressed in terms of components along the same mean axes, which is a very tedious task at best.

The motion of *force-free rigid bodies* in space is unstable. Under certain circumstances, the motion of rigid bodies can be stabilized by imparting them some spin about the axis of either the minimum or the maximum moment of inertia. On the other hand, *flexible bodies* cannot be stabilized if the spin is about the axis of minimum moment of inertia. The preceding statements imply that the motion takes place in vacuum, such as in the case of a spacecraft. Matters are entirely different for flexible aircraft, which are neither force-free, nor do they operate in vacuum. In fact, aircraft are subjected to aerodynamic and wind forces, and any stabilization is done by active means, namely, by the engine throttle and control surfaces, where the latter consist of the aileron, elevator and rudder.

The flight of aircraft tends to be quite diverse, ranging from steady level cruise to complex maneuvers, and stabilization requires the use of controls permitting the aircraft to carry out the intended maneuver while suppressing any deviations from it, whether in the form of rigid body displacements or elastic deformations. Both flight dynamics and aeroelasticity are concerned with aircraft stability. But, whereas flight dynamics is concerned mainly with rigid body motions, aeroelasticity is concerned with vibration and flutter.

A stability analysis tends to be limited in scope, in the sense that it can only yield a qualitative statement about the nature of motion in the neighborhood of an equilibrium state of a system. More specifically, it can state whether the equilibrium is merely stable, asymptotically stable, or unstable. The time plays no role in a stability analysis. In fact, stability analyses tend to be limited to cases in which the time variable can be eliminated, such as when the equations of motion can be reduced to an eigenvalue problem. The stability of time-dependent maneuvers can only be evaluated numerically.

To obtain information going beyond stability statements, such as the time response of aircraft to external stimuli, it is necessary to undertake a simulation of the equations of motion, which amounts to the integration of the equations of motion. Such a dynamic simulation can be used for parametric studies in preliminary design. Moreover, it can be used to determine aircraft performance, thus reducing the time required for flight testing by "flying the aircraft on a computer."

The choice in this paper is to work with a reference frame attached to the undeformed aircraft, which has many advantages over mean axes. But, because the elastic deformations prevent the origin of a frame attached to the undeformed body from coinciding with the mass center and the axes themselves from coinciding with the principal axes for all times, there is no preferred choice of a reference frame; we base the choice on geometric considerations. In particular, we attach a set of body axes to the undeformed fuselage, where one of the axes is along the symmetry axis. For convenience, sets of body axes are also attached to the other flexible components, such as the wing and the empennage. Ultimately, however, all motions are referred to the fuselage body axes, which act as a reference frame for the whole aircraft.

The mathematical formulation is based on equations of motion in terms of quasi-coordinates derived earlier by the first author for flexible spacecraft and later adapted by him to flexible aircraft. The formulation is hybrid in nature, in the sense that it consists of ordinary differential equations for the rigid body translations and rotations of the aircraft as a whole and boundary-value problems for the elastic deformations of the flexible components of the aircraft, namely, the fuselage, wing and empennage. For practical reasons, the distributed variables describing the boundary-value problems for the individual components are discretized in space, obtaining a relatively large set of second-order ordinary differential equations for the whole aircraft. The discretization process amounts to representing the distributed variables as finite series of known space-dependent shape functions multiplied by time-dependent generalized coordinates. The derivation of the equations of motion in conjunction with the extended Hamilton principle requires expressions for the kinetic energy, potential energy and virtual work, all scalar quantities. In turn, the kinetic energy requires the velocity of every point of the aircraft, which can be obtained by means of an orderly kinematical synthesis, going from the fuselage to the wing and to the empennage. The potential energy is merely equal to the strain energy. Moreover, the aerodynamic, propulsion, control and gravity forces are accounted for through the virtual work. Rather than deriving first hybrid equations of motion and then discretizing them in space, it is perhaps more expeditious to carry out the discretization directly in the kinetic energy, potential energy and virtual work, thus obtaining the desired set of ordinary differential equations for the whole flexible aircraft without the need to derive boundary-value problems. For integration of the differential equations and for control design, it is necessary to transform the set of second-order differential equations into a set of first-order differential equations, namely, into a set of state equations. It turns out that, for the problem at hand, it is more convenient to work with momenta rather than with velocities. Although the resulting first-order equations actually represent phase equations, we shall continue to refer to them as state equations.

The simulation of the flight of an aircraft amounts essentially to integration of the state equations. Because of various nonlinearities involved, such as those due to rigid body motions and aerodynamic forces, the integration must be carried out numerically on a computer. In one way or another, computer integration can only be done in discrete time, which raises the question of the size of the sampling period, or time step. Of course, the answer depends on the desired accuracy of the simulation, and it is intimately related to the dynamic characteristics of the system. If the aircraft is to be controlled by an autopilot, then the simulation must be carried out in real time. If the dynamic characteristics are such that the time step must be relatively short, perhaps of the order of 0.01s, most aerodynamic theories in current use must be ruled out, as the computation of the dynamic pressure over the entire aircraft is sure to take considerably longer time than that. Hence, a new method for computing the dynamic pressure must be developed, one characterized by high computational speed, even if some accuracy must be sacrificed. Moreover, the method for computing the dynamic pressure must be compatible with the method for modeling the airframe. If the formulation is to be used for aircraft design, then real-time simulation may not really be necessary, although on-line simulation may. But, the size of the sampling period, which is determined by the system dynamic characteristics, remains the same regardless of whether the simulation is in real time or only on-line. The implication is that the computation of the dynamic pressure must still be relatively fast. Indeed, a mere 10 s simulation requires 1,000 time steps. Hence if the computation of the dynamic pressure takes one hour, the simulation requires over 40 days. This demonstrates the need for a method for computing the dynamic pressure in a very short time period. In this regard, a reasonably accurate approximate method may be acceptable.

As indicated above, the equations of motion for a flying flexible aircraft are nonlinear, where the nonlinearity is due to the rigid body motions and the aerodynamic forces. Moreover, the equations tend to be of high order, the order depending on the discretization procedure employed. Hence, one can expect difficulties both with a stability analysis and with control design. In addition, difficulties can be experienced in the integration process, because some of the variables describing the aircraft rigid body motions tend to be large and the variables describing the elastic displacements tend to be small. A perturbation approach to the solution can obviate many of these difficulties. More specifically, the solution can be represented as the sum of a zero-order part for the large rigid body variables and a first-order part for the small elastic variables and perturbations in the rigid body variables, where the zero-order quantities are larger than the first-order quantities by at least one order of magnitude. Then, the equations of motion can be separated into a *zero-order problem* for the rigid body motions alone and a *first-order problem* for the elastic displacements and the perturbations in the rigid body motions. The state equations for the zero-order problem are of order 12 at most; they can be identified as the equations of *flight dynamics* and can be used to describe aircraft maneuvers. On the other hand, the state equations for the first-order problem are of order $12 + 2n_e$, where n_e is the number of elastic degrees of freedom; they represent the *extended aeroelasticity* equations, where "extended" is in the sense that they include not only the elastic displacements but also perturbations in the rigid body variables, where the latter are sometimes referred to as "body freedoms."

The flight dynamics equations are in general *nonlinear* and describe the translations and rotations of the aircraft as if it were rigid. They can be used to design given maneuvers of an aircraft, which amounts to solving an "inverse" problem. In the commonly encountered direct problems in dynamics of rigid bodies, the forces are given and the equations of motion are solved for the state, i.e., for the positions and velocities. In the context of the present formulation unifying flight dynamics and aeroelasticity, however, the state representing a desired maneuver is given and the problem amounts to determining the engine thrust and the control surface forces permitting the realization of the maneuver; this represents an inverse problem. On the other hand, the extended aeroelasticity equations are *linear*, but they contain the state and forces from the flight dynamics problem as coefficients and as an input. Hence, *there is a set of extended aeroelasticity equations for every conceivable aircraft maneuver.* If the flight dynamics problem represents steady level cruise or a steady level turn maneuver, then the zero-order state and forces are constant and the system of extended aeroelasticity equations is linear time-invariant. In this case, the state equations lend themselves to a standard stability check, such as one based on the roots of the eigenvalue problem, to control design by commonly used techniques, such as the LQG method, and to ready integration for simulation of the aircraft response to external stimuli. If the flight dynamics problem represents a time-dependent maneuver, such as the transition from one steady state to another, then the zero-order state and forces depend on time and the extended aeroelasticity state equations are linear time-varying, which precludes a standard stability analysis. However, the state equations still permit control design and response simulation.

The following literature review should help relate the present paper to previous investigations: Although flight dynamics and aeroelasticity have been developed traditionally as separate disciplines, the need for considering interacting efforts was recognized quite early.[1-3] Still, relatively few attempts have been made to link the two disciplines, and when such attempts were made almost invariably the scope was quite limited. This lack of interest in linking flight dynamics and aeroelasticity can be attributed to a reluctance to increase the complexity of the problem to a significant extent at a time when powerful computers capable of solving such problems were not available. As a result, problems combining flight dynamics and aeroelasticity effects have tended to be subjected to many simplifying assumptions designed to permit largely analytical solutions. In one of the first references on the subject, Bisplinghoff and Ashley[4] derived scalar equations of motion for an unrestrained flexible vehicle. The equations consisted of three inertially decoupled sets, one for the rigid body translations, one for the rigid body rotations and one for the elastic deformations, the latter expressed in terms of aircraft structural natural modes. Although not stated explicitly, this implies the use of principal mean axes with the origin at the vehicle mass center. Moreover, the inertia matrix was assumed to be constant, which implies that the contributions from the elastic deformations to the inertia matrix were ignored. Aerodynamic forces for the case of small disturbed motions from steady rectilinear flight were given in terms of an influence function for an unrestrained aircraft. An integrated analytical treatment of the equilibrium and stability of flexible aircraft was presented by Milne.[5] In Part I, he derived linearized equations of motion about a steady state, assuming not only that the elastic deformations but also the rigid body translations and rotations were small. Although the constraint equations defining the mean axes were given, the formulation seems to have used body axes attached to the undeformed aircraft. The equations are expressed in a vector-dyadic form that does not permit a ready check for missing terms and, more importantly, does not lend itself to ready computer solutions. In Part II, the general analysis was applied to the study of equilibrium and longitudinal stability about equilibrium of an aircraft having longitudinal flexibility only. A monograph by Taylor and Woodcock[6] consists of two parts representing different approaches to the same problem. In Part I, Taylor presents a very lucid summary of the equations of motion for deformable aircraft derived by Bisplinghoff and Ashley[4] and by Milne.[5] Following a reduction to scalar form, the equations are simplified to permit the study of some special cases. In Part II, Woodcock uses an unorthodox form of Lagrange's equations to derive scalar perturbation equations of motion about a given "datum motion," not necessarily corresponding to steady level rectilinear flight; the equations are in terms of body-fixed axes. The question of aerodynamics receives scant attention in both parts. An extensive report by Dusto et al.,[7] resulting in a computer program known as FLEXSTAB, integrates flexible body mechanics with a low frequency aerodynamics employing linear influence coefficients. The flexible aircraft mechanics uses free vibration modes superimposed on rigid body dynamics. Aerodynamic influence coefficients are derived using a paneling scheme lending itself to empirical corrections. The equations are expressed in terms of steady perturbations about a reference motion to determine dynamic stability by characteristic roots or by time histories following an initial perturbation or some gust disturbance. There are two major concerns. The first consists of the fact that the structural dynamics formulation is in terms of mean axes and the aerodynamics is in terms of a different set of axes, namely, "fluid axes," where the latter move with a steady velocity relative to the undeformed aircraft body axes; using two different sets of axes in the same formulation, without making the necessary transformation from one set to another, is a very questionable proposition. The second source of concern is the time required to run FLEXSTAB (see Ref. 24). Several analytical methods for mathematical modeling of aircraft active control system design are described by Roger,[8] placing the emphasis on aerodynamics. Inconsistencies in control configured vehicles are highlighted by Schwanz.[9] He suggests that familiarity of flight control specialists with a broad spectrum of pertinent disciplines, including aerodynamics, structures, modern dynamics and control, can minimize and perhaps avoid altogether these inconsistencies. Free-free dynamic analyses of forward swept wing aircraft by Miller, Wykes and Brosnan[10] have shown that the static aeroelastic divergence exhibited by a cantilevered forward swept wing is replaced by a low-frequency flutter mode due to coupling between the wing divergent mode and the aircraft short-period mode. This coupling is shown to have detrimental effects on flying qualities, ride qualities and gust loads, but these effects can be minimized by an active flutter control system. In the same spirit, Weisshaar and Zeiler[11] discuss the importance of including aircraft rigid-body modes in the aeroelastic analysis of forward swept wing aircraft. They show that body-freedom flutter and aircraft aeroelastic divergence, not wing divergence, are the primary aeroelastic instabilities. Rodden and Love[12] point out that equations of motion derived using mean axes for the inertial terms and axes attached to the undeformed structure for the flexibility terms are likely to be incorrect; such flexibility terms are obtained when using structural influence coefficients. Cerra, Calico and Noll [13] developed a linear model of an elastic aircraft providing the capability of analyzing the coupling between the rigid body motions and the elastic motions. The model can be used for stability and control analyses. As in Ref. 4, the rigid body translations, rigid body rotations and elastic deformations are assumed to be inertially decoupled. A framework for constructing simulation models for flexible aircraft is described by Arbuckle, Buttrill and Zeiler.[14] The objectives are to increase simulation model fidelity and to reduce the time required for developing and modifying these models. The framework has been applied to the development of an open-loop F/A-18 simulation model. Buttrill, Zeiler and Arbuckle[15] considered a mathematical model integrating nonlinear rigid body mechanics and linear aeroelasticity in conjunction with Lagrangian mechanics to derive the equations of motion for flexible aircraft. Undamped vibration modes satisfying first-order mean axes constraints were used as generalized coordinates. Considering a model of an F/A-18 aircraft, elastic modes significantly affected by inertial coupling were found to be aerodynamically decoupled from the rest of the model. Zeiler and Buttrill[16] used the extended Hamilton principle to derive equations of motion for a flexible body. The equations include inertial terms due to flexibility, as well as terms coupling rigid body and flexible momenta. In addition, a nonlinear strain-displacement relation permits centrifugal stiffening to be taken into account. The equations are used to simulate the motion of a structure spinning initially about an unstable principal axis in gravity-free vacuum. Using Lagrange's equations, Waszak and Schmidt[17] derived the equations of motion for a flexible aircraft. The strip theory was used to obtain closed-form integral expressions for the generalized aerodynamic forces. Moreover, the use of mean axes permitted inertial decoupling of the rigid body translations, rigid body rotations and elastic deformations, the latter being expressed in terms of aircraft vibration modes. The modeling method was applied to a generic elastic aircraft, and the model was used for a parametric study of the flexibility effects. Nonlinear equations of motion for elastic panels in an aircraft executing a pull-up maneuver of given velocity and angular velocity were derived by Sipcic and Morino.[18] The effect of the maneuver on the flutter speed and on the limit cycle amplitude was discussed for various load conditions. Accurate modeling of aeroelastic vehicles, with emphasis on the rigid body and elastic degrees of freedom, was discussed by Waszak, Buttrill and Schmidt.[19] A comparison of the approach of Ref. 17 on the one hand and that of Refs. 15 and 16 on the other hand was presented and various model reduction techniques were reviewed. An integrated analytical framework for modeling elastic hypersonic flight vehicles was developed by Bilimoria and Schmidt.[20] A Lagrangian approach was used to derive equations of motion including rigid body motions and elastic deformations, as well as effects due to fluid flow, rotating machinery, wind and a spherical rotating Earth. The elastic deformations are represented in terms of modal coordinates relative to mean axes. A paper by Olsen[21] reveals new insights in the aeroelasticity and flight mechanics of flexible aircraft by obtaining and solving the equations of motion for an accelerating, rotating aircraft. General equations in terms of quasi-coordinates are first obtained and then reduced to the case of a "flat" airplane. The influence of gusts on the dynamics of large flexible aircraft is analyzed by Teufel, Hanel and Well,[22] who present an integrated flight and aeroelastic control law reducing gust sensitivity. Moreover, the control laws, designed by μ-synthesis, are such that flight maneuvers do not excite elastic motions. König and Schuler[23] describe how an integral model for large flexible aircraft can be derived and how an integral control, covering flight control, load control and structural mode control, can be designed by multiobjective parameter optimization. Samareh and Bhatia[24] presented a unified three-dimensional approach that reduces the number of interactions among various disciplines by using a computer-aided design model. Results were presented for a blended wing body and a high-speed civil transport. Schmidt and Raney[25] considered the effects of flexibility on the flight dynamics of large flexible aircraft. In particular, when the frequencies of the lower elastic modes approach those of the rigid body modes the handling characteristics can suffer and the flight control system design tends to become significantly more complex. Expressing the motion in terms of components along mean axes, they add the flexible degrees of freedom to an existing simulation model of the vehicle's rigid body dynamics. The NASA Langley Research Center simulation facility was used to obtain the dynamic response of two different aircraft.

With some exceptions, the equations of motion in Refs. 3-23,25 were derived either by means of Newtonian mechanics or by means of standard Lagrange's equations. These approaches are more suitable when the motions are expressed in terms of inertial axes and/or when the rotations are in terms of Euler's angles. Yet, in the case of aircraft it is more convenient to express the motion in terms of components along body axes. In this regard, we should point out that this is common practice in flight dynamics, in which case the angular veolcities in terms of body axes are the well-known roll, pitch and yaw. Of course, equations in terms of inertial axes and/or Eulerian angles can always be transformed into equations in terms of body axes through coordinate transformations. It is appreciably simpler, however, to derive the equations of motion directly in terms of body axes, which can be done through the use of Lagrange's equations in terms of quasi-coordinates.[26]

Motivated by problems in dynamics of spacecraft with flexible appendages, Meirovitch and Nelson[27] derived for the first time hybrid (ordinary and partial) differential equations of motion coupling rigid body rotations and elastic deformations. The elastic deformations were measured relative to a set of body axes attached to the undeformed spacecraft and the rotational motions were in terms of quasi-coordinates. The explicit formulation of Ref. 27 was extended by Meirovitch[28] to a generic whole flexible body by deriving a set of hybrid equations of motion in terms of quasi-coordinates, treating for the first time translational velocities as quasi-velocities; the equations were then cast in state form. The equations of motion in terms of quasi-coordinates of Ref. 27 were used by Platus[29] to derive coupled equations of motion governing the aeroelastic stability of spinning flexible missiles. The coupling between the elastic deflections and rigid-body motions was nonlinear, but the equations were linearized so as to permit a stability analysis. The developments of Ref. 28 were extended by Meirovitch[30] and Meirovitch and Stemple[31] to flexible multibody systems. Then, the approach of Refs. 28, 30 and 31 was used by Meirovitch[32] to produce a definitive unified theory for the flight dynamics and aeroelasticity of whole aircraft. Generic state equations describing the flight of flexible aircraft were first derived in hybrid form and subsequently discretized in space. Then, using a perturbation approach, the discrete state equations were separated into a set of nonlinear flight dynamics equations for the rigid body variables and a set of linear extended aeroelasticity equations for the elastic variables and perturbations in the rigid body variables. Nydick and Friedmann[33] applied the equations of motion in terms of quasi-coordinates derived in Ref. 28 to the analysis of a hypersonic vehicle in free flight. To this end, they simplified the equations by considering only the pitch and plunge rigid body degrees of freedom and small elastic displacements. The nonlinear equations were linearized about a trim state obtained by using a rigid body trim model and steady hypersonic aerodynamics. Flutter derivatives were calculated by means of piston theory. The generic formulation of Ref. 32 was used by Meirovitch and Tuzcu[34] to carry out the derivation of explicit equations of motion in terms of quasi-coordinates for a flexible aircraft model and to cast the equations in a special state form suitable for simulation on a computer. Due to relative ease of integration into the unified formulation and computational speed advantages, the aerodynamic forces were derived by means of strip theory. Then, equations for flight dynamics and extended aeroelasticity were derived. An approach entirely different from that in Ref. 34 is proposed by Fornasier et al.[35] Indeed, Ref. 35 is concerned essentially with the fluid-structure interaction in a flexible aircraft. To this end, it uses "temporal and spatial algorithms" to make two independently developed computer codes, one for the aerodynamics (CFD) and one for structural mechanics (CSM), work together. The scope of Ref. 35 is relatively limited, as the aircraft is assumed to follow a known preset trajectory, so that there are no rigid body degrees of freedom, and there are no controls. Worthy of notice is the fact that several 5 s simulations, including some of the wing tip displacement, took approximately 35 hrs on a 32-processor Sgi computer.

The present paper represents an extension of the developments in Ref. 34. In addition to some modeling refinements, the paper contains a numerical example for a model of a flexible aircraft containing 76 states, 12 rigid body states and 64 elastic states. Two flight dynamics problems are considered, the steady level cruise and a steady level turn maneuver. The corresponding extended aeroelasticity problems are derived and used to design feedback controls guaranteeing the vanishing of the rigid body perturbations and the elastic vibration, and hence the stability of the maneuver and the comfort of the flight. The control design consists of a linear quadratic regulator in conjunction with a stochastic observer. The integrated process is demonstrated by means of a numerical example including a variety of rigid body and elastic displacements time simulations together with the corresponding controls time histories, all carried out on a 1 GHz PC using MATHEMATICA.

2. Hybrid Equations of Motion in Terms of Quasi-Coordinates

We regard the aircraft model shown in Fig. 1 as a flexible multibody system subjected to gravity, aerodynamic, propulsion and control forces, where the bodies can be broadly identified as the fuselage, wing and empennage. The motion of the aircraft can be conveniently described by attaching a reference frame $x_f y_f z_f$ to the undeformed fuselage (Fig. 1), as well as corresponding reference frames $x_w y_w z_w$ and $x_e y_e z_e$ to the wing and empennage, where the various reference frames represent respective body axes. Then, the motion can be described by six rigid body degrees of freedom of the fuselage body axes, three translations and three rotations, and by the elastic deformation of every point of each flexible component relative to the respective body axes.

From Ref. 32, and making provisions for members in torsion, as well as for structural damping, the hybrid equations of motion for the whole flexible aircraft in terms of quasi-coordinates have

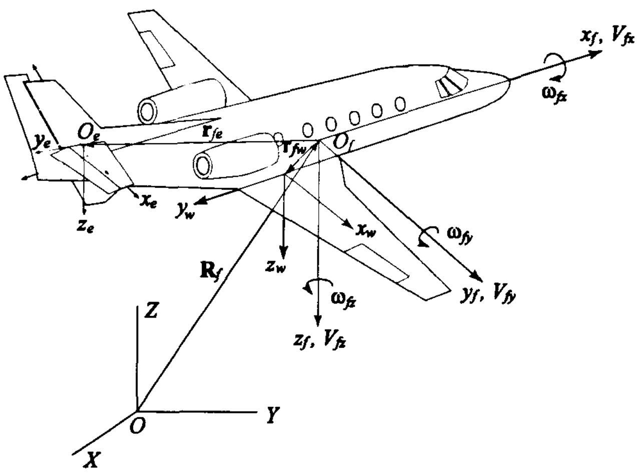

Figure 1. Flexible Aircraft Model

the generic form

$$\begin{aligned}
&\frac{d}{dt}\left(\frac{\partial L}{\partial \mathbf{V}_f}\right) + \tilde{\omega}_f \frac{\partial L}{\partial \mathbf{V}_f} - C_f \frac{\partial L}{\partial \mathbf{R}_f} = \mathbf{F} \\
&\frac{d}{dt}\left(\frac{\partial L}{\partial \boldsymbol{\omega}_f}\right) + \tilde{V}_f \frac{\partial L}{\partial \mathbf{V}_f} + \tilde{\omega}_f \frac{\partial L}{\partial \boldsymbol{\omega}_f} - (E_f^T)^{-1} \frac{\partial L}{\partial \boldsymbol{\theta}_f} = \mathbf{M} \\
&\frac{\partial}{\partial t}\left(\frac{\partial \hat{L}_i}{\partial \mathbf{v}_i}\right) - \frac{\partial \hat{L}_i}{\partial \mathbf{u}_i} + \frac{\partial \hat{\mathcal{F}}_{ui}}{\partial \dot{\mathbf{u}}_i} + \mathcal{L}_{ui}\mathbf{u}_i = \hat{\mathbf{U}}_i, \quad \frac{\partial}{\partial t}\left(\frac{\partial \hat{L}_i}{\partial \boldsymbol{\alpha}_i}\right) + \frac{\partial \hat{\mathcal{F}}_{\alpha i}}{\partial \dot{\boldsymbol{\psi}}_i} + \mathcal{L}_{\psi i}\boldsymbol{\psi}_i = \hat{\boldsymbol{\Psi}}_i, \\
&\qquad i = f \text{ (fuselage)},\ w \text{ (wing)},\ e \text{ (empennage)}
\end{aligned} \tag{1}$$

where

L = Lagrangian for the whole aircraft

$\mathbf{V}_f, \boldsymbol{\omega}_f$ = vector of translational, angular quasi-velocities of $x_f y_f z_f$

$\tilde{V}_f, \tilde{\omega}_f$ = skew symmetric matrices derived from $\mathbf{V}_f$, $\boldsymbol{\omega}_f$

C_f = matrix of direction cosines between $x_f y_f z_f$ and XYZ (inertial axes)

$\mathbf{R}_f = \mathbf{R}_f(X_f, Y_f, Z_f)$ = position vector of origin O_f of $x_f y_f z_f$ relative to XYZ

E_f = matrix relating Eulerian velocities to angular quasi-velocities

$\boldsymbol{\theta}_f$ = symbolic vector of Eulerian angles between $x_f y_f z_f$ and XYZ

$\mathbf{u}_i, \mathbf{v}_i$ = elastic displacement, velocity vectors for body i

$\boldsymbol{\psi}_i, \boldsymbol{\alpha}_i$ = elastic angular displacement, velocity vectors for body i

$\hat{L}_i$ = Lagrangian density for body i exclusive of strain energy

$\hat{\mathcal{F}}_{ui}, \hat{\mathcal{F}}_{\psi i}$ = Rayleigh's dissipation function[37] densities for body i

$\mathcal{L}_{ui}, \mathcal{L}_{\psi i}$ = matrices of stiffness differential operators for body i

$\mathbf{F}, \mathbf{M}$ = resultant of gravity, aerodynamic, propulsion and control force, moment vectors acting on the whole aircraft in terms of fuselage body axes components

$\hat{\mathbf{U}}_i, \boldsymbol{\Psi}_i$ = resultant of gravity, aerodynamic, propulsion and control force, moment density vectors for body i

Assuming that axes $x_f y_f z_f$ are obtained from axes XYZ through the sequence of rotations ψ about Z to axes $x_1 y_1 z_1$, θ about y_1 to $x_2 y_2 z_2$ and ϕ about x_2 to $x_f y_f z_f$, the matrices C_f and E_f have the form[36]

$$C_f = \begin{bmatrix} \mathrm{c}\psi\mathrm{c}\theta & \mathrm{s}\psi\mathrm{c}\theta & -\mathrm{s}\theta \\ \mathrm{c}\psi\mathrm{s}\theta\mathrm{s}\phi - \mathrm{s}\psi\mathrm{c}\phi & \mathrm{s}\psi\mathrm{s}\theta\mathrm{s}\phi + \mathrm{c}\psi\mathrm{c}\phi & \mathrm{c}\theta\mathrm{s}\phi \\ \mathrm{c}\psi\mathrm{s}\theta\mathrm{c}\phi + \mathrm{s}\psi\mathrm{s}\phi & \mathrm{s}\psi\mathrm{s}\theta\mathrm{c}\phi - \mathrm{c}\psi\mathrm{s}\phi & \mathrm{c}\theta\mathrm{c}\phi \end{bmatrix}$$
$$E_f = \begin{bmatrix} 1 & 0 & -\mathrm{s}\theta \\ 0 & \mathrm{c}\phi & \mathrm{c}\theta\mathrm{s}\phi \\ 0 & -\mathrm{s}\phi & \mathrm{c}\theta\mathrm{c}\phi \end{bmatrix} \tag{2}$$

in which s = sin, c = cos. The elastic displacement vectors $\mathbf{u}_i$ and $\boldsymbol{\psi}_i$ are subject to given boundary conditions at the interface between bodies. Equations (1) involve the Lagrangian $L = T - V$, in which T is the kinetic energy and V the potential energy, the Rayleigh dissipation function densities $\hat{\mathcal{F}}_{ui}$ and $\hat{\mathcal{F}}_{\psi i}$, which contain the information about the structural damping, and the stiffness operators $\mathcal{L}_{ui}$ and $\mathcal{L}_{\psi i}$, which are related to the strain energy. Before more explicit equations of motion can be derived, it is necessary to produce these quantities. The kinetic energy for the whole aircraft can be written as

$$T = T_f + T_w + T_e \tag{3}$$

where

$$T_i = \tfrac{1}{2}\int \bar{\mathbf{V}}_i^T \bar{\mathbf{V}}_i dm_i, \; i = f, w, e \tag{4}$$

are kinetic energies of the individual components, in which $\bar{\mathbf{V}}_i$ are velocity vectors of typical points in the components and dm_i are corresponding mass differential elements. The velocity of a point in the fuselage can be written as

$$\begin{aligned} \bar{\mathbf{V}}_f(\mathbf{r}_f, t) &= \mathbf{V}_f(t) + [\tilde{r}_f + \tilde{u}_f(\mathbf{r}_f, t)]^T [\boldsymbol{\omega}_f(t) + \boldsymbol{\alpha}_f(\mathbf{r}_f, t)] + \mathbf{v}_f(\mathbf{r}_f, t) \\ &\cong \mathbf{V}_f + (\tilde{r}_f + \tilde{u}_f)^T \boldsymbol{\omega}_f + \tilde{r}_f^T \boldsymbol{\alpha}_f + \mathbf{v}_f \end{aligned} \tag{5}$$

where $\mathbf{r}_f$ is the nominal position of the mass element dm_f, $\tilde{r}_f$ and $\tilde{u}_f$ are skew symmetric matrices[26] corresponding to $\mathbf{r}_f$ and $\mathbf{u}_f$ and $\mathbf{v}_f$ and $\boldsymbol{\alpha}_f$ are elastic velocities associated with bending and torsion, respectively. Then, denoting by C_w the matrix of direction cosines between $x_w y_w z_w$ and

$x_f y_f z_f$, the velocity of a point on the wing has the expression

$$\begin{aligned}\bar{\mathbf{V}}_w(\mathbf{r}_w, t) &= C_w \bar{\mathbf{V}}_f(\mathbf{r}_{fw}, t) + \tilde{r}_w^T C_w[\boldsymbol{\Omega}_f(\mathbf{r}_{fw}, t) + \boldsymbol{\alpha}_f(\mathbf{r}_{fw}, t)] + [\tilde{r}_w + \tilde{u}_w(\mathbf{r}_w, t)]^T[\boldsymbol{\omega}_w(t) \\ &\quad + \boldsymbol{\alpha}_w(\mathbf{r}_w, t)] + \mathbf{v}_w(\mathbf{r}_w, t) \\ &\cong C_w \mathbf{V}_f + [C_w(\tilde{r}_{fw} + \tilde{u}_{fw})^T + (\tilde{r}_w + \tilde{u}_w)^T C_w]\boldsymbol{\omega}_f + \tilde{r}_w^T C_w(\boldsymbol{\Omega}_{fw} + \boldsymbol{\alpha}_{fw}) \\ &\quad + C_w(\mathbf{v}_{fw} + \tilde{r}_{fw}^T \boldsymbol{\alpha}_{fw}) + \tilde{r}_w^T \boldsymbol{\alpha}_w + \mathbf{v}_w \end{aligned} \tag{6}$$

in which $\mathbf{r}_{fw}$ is the radius vector from the origin of $x_f y_f z_f$ to the origin of $x_w y_w z_w$,

$$\boldsymbol{\Omega}_{fw} = [0 \quad -\partial \dot{u}_{fz}/\partial x_f \quad \partial \dot{u}_{fy}/\partial x_f]\big|_{\mathbf{r}_{fw}}^T \tag{7}$$

is the angular velocity of the fuselage at $\mathbf{r}_{fw}$ due to bending and $\boldsymbol{\alpha}_{fw} = [\alpha_{fw} \ \ 0 \ \ 0]\big|_{\mathbf{r}_{fw}}^T$ is the elastic velocity of the fuselage at $\mathbf{r}_{fw}$ due to torsion. The velocity $\bar{\mathbf{V}}_e(\mathbf{r}_e, t)$ of a point on the empennage can be obtained from Eq. (6) by simply replacing w by e. The total kinetic energy can be expressed in the general form

$$T = \tfrac{1}{2}\int \bar{\mathbf{V}}_f^T \bar{\mathbf{V}}_f dm_f + \tfrac{1}{2}\int \bar{\mathbf{V}}_w^T \bar{\mathbf{V}}_w dm_w + \tfrac{1}{2}\int \bar{\mathbf{V}}_e^T \bar{\mathbf{V}}_e dm_e \tag{8}$$

The potential energy can be expressed in terms of the operators $\mathcal{L}_{ui}$, $\mathcal{L}_{\psi i}$ $(i = f, w, e)$, but is more conveniently expressed as the strain energy. Moreover, the Rayleigh dissipation function densities can be expressed in the form

$$\hat{\mathcal{F}}_{ui} = \tfrac{1}{2} c_{ui} EI_i \frac{\partial^2 \dot{\mathbf{u}}_i^T}{\partial x_i^2} \frac{\partial^2 \dot{\mathbf{u}}_i}{\partial x_i^2}, \ \hat{\mathcal{F}}_{\psi i} = \tfrac{1}{2} c_{\psi i} GJ_i \frac{\partial \dot{\boldsymbol{\psi}}_i^T}{\partial x_i} \frac{\partial \dot{\boldsymbol{\psi}}_i}{\partial x_i}, \ i = f, w, e \tag{9}$$

where c_{ui}, $c_{\psi i}$ are damping functions and EI_i, GJ_i are flexural and torsional rigidities $(i = f, w, e)$.

Equation (8), the potential energy V, the functions $\hat{\mathcal{F}}_{ui}$ and $\hat{\mathcal{F}}_{\psi i}$ and the operators $\mathcal{L}_{ui}$ and $\mathcal{L}_{\psi i}$, when inserted into Eqs. (1), permit the derivation of explicit hybrid equations of motion. Because for all practical purposes it is not feasible to work with hybrid equations, we do not pursue this subject any farther, and approximate instead the partial differential equations by sets of ordinary differential equations.

3. Spatial Discretization of the Distributed Variables

For the most part, aircraft are modeled as discrete systems, either by regarding the inertia and stiffness properties as lumped from the onset or by describing their elastic motions in terms of aircraft structural modes. For undamped structures in vacuum, the use of structural modes yields complete decoupling, i.e., it yields a set of independent modal equations of motion. In the case of aircraft, however, complete decoupling is not possible, even when aircraft structural modes are used, as the aerodynamic forces guarantee that the equations of motion remain coupled. Spatial discretization using aircraft structural modes not only does not offer any particular advantage but also has the disadvantage that some geometric details of the aircraft are lost in the process. Hence, a discretization procedure that does not require the structural modes, which may not be readily available and/or may not be compatible with the rest of the formulation, and retains some sense of the aircraft geometry seems desirable. Consistent with this, we consider spatial discretization of the individual aircraft components separately. To this end, we use either the Galerkin method or the finite element method[37] and introduce the expansions

$$\mathbf{u}_i(\mathbf{r}_i,t) = \Phi_{ui}(\mathbf{r}_i)\mathbf{q}_{ui}(t),\ \boldsymbol{\psi}_i(\mathbf{r}_i,t) = \Phi_{\psi i}(\mathbf{r}_i)\mathbf{q}_{\psi i}(t),\ i = f, w, e \tag{10}$$

where Φ_{ui} and $\Phi_{\psi i}$ are matrices of shape functions and $\mathbf{q}_{ui}$ and $\mathbf{q}_{\psi i}$ are corersponding vectors of generalized coordinates. Note that the choice of shape functions is very important. Indeed, for accurate modeling, the shape functions must reflect the mass and stiffness characteristics of the components. Some guidelines concerning the choice of shape functions can be found in Ref. 37. Moreover, we denote the associated generalized velocities by

$$\mathbf{s}_{ui}(t) = \dot{\mathbf{q}}_{ui}(t),\ \mathbf{s}_{\psi i}(t) = \dot{\mathbf{q}}_{\psi i}(t),\ i = f, w, e \tag{11}$$

In anticipation of later needs, we write the velocity vectors for points on the individual components in the two discrete forms

$$\begin{aligned}
\bar{\mathbf{V}}_f(\mathbf{r}_f,t) &= \mathbf{V}_f + (\tilde{r}_f + \widetilde{\Phi_{uf}\mathbf{q}_{uf}})^T\boldsymbol{\omega}_f + \Phi_{uf}\mathbf{s}_{uf} + \tilde{r}_f^T\Phi_{\psi f}\mathbf{s}_{\psi f} \\
&= \mathbf{V}_f + \tilde{r}_f^T\boldsymbol{\omega}_f + \tilde{\omega}_f\Phi_{uf}\mathbf{q}_{uf} + \Phi_{uf}\mathbf{s}_{uf} + \tilde{r}_f^T\Phi_{\psi f}\mathbf{s}_{\psi f} \\
\bar{\mathbf{V}}_w(\mathbf{r}_w,t) &= C_w\mathbf{V}_f + [C_w(\tilde{r}_{fw} + \widetilde{\Phi_{ufw}\mathbf{q}_{uf}})^T + (\tilde{r}_w + \widetilde{\Phi_{uw}\mathbf{q}_{uw}})^T C_w]\boldsymbol{\omega}_f \\
&\quad + (\tilde{r}_w^T C_w\Delta\Phi_{ufw} + C_w\Phi_{ufw})\mathbf{s}_{uf} + \Phi_{uw}\mathbf{s}_{uw} \\
&\quad + (\tilde{r}_w^T C_w\Phi_{\psi fw} + C_w\tilde{r}_{fw}^T\Phi_{\psi fw})\mathbf{s}_{\psi f} + \tilde{r}_w^T\Phi_{\psi w}\mathbf{s}_{\psi w} \\
&= C_w\mathbf{V}_f + (C_w\tilde{r}_{fw}^T + \tilde{r}_w^T C_w)\boldsymbol{\omega}_f + C_w\tilde{\omega}_f\Phi_{ufw}\mathbf{q}_{uf} + \widetilde{C_w\boldsymbol{\omega}_f}\Phi_{uw}\mathbf{q}_{uw} \\
&\quad + (\tilde{r}_w^T C_w\Delta\Phi_{ufw} + C_w\Phi_{ufw})\mathbf{s}_{uf} + \Phi_{uw}\mathbf{s}_{uw} \\
&\quad + (\tilde{r}_w^T C_w\Phi_{\psi fw} + C_w\tilde{r}_{fw}^T\Phi_{\psi fw})\mathbf{s}_{\psi f} + \tilde{r}_w^T\Phi_{\psi w}\mathbf{s}_{\psi w}
\end{aligned} \tag{12}$$

in which

$$\Delta = \begin{bmatrix} 0 & 0 \\ 0 & -\partial/\partial x_f \\ \partial/\partial x_f & 0 \end{bmatrix},\ \Phi_{uf} = \begin{bmatrix} \boldsymbol{\phi}_{ufy}^T & \mathbf{0}^T \\ \mathbf{0}^T & \boldsymbol{\phi}_{ufz}^T \end{bmatrix},\ \Phi_{ufw} = \Phi_{uf}(\mathbf{r}_{fw}) \tag{13}$$

Expression analogous to Φ_{uf} can be written for $\Phi_{\psi f}$ and $\Phi_{\psi fw}$. Moreover, $\bar{\mathbf{V}}_e(\mathbf{r}_e,t)$ can be obtained from $\bar{\mathbf{V}}_w(\mathbf{r}_w,t)$ by simply replacing w by e. Inserting the first forms of Eqs. (12) into Eq. (8) and carrying out the indicated operations, we can write the kinetic energy in the compact form

$$T = \frac{1}{2}\int \bar{\mathbf{V}}_f^T \bar{\mathbf{V}}_f dm_f + \frac{1}{2}\int \bar{\mathbf{V}}_w^T \bar{\mathbf{V}}_w dm_w + \frac{1}{2}\int \bar{\mathbf{V}}_e^T \bar{\mathbf{V}}_e dm_e = \frac{1}{2}\mathbf{V}^T M \mathbf{V} \tag{14}$$

where $\mathbf{V} = [\mathbf{V}_f^T\ \boldsymbol{\omega}_f^T\ \mathbf{s}_{uf}^T\ \mathbf{s}_{uw}^T\ \mathbf{s}_{ue}^T\ \mathbf{s}_{\psi f}^T\ \mathbf{s}_{\psi w}^T\ \mathbf{s}_{\psi e}^T]^T = [\mathbf{V}_1^T\ \mathbf{V}_2^T \ldots \mathbf{V}_8^T]^T$ is the discrete system velocity vector and $M = [M_{ij}]$ is the system mass matrix, a matrix that can be expressed in partitioned form with the submatrices

$$\begin{aligned}
&M_{11} = mI,\ M_{12} = \tilde{S}^T, \\
&M_{13} = \int \Phi_{uf} dm_f + \int C_w^T(\tilde{r}_w^T C_w \Delta\Phi_{ufw} + C_w \Phi_{ufw}) dm_w + \int C_e^T(\tilde{r}_e^T C_e \Delta\Phi_{ufe} + C_e \Phi_{ufe}) dm_e \\
&M_{14} = C_w^T \int \Phi_{uw} dm_w,\ M_{15} = C_e^T \int \Phi_{ue} dm_e \\
&M_{16} = \int \tilde{r}_f^T \Phi_{\psi f} dm_f + C_w^T \int (\tilde{r}_w^T C_w \Phi_{\psi fw} + C_w \tilde{r}_{fw}^T \Phi_{\psi fw}) dm_w + C_e^T \int (\tilde{r}_e^T C_e \Phi_{\psi fe} \\
&\qquad + C_e \tilde{r}_{fe}^T \Phi_{\psi fe}) dm_e \\
&M_{17} = C_w^T \int \tilde{r}_w^T \Phi_{\psi w} dm_w,\ M_{18} = C_e^T \int \tilde{r}_e^T \Phi_{\psi e} dm_e \\
&M_{21} = M_{12}^T,\ M_{22} = J \\
&M_{23} = \int (\tilde{r}_f + \widetilde{\Phi_{uf}\mathbf{q}_{uf}}) \Phi_{uf} dm_f + \int [C_w(\tilde{r}_{fw} + \widetilde{\Phi_{ufw}\mathbf{q}_{uf}})^T + (\tilde{r}_w + \widetilde{\Phi_{uw}\mathbf{q}_{uw}})^T C_w]^T \\
&\qquad \times (\tilde{r}_w^T C_w \Delta\Phi_{ufw} + C_w \Phi_{ufw}) dm_w + \int [C_e(\tilde{r}_{fe} + \widetilde{\Phi_{ufe}\mathbf{q}_{uf}})^T + (\tilde{r}_e + \widetilde{\Phi_{ue}\mathbf{q}_{ue}})^T C_e]^T \\
&\qquad \times (\tilde{r}_e^T C_e \Delta\Phi_{ufe} + C_e \Phi_{ufe}) dm_e \\
&M_{24} = \int [C_w(\tilde{r}_{fw} + \widetilde{\Phi_{ufw}\mathbf{q}_{uf}})^T + (\tilde{r}_w + \widetilde{\Phi_{uw}\mathbf{q}_{uw}})^T C_w]^T \Phi_{uw} dm_w \\
&M_{25} = \int [C_e(\tilde{r}_{fe} + \widetilde{\Phi_{ufe}\mathbf{q}_{uf}})^T + (\tilde{r}_e + \widetilde{\Phi_{ue}\mathbf{q}_{ue}})^T C_e]^T \Phi_{ue} dm_e \\
&M_{26} = \int (\tilde{r}_f + \widetilde{\Phi_{uf}\mathbf{q}_{uf}}) \tilde{r}_f^T \Phi_{\psi f} dm_f + \int [C_w(\tilde{r}_{fw} + \widetilde{\Phi_{ufw}\mathbf{q}_{uf}})^T + (\tilde{r}_w + \widetilde{\Phi_{uw}\mathbf{q}_{uw}})^T C_w]^T \\
&\qquad \times (\tilde{r}_w^T C_w \Phi_{\psi fw} + C_w \tilde{r}_{fw}^T \Phi_{\psi fw}) dm_w + \int [C_e(\tilde{r}_{fe} + \widetilde{\Phi_{ufe}\mathbf{q}_{uf}})^T + (\tilde{r}_e + \widetilde{\Phi_{ue}\mathbf{q}_{ue}})^T C_e]^T \\
&\qquad \times (\tilde{r}_e^T C_e \Phi_{\psi fe} + C_e \tilde{r}_{fe}^T \Phi_{\psi fe}) dm_e \\
&M_{27} = \int [C_w(\tilde{r}_{fw} + \widetilde{\Phi_{ufw}\mathbf{q}_{uf}})^T + (\tilde{r}_w + \widetilde{\Phi_{uw}\mathbf{q}_{uw}})^T C_w]^T \tilde{r}_w^T \Phi_{\psi w} dm_w \\
&M_{28} = \int [C_e(\tilde{r}_{fe} + \widetilde{\Phi_{ufe}\mathbf{q}_{uf}})^T + (\tilde{r}_e + \widetilde{\Phi_{ue}\mathbf{q}_{ue}})^T C_e]^T \tilde{r}_e^T \Phi_{\psi e} dm_e \\
&M_{31} = M_{13}^T,\ M_{32} = M_{23}^T \\
&M_{33} = \int \Phi_{uf}^T \Phi_{uf} dm_f + \int (\tilde{r}_w^T C_w \Delta\Phi_{ufw} + C_w \Phi_{ufw})^T (\tilde{r}_w^T C_w \Delta\Phi_{ufw} + C_w \Phi_{ufw}) dm_w \\
&\qquad + \int (\tilde{r}_e^T C_e \Delta\Phi_{ufe} + C_e \Phi_{ufe})^T (\tilde{r}_e^T C_e \Delta\Phi_{ufe} + C_e \Phi_{ufe}) dm_e \\
&M_{34} = \int (\tilde{r}_w^T C_w \Delta\Phi_{ufw} + C_w \Phi_{ufw})^T \Phi_{uw} dm_w \\
&M_{35} = \int (\tilde{r}_e^T C_e \Delta\Phi_{ufe} + C_e \Phi_{ufe})^T \Phi_{ue} dm_e \\
&M_{36} = \int \Phi_{uf}^T \tilde{r}_f^T \Phi_{\psi f} dm_f + \int (\tilde{r}_w^T C_w \Delta\Phi_{ufw} + C_w \Phi_{ufw})^T (\tilde{r}_w^T C_w \Phi_{\psi fw} + C_w \tilde{r}_{fw}^T \Phi_{\psi fw}) dm_w \\
&\qquad + \int (\tilde{r}_e^T C_e \Delta\Phi_{ufe} + C_e \Phi_{ufe})^T (\tilde{r}_e^T C_e \Phi_{\psi fe} + C_e \tilde{r}_{fe}^T \Phi_{\psi fe}) dm_e \\
&M_{37} = \int (\tilde{r}_w^T C_w \Delta\Phi_{ufw} + C_w \Phi_{ufw})^T \tilde{r}_w^T \Phi_{\psi w} dm_w \\
&M_{38} = \int (\tilde{r}_e^T C_e \Delta\Phi_{ufe} + C_e \Phi_{ufe})^T \tilde{r}_e^T \Phi_{\psi e} dm_e \\
&M_{41} = M_{14}^T,\ M_{42} = M_{24}^T,\ M_{43} = M_{34}^T,\ M_{44} = \int \Phi_{uw}^T \Phi_{uw} dm_w,\ M_{45} = 0
\end{aligned} \tag{15}$$

$$M_{46} = \int \Phi_{uw}^T(\tilde{r}_w^T C_w \Phi_{\psi fw} + C_w \tilde{r}_{fw}^T \Phi_{\psi fw}) dm_w,\ M_{47} = \int \Phi_{uw}^T \tilde{r}_w^T \Phi_{\psi w} dm_w\ , M_{48} = 0$$
$$M_{51} = M_{15}^T,\ M_{52} = M_{25}^T,\ M_{53} = M_{35}^T,\ M_{54} = M_{45}^T,\ M_{55} = \int \Phi_{ue}^T \Phi_{ue} dm_e$$
$$M_{56} = \int \Phi_{ue}^T(\tilde{r}_e^T C_e \Phi_{\psi fe} + C_e \tilde{r}_{fe}^T \Phi_{\psi fe}) dm_e,\ M_{57} = 0,\ M_{58} = \int \Phi_{ue}^T \tilde{r}_e^T \Phi_{\psi e} dm_e$$
$$M_{61} = M_{16}^T,\ M_{62} = M_{26}^T,\ M_{63} = M_{36}^T,\ M_{64} = M_{46}^T,\ M_{65} = M_{56}^T$$
$$M_{66} = \int \Phi_{\psi f}^T \tilde{r}_f \tilde{r}_f^T \Phi_{\psi f} dm_f + \int (\tilde{r}_w^T C_w \Phi_{\psi fw} + C_w \tilde{r}_{fw}^T \Phi_{\psi fw})^T (\tilde{r}_w^T C_w \Phi_{\psi fw} + C_w \tilde{r}_{fw}^T \Phi_{\psi fw}) dm_w$$
$$+ \int (\tilde{r}_e^T C_e \Phi_{\psi fe} + C_e \tilde{r}_{fe}^T \Phi_{\psi fe})^T (\tilde{r}_e^T C_e \Phi_{\psi fe} + C_e \tilde{r}_{fe}^T \Phi_{\psi fe}) dm_e$$
$$M_{67} = \int (\tilde{r}_w^T C_w \Phi_{\psi fw} + C_w \tilde{r}_{fw}^T \Phi_{\psi fw})^T \tilde{r}_w^T \Phi_{\psi w} dm_w$$
$$M_{68} = \int (\tilde{r}_e^T C_e \Phi_{\psi fe} + C_e \tilde{r}_{fe}^T \Phi_{\psi fe})^T \tilde{r}_e^T \Phi_{\psi e} dm_e$$
$$M_{71} = M_{17}^T,\ M_{72} = M_{27}^T,\ M_{73} = M_{37}^T,\ M_{74} = M_{47}^T,\ M_{75} = M_{57}^T,\ M_{76} = M_{67}^T$$
$$M_{77} = \int \Phi_{\psi w}^T \tilde{r}_w \tilde{r}_w^T \Phi_{\psi w} dm_w,\ M_{78} = 0$$
$$M_{81} = M_{18}^T,\ M_{82} = M_{28}^T,\ M_{83} = M_{38}^T,\ M_{84} = M_{48}^T,\ M_{85} = M_{58}^T,\ M_{86} = M_{68}^T,\ M_{87} = M_{78}^T$$
$$M_{88} = \int \Phi_{\psi e}^T \tilde{r}_e \tilde{r}_e^T \Phi_{\psi e} dm_e$$

in which m is the aircraft total mass,

$$\tilde{S} = \int (\tilde{r}_f + \widetilde{\Phi_{uf}\mathbf{q}_{uf}}) dm_f + \int [(\tilde{r}_{fw} + \widetilde{\Phi_{ufw}\mathbf{q}_{uf}}) C_w^T + C_w^T(\tilde{r}_w + \widetilde{\Phi_{uw}\mathbf{q}_{uw}})] C_w dm_w$$
$$+ \int [(\tilde{r}_{fe} + \widetilde{\Phi_{ufe}\mathbf{q}_{uf}}) C_e^T + C_e^T(\tilde{r}_e + \widetilde{\Phi_{ue}\mathbf{q}_{ue}})] C_e dm_e \tag{16}$$

is the matrix of first moments of inertia of the *deformed* aircraft and

$$J = \int (\tilde{r}_f + \widetilde{\Phi_{uf}\mathbf{q}_{uf}})^T (\tilde{r}_f + \widetilde{\Phi_{uf}\mathbf{q}_{uf}}) dm_f + \int [C_w(\tilde{r}_{fw} + \widetilde{\Phi_{ufw}\mathbf{q}_{uf}})^T + (\tilde{r}_w + \widetilde{\Phi_{uw}\mathbf{q}_{uw}})^T C_w]^T$$
$$\times [C_w(\tilde{r}_{fw} + \widetilde{\Phi_{ufw}\mathbf{q}_{uf}})^T + (\tilde{r}_w + \widetilde{\Phi_{uw}\mathbf{q}_{uw}})^T C_w] dm_w + \int [C_e(\tilde{r}_{fe} + \widetilde{\Phi_{ufe}\mathbf{q}_{uf}})^T$$
$$+ (\tilde{r}_e + \widetilde{\Phi_{ue}\mathbf{q}_{ue}})^T C_e]^T [C_e(\tilde{r}_{fe} + \widetilde{\Phi_{ufe}\mathbf{q}_{uf}})^T + (\tilde{r}_e + \widetilde{\Phi_{ue}\mathbf{q}_{ue}})^T C_e] dm_e \tag{17}$$

is the inertia matrix of the deformed aircraft.

In a similar fashion, we insert Eqs. (10) into Eqs. (9), integrate over the respective components domains and obtain the generalized Rayleigh's dissipation functions

$$\begin{aligned} \mathcal{F}_{ui} &= \int_{D_i} \hat{\mathcal{F}}_{ui} dD_i = \tfrac{1}{2} \int_{D_i} c_{ui} EI_i \dot{\mathbf{q}}_{ui}^T \frac{d^2\Phi_{ui}^T}{dx_i^2} \frac{d^2\Phi_{ui}}{dx_i^2} \dot{\mathbf{q}}_{ui} dD_i = \tfrac{1}{2} \dot{\mathbf{q}}_{ui}^T C_{ui} \dot{\mathbf{q}}_{ui}, \\ \mathcal{F}_{\psi i} &= \int_{D_i} \hat{\mathcal{F}}_{\psi i} dD_i = \tfrac{1}{2} \int_{D_i} c_{\psi i} GJ_i \dot{\mathbf{q}}_{\psi i}^T \frac{d\Phi_{\psi i}^T}{dx_i} \frac{d\Phi_{\psi i}}{dx_i} \dot{\mathbf{q}}_{\psi i} dD_i = \tfrac{1}{2} \dot{\mathbf{q}}_{\psi i}^T C_{\psi i} \dot{\mathbf{q}}_{\psi i}, \end{aligned} \quad i = f, w, e \tag{18}$$

where

$$C_{ui} = \int_{D_i} c_{ui} EI_i \frac{d^2\Phi_{ui}^T}{dx_i^2} \frac{d^2\Phi_{ui}}{dx_i^2} dD_i,\ C_{\psi i} = \int_{D_i} c_{\psi i} GJ_i \frac{d\Phi_{\psi i}^T}{dx_i} \frac{d\Phi_{\psi i}}{dx_i} dD_i,\ i = f, w, e \tag{19}$$

are damping matrices.

Next, we denote the momentum vector for the whole aircraft by $\mathbf{p} = [\mathbf{p}_{Vf}^T\ \mathbf{p}_{\omega f}^T\ \mathbf{p}_{uf}^T\ \mathbf{p}_{uw}^T\ \mathbf{p}_{ue}^T\ \mathbf{p}_{\psi f}^T\ \mathbf{p}_{\psi w}^T\ \mathbf{p}_{\psi e}^T]^T = [\mathbf{p}_1^T\ \mathbf{p}_2^T \dots \mathbf{p}_8^T]^T$, so that we can write

$$\mathbf{p} = \partial T / \partial \mathbf{V} = M\mathbf{V} \tag{20}$$

where the individual momenta are given by

$$
\begin{aligned}
\mathbf{p}_{Vf} &= \partial T/\partial \mathbf{V}_f = \mathbf{p}_1 = \sum_{j=1}^{8} M_{1j}\mathbf{V}_j \\
\mathbf{p}_{\omega f} &= \partial T/\partial \boldsymbol{\omega}_f = \mathbf{p}_2 = \sum_{j=1}^{8} M_{2j}\mathbf{V}_j \\
\mathbf{p}_{uf} &= \partial T/\partial \mathbf{s}_{uf} = \mathbf{p}_3 = \sum_{j=1}^{8} M_{3j}\mathbf{V}_j \\
&- \\
\mathbf{p}_{\psi e} &= \partial T/\partial \mathbf{s}_{\psi e} = \mathbf{p}_8 = \sum_{j=1}^{8} M_{8j}\mathbf{V}_j
\end{aligned}
\tag{21}
$$

Finally, adding some obvious kinematical identities to the discretized version of Eqs. (1), the state equations can be written in the special form

$$
\begin{aligned}
&\dot{\mathbf{R}}_f = C_f^T\mathbf{V}_f,\ \dot{\boldsymbol{\theta}}_f = E_f^{-1}\boldsymbol{\omega}_f;\ \dot{\mathbf{q}}_{ui} = \mathbf{s}_{ui},\ \dot{\mathbf{q}}_{\psi i} = \mathbf{s}_{\psi i},\ i = f, w, e \\
&\dot{\mathbf{p}}_{Vf} = -\tilde{\omega}_f\mathbf{p}_{Vf} + \mathbf{F},\ \dot{\mathbf{p}}_{\omega f} = -\tilde{V}_f\mathbf{p}_{Vf} - \tilde{\omega}_f\mathbf{p}_{\omega f} + \mathbf{M} \\
&\left.\begin{aligned}
\dot{\mathbf{p}}_{ui} &= \partial T/\partial \mathbf{q}_{ui} - K_{ui}\mathbf{q}_{ui} - C_{ui}\mathbf{s}_{ui} + \mathbf{Q}_{ui} \\
\dot{\mathbf{p}}_{\psi i} &= -K_{\psi i}\mathbf{q}_{\psi i} - C_{\psi i}\mathbf{s}_{\psi i} + \mathbf{Q}_{\psi i}
\end{aligned}\right\} i = f, w, e
\end{aligned}
\tag{22}
$$

where, using Eq. (8) in conjunction with the second form of $\bar{\mathbf{V}}_f$, $\bar{\mathbf{V}}_w$ and $\bar{\mathbf{V}}_e$, Eqs. (12),

$$
\begin{aligned}
\frac{\partial T}{\partial \mathbf{q}_{uf}} &= \frac{\partial \bar{\mathbf{V}}_f^T}{\partial \mathbf{q}_{uf}}\frac{\partial T}{\partial \bar{\mathbf{V}}_f} + \frac{\partial \bar{\mathbf{V}}_w^T}{\partial \mathbf{q}_{uf}}\frac{\partial T}{\partial \bar{\mathbf{V}}_w} + \frac{\partial \bar{\mathbf{V}}_e^T}{\partial \mathbf{q}_{uf}}\frac{\partial T}{\partial \bar{\mathbf{V}}_e} \\
&= \int \Phi_{uf}^T\tilde{\omega}_f^T\bar{\mathbf{V}}_f dm_f + \Phi_{ufw}^T\tilde{\omega}_f^T C_w^T \int \bar{\mathbf{V}}_w dm_w + \Phi_{ufe}^T\tilde{\omega}_f^T C_e^T \int \bar{\mathbf{V}}_e dm_e \\
\frac{\partial T}{\partial \mathbf{q}_{uw}} &= \frac{\partial \bar{\mathbf{V}}_f^T}{\partial \mathbf{q}_{uw}}\frac{\partial T}{\partial \bar{\mathbf{V}}_f} + \frac{\partial \bar{\mathbf{V}}_w^T}{\partial \mathbf{q}_{uw}}\frac{\partial T}{\partial \bar{\mathbf{V}}_w} + \frac{\partial \bar{\mathbf{V}}_e^T}{\partial \mathbf{q}_{uw}}\frac{\partial T}{\partial \bar{\mathbf{V}}_e} = \Phi_{uw}^T\widetilde{C_w\boldsymbol{\omega}_f}^T \int \bar{\mathbf{V}}_w dm_w \\
\frac{\partial T}{\partial \mathbf{q}_{ue}} &= \frac{\partial \bar{\mathbf{V}}_f^T}{\partial \mathbf{q}_{ue}}\frac{\partial T}{\partial \bar{\mathbf{V}}_f} + \frac{\partial \bar{\mathbf{V}}_w^T}{\partial \mathbf{q}_{ue}}\frac{\partial T}{\partial \bar{\mathbf{V}}_w} + \frac{\partial \bar{\mathbf{V}}_e^T}{\partial \mathbf{q}_{ue}}\frac{\partial T}{\partial \bar{\mathbf{V}}_e} = \Phi_{ue}^T\widetilde{C_e\boldsymbol{\omega}_f}^T \int \bar{\mathbf{V}}_e dm_e
\end{aligned}
\tag{23}
$$

Moreover,

$$
K_{ui} = \int \Phi_{ui}^T \mathcal{L}_{ui}\Phi_{ui} dD_i,\ K_{\psi i} = \int \Phi_{\psi i}^T \mathcal{L}_{\psi i}\Phi_{\psi i} dD_i,\ i = f, w, e \tag{24}
$$

are component stiffness matrices. In practice, K_{ui} and $K_{\psi i}$ $(i = f, w, e)$ can be obtained with greater ease from the strain energy directly, as shown in the **Numerical Example**.

The quantities $\mathbf{F}$, $\mathbf{M}$, $\mathbf{Q}_{ui}$ and $\mathbf{Q}_{\psi i}$ $(i = f, w, e)$ appearing in the state equations, Eqs. (22), represent generalized forces. They are related to the actual forces, which consist of the distributed force $\mathbf{f}_i(\mathbf{r}_i, t)$ over component i due to gravity, aerodynamics and controls and the engine thrust $\mathbf{F}_E\delta(\mathbf{r} - \mathbf{r}_E)$, where $\delta(\mathbf{r} - \mathbf{r}_E)$ is a spatial Dirac delta function,[37] in which $\mathbf{r}_E$ denotes the location of the engines. If some control forces are concentrated, they can also be treated as distributed, as in the case of the engine thrust. The relation between the generalized forces and the actual forces can be obtained by means of the virtual work, which can be expressed as

$$\delta\bar{W} = \sum_i \int_{D_i} [\mathbf{f}_i^T + \mathbf{F}_E^T \delta(\mathbf{r} - \mathbf{r}_E)] \delta\bar{\mathbf{R}}_i^* dD_i \tag{25}$$

where $\delta\bar{\mathbf{R}}_i^*$ is the virtual quasi-displacement vector of a typical point on component i ($i = f, w, e$). The vector $\delta\bar{\mathbf{R}}_i^*$ is related to the virtual quasi-displacement vectors corresponding to the quasi-velocities used to describe the motion of the aircraft components. Indeed, using Eqs. (12), we can write

$$\begin{aligned} \delta\bar{\mathbf{R}}_f^* &= \delta\mathbf{R}_f^* + (\tilde{r}_f + \widetilde{\Phi_{uf}\mathbf{q}_{uf}})^T \delta\boldsymbol{\theta}_f^* + \Phi_{uf}\delta\mathbf{q}_{uf} + \tilde{r}_f^T \Phi_{\psi f}\delta\mathbf{q}_{\psi f} \\ \delta\bar{\mathbf{R}}_w^* &= C_w \delta\mathbf{R}_f^* + [C_w(\tilde{r}_{fw} + \widetilde{\Phi_{ufw}\mathbf{q}_{uf}})^T + (\tilde{r}_w + \widetilde{\Phi_{uw}\mathbf{q}_{uw}})^T C_w] \delta\boldsymbol{\theta}_f^* \\ &\quad + (\tilde{r}_w^T C_w \Delta\Phi_{ufw} + C_w \Phi_{ufw})\delta\mathbf{q}_{uf} + \Phi_{uw}\delta\mathbf{q}_{uw} \\ &\quad + (\tilde{r}_w^T C_w \Phi_{\psi fw} + C_w \tilde{r}_{fw}^T \Phi_{\psi fw})\delta\mathbf{q}_{\psi f} + \tilde{r}_w^T \Phi_{\psi w}\delta\mathbf{q}_{\psi w} \end{aligned} \tag{26}$$

and we note that $\delta\bar{\mathbf{R}}_e^*$ can be obtained from $\delta\bar{\mathbf{R}}_w^*$ by replacing w by e. Inserting Eqs. (26) into Eq. (25), and collecting terms, we can write the virtual work in terms of virtual generalized displacements as follows:

$$\delta\bar{W} = \mathbf{F}^T \delta\mathbf{R}_f^* + \mathbf{M}^T \delta\boldsymbol{\theta}_f^* + \sum_i (\mathbf{Q}_{ui}^T \delta\mathbf{q}_{ui} + \mathbf{Q}_{\psi i}^T \delta\mathbf{q}_{\psi i}) \tag{27}$$

from which, assuming that the engines are mounted on the fuselage (Fig. 1), we obtain

$$\begin{aligned} \mathbf{F} &= \int_{D_f} [\mathbf{f}_f + \mathbf{F}_E \delta(\mathbf{r} - \mathbf{r}_E)] dD_f + C_w^T \int_{D_w} \mathbf{f}_w dD_w + C_e^T \int_{D_e} \mathbf{f}_e dD_e \\ \mathbf{M} &= \int_{D_f} (\tilde{r}_f + \widetilde{\Phi_{uf}\mathbf{q}_{uf}}) [\mathbf{f}_f + \mathbf{F}_E \delta(\mathbf{r} - \mathbf{r}_E)] dD_f + \int_{D_w} [(\tilde{r}_{fw} + \widetilde{\Phi_{ufw}\mathbf{q}_{uf}}) C_w^T \\ &\quad + C_w^T (\tilde{r}_w + \widetilde{\Phi_{uw}\mathbf{q}_{uw}})] \mathbf{f}_w dD_w + \int_{D_e} [(\tilde{r}_{fe} + \widetilde{\Phi_{ufe}\mathbf{q}_{uf}}) C_e^T + C_e^T (\tilde{r}_e + \widetilde{\Phi_{ue}\mathbf{q}_{ue}})] \mathbf{f}_e dD_e \\ \mathbf{Q}_{uf} &= \int_{D_f} \Phi_{uf}^T [\mathbf{f}_f + \mathbf{F}_E \delta(\mathbf{r} - \mathbf{r}_E)] dD_f + \int_{D_w} (\tilde{r}_w^T C_w \Delta\Phi_{ufw} + C_w \Phi_{ufw})^T \mathbf{f}_w dD_w \\ &\quad + \int_{D_e} (\tilde{r}_e^T C_e \Delta\Phi_{ufe} + C_e \Phi_{ufe})^T \mathbf{f}_e dD_e, \\ \mathbf{Q}_{\psi f} &= \int_{D_f} \Phi_{\psi f}^T \tilde{r}_f [\mathbf{f}_f + \mathbf{F}_E \delta(\mathbf{r} - \mathbf{r}_E)] dD_f + \int_{D_w} (\tilde{r}_w^T C_w \Phi_{\psi fw} + C_w \tilde{r}_{fw}^T \Phi_{\psi fw})^T \mathbf{f}_w dD_w \\ &\quad + \int_{D_e} (\tilde{r}_e^T C_e \Phi_{\psi fe} + C_e \tilde{r}_{fe}^T \Phi_{\psi fe})^T \mathbf{f}_e dD_e \\ \mathbf{Q}_{ui} &= \int_{D_i} \Phi_{ui}^T \mathbf{f}_i dD_i, \; \mathbf{Q}_{\psi i} = \int_{D_i} \Phi_{\psi i}^T \tilde{r}_i \mathbf{f}_i dD_i, \; i = w, e \end{aligned} \tag{28}$$

To complete the state equations, Eqs. (22), it is necessary to derive the stiffness matrices K_{ui} and $K_{\psi i}$ ($i = f, w, e$), the aerodynamic forces and the control forces.

4. The Aerodynamic and Gravity Forces

The forces acting on the aircraft can be identified as the aerodynamic, propulsion, control and gravity forces. Equations (28) give the generalized forces in terms of actual distributed and concentrated forces, where the first imply prescribing the forces at every point of the aircraft. Of the forces acting on an aircraft, the aerodynamic and control forces require special attention. We discuss the aerodynamic forces in this section and the control forces in a later section.

There are a number of aerodynamic theories available, some of them capable of prescribing the pressure distribution at every point of the aircraft. However, as pointed out in the **Introduction and Literature Review**, any aerodynamic theory to be used in a dynamic simulation such as that described in this paper must satisfy certain requirements. Indeed, one of the requirements is that the aerodynamic forces be expressed in a form compatible with the present general dynamic formulation, which implies that they be in terms of the same variables and be referred to the same body axes attached to the undeformed aircraft as here. Another requirement is that the aerodynamic forces lend themselves to sufficiently fast computation as to permit time simulation of the aircraft behavior. Such computational efficiency does not appear to be within the state of the art. Hence, an aerodynamic theory capable of fitting within the framework of a computer simulation of the type envisioned here must yet be developed. Such a theory need not be unduly accurate, because a feedback control design tends to be sufficiently forgiving to tolerate small deviations from the actual aerodynamic forces. Until such a theory becomes reality, it is still possible to demonstrate how aerodynamics fits in the integration process by using an existing theory satisfying the requirement described above, namely, strip theory,[38] even though the theory may not be entirely suitable otherwise.

To derive the aerodynamic forces included in the distributed forces $\mathbf{f}_i$ $(i = f, \omega, e)$ acting on the aircraft by means of strip theory, we regard the fuselage, wing and empennage as two-dimensional aerodynamic surfaces. The lift force per unit span of fuselage can be written as[38]

$$\ell_f = q_f c_f C_{L\alpha f} \alpha_f = q_f c_f C_{Lf} \tag{29}$$

where c_f is the chord, $C_{L\alpha f}$ the slope of the lift curve, C_{Lf} the lift coefficient and

$$q_f = \tfrac{1}{2}\rho(\bar{V}_{fx}^2 + \bar{V}_{fz}^2),\ \alpha_f = \tan^{-1}(\bar{V}_{fz}/\bar{V}_{fx}) \tag{30}$$

are the dynamic pressure and angle of attack, respectively, in which ρ is the air density and $\bar{V}_{fx}$ and $\bar{V}_{fz}$ are components of the velocity vector $\bar{\mathbf{V}}_f$, Eq. (5). Similarly, the drag force per unit span of fuselage is given by

$$d_f = q_f c_f C_{Df} = q_f c_f (C_{Df0} + k_f C_{Lf}^2) = q_f c_f (C_{Df0} + k_f C_{L\alpha f}^2 \alpha_f^2) \tag{31}$$

where C_{Df0} is the drag coefficient corresponding to $\alpha_f = 0$ and k_f is a constant. The fuselage has also vertical surfaces subjected to aerodynamic forces. The lateral force per unit span can be expressed as

$$s_f = q_{sf} c_{sf} C_{s\beta f} \beta_f = q_{sf} c_{sf} C_{sf} \tag{32}$$

where c_{sf} is the lateral chord, $C_{s\beta f}$ the slope of the lateral force curve, C_{sf} the lateral force coefficient and

$$q_{sf} = \tfrac{1}{2}\rho(\bar{V}_{fx}^2 + \bar{V}_{fy}^2),\ \beta_f = \tan^{-1}(\bar{V}_{fy}/\bar{V}_{fx}) \tag{33}$$

are the dynamic pressure and the angle of attack of the lateral force, respectively, in which $\bar{V}_{fx}$ and $\bar{V}_{fy}$ are components of $\bar{\mathbf{V}}_f$. Hence, the aerodynamic forces on the fuselage can be written in the vector form

$$\mathbf{f}_{af} = \begin{bmatrix} \ell_f \sin\alpha_f - d_f \cos\alpha_f \\ 0 \\ -\ell_f \cos\alpha_f - d_f \sin\alpha_f \end{bmatrix}, \ \mathbf{f}_{sf} = \begin{bmatrix} s_f \sin\beta_f \\ -s_f \cos\beta_f \\ 0 \end{bmatrix} \tag{34}$$

In a similar fashion, the lift and drag per unit span of wing are given by

$$\ell_w = q_w c_w (C_{L\alpha w}\alpha_w + C_{L\delta a}\delta_a),\ d_w = q_w c_w (C_{Dw0} + k_w C_{Lw}^2) = q_w c_w (C_{Dw0} + k_w C_{L\alpha w}^2 \alpha_w^2) \tag{35}$$

where c_w is the chord, δ_a an aileron rotation, $C_{L\delta a}$ a control effectiveness coefficient[17] and

$$q_w = \tfrac{1}{2}\rho(\bar{V}_{wy}^2 + \bar{V}_{wz}^2),\ \alpha_w = \tan^{-1}(\bar{V}_{wz}/\bar{V}_{wy}) + \psi_{wx} \tag{36}$$

in which the velocity components $\bar{V}_{wy}$ and $\bar{V}_{wz}$ of $\bar{\mathbf{V}}_w$ can be obtained from Eq. (6). Moreover, ψ_{wx} is the angular displacement of the wing about axis x_w due to torsion. There is no meaningful lateral force on the wing, so that

$$\mathbf{f}_{aw} = \begin{bmatrix} 0 \\ \ell_w \sin\alpha_w - d_w \cos\alpha_w \\ -\ell_w \cos\alpha_w - d_w \sin\alpha_w \end{bmatrix} \tag{37}$$

The empennage has both lift and lateral surfaces. The lift, drag and lateral forces per unit span of empennage are

$$\ell_e = q_e c_e (C_{L\alpha e}\alpha_e + C_{L\delta e}\delta_e),\ d_e = q_e c_e (C_{De0} + k_e C_{L\alpha e}^2 \alpha_e^2),\ s_e = q_{se} c_{se} (C_{s\beta e}\beta_e + C_{s\delta r}\delta_r) \tag{38}$$

where c_e and c_{se} are the chords, δ_e and δ_r are rotations of the elevator and ruder, $C_{L\delta e}$ and $C_{s\delta r}$ are respective control effectiveness coefficients and

$$\begin{aligned} q_e &= \tfrac{1}{2}\rho(\bar{V}_{ey}^2 + \bar{V}_{ez}^2),\ \alpha_e = \tan^{-1}(\bar{V}_{ez}/\bar{V}_{ey}) + \psi_{ex} \\ q_{se} &= \tfrac{1}{2}\rho(\bar{V}_{ey}^2 + \bar{V}_{ez}^2),\ \beta_e = \tan^{-1}(\bar{V}_{ez}/\bar{V}_{ey}) + \psi_{ex} \end{aligned} \tag{39}$$

Hence, the aerodynamic force vectors per unit span of empennage can be written as

$$\mathbf{f}_{ae} = \begin{bmatrix} 0 \\ \ell_e \sin\alpha_e - d_e \cos\alpha_e \\ -\ell_e \cos\alpha_e - d_e \sin\alpha_e \end{bmatrix}, \ \mathbf{f}_{se} = \begin{bmatrix} 0 \\ s_e \sin\beta_e \\ -s_e \cos\beta_e \end{bmatrix} \tag{40}$$

For a typical component, the lift, lateral force and drag per unit span are applied at the line of aerodynamic centers. Hence, in Eqs. (28), the domain of integration for the terms involving the aerodynamic forces is the line of aerodynamic centers. The gravity forces per unit volume of components are simply

$$\mathbf{f}_{gf} = C_f \begin{bmatrix} 0 \\ 0 \\ \rho_f g \end{bmatrix}, \ \mathbf{f}_{gw} = C_w C_f \begin{bmatrix} 0 \\ 0 \\ \rho_w g \end{bmatrix}, \ \mathbf{f}_{ge} = C_e C_f \begin{bmatrix} 0 \\ 0 \\ \rho_e g \end{bmatrix} \tag{41}$$

Note that the aerodynamic and gravity forces are in terms of respective component body axes.

5. A Unified Theory for Flight Dynamics and Aeroelasticity

To complete the discussion of the forces acting on an aircraft, we turn our attention to the control forces. Aircraft control is carried out by means of control surfaces, as well as by the engine thrust. Before we consider the problem of control design, it will prove beneficial to examine the nature of the controls. Controls are of two general types, one designed to steer the aircraft as a whole and the other to suppress the effects of any undesirable disturbances. The first type involves rigid body motions of the aircraft, which are in general large, and traditionally lies in the domain of flight dynamics. On the other hand, the second type involves elastic deformations of the aircraft, which tend to be small compared to the rigid body motions, and traditionally lies in the domain of aeroelasticity. Hence, the formulation given by Eqs. (22) can be regarded as spanning the fields of flight dynamics and aeroelasticity.

From the above discussion, it appears that control of the aircraft as a whole is likely to be different in nature from control of disturbances. In this regard, we observe that the state equations, Eqs. (22), are in general nonlinear and of high dimension, where the nonlinearity can be traced to the large rigid body variables. On the other hand, the high dimensionality can be traced to the small elastic variables. In view of this, a solution by a perturbation approach seems indicated, which amounts to a separation of the problem into a *zero-order problem* for the large variables and a *first-order problem* for the small variables, where the difference between the large and small variables is one order of magnitude, or more. Physically, in the zero-order problem the aircraft executes a given maneuver as if it were rigid, in which case the mathematical formulation consists of a maximum of six coupled, generally nonlinear ordinary differential equations, three for rigid body translations and three for rigid body rotations. They correspond to the equations commonly used in *flight dynamics*. On the other hand, the first-order problem involves the elastic deformations, as well as small perturbations in the rigid body variables. In view of the inclusion of the latter, the first-order problem defined here represents an *extended aeroelasticity theory*, in which the rigid body degrees of freedom are included in a natural manner. This is in contrast with some occasional practice,[11,39] in which "body freedoms" are included in an ad hoc manner. We note that the solution of the zero-order problem enters into the first-order problem, so that *this new theory provides one set of extended aeroelasticity equations for every conceivable rigid body maneuver of the aircraft*, rather than the single set of equations commonly associated with steady cruise. We express the perturbation solution as follows:

$$\begin{gathered}\mathbf{R}_f = \mathbf{R}_f^{(0)} + \mathbf{R}_f^{(1)},\ \boldsymbol{\theta}_f = \boldsymbol{\theta}_f^{(0)} + \boldsymbol{\theta}_f^{(1)},\ \mathbf{V}_f = \mathbf{V}_f^{(0)} + \mathbf{V}_f^{(1)},\ \boldsymbol{\omega}_f = \boldsymbol{\omega}_f^{(0)} + \boldsymbol{\omega}_f^{(1)} \\ \mathbf{p}_{Vf} = \mathbf{p}_{Vf}^{(0)} + \mathbf{p}_{Vf}^{(1)},\ \mathbf{p}_{\omega f} = \mathbf{p}_{\omega f}^{(0)} + \mathbf{p}_{\omega f}^{(1)},\ \mathbf{F} = \mathbf{F}^{(0)} + \mathbf{F}^{(1)},\ \mathbf{M} = \mathbf{M}^{(0)} + \mathbf{M}^{(1)}\end{gathered} \tag{42}$$

where the superscripts (0) and (1) denote orders of magnitude. All the quantities related to the elastic deformations are regarded as being of first order. Then, inserting Eqs. (42) into the state equations, Eqs. (22), and separating different orders of magnitude, we obtain the zero-order problem, or the *flight dynamics problem*

$$\begin{gathered}\dot{\mathbf{R}}_f^{(0)} = C_f^{(0)T}\mathbf{V}_f^{(0)},\ \dot{\boldsymbol{\theta}}_f^{(0)} = (E_f^{(0)})^{-1}\boldsymbol{\omega}_f^{(0)} \\ \dot{\mathbf{p}}_{Vf}^{(0)} = -\tilde{\omega}_f^{(0)}\mathbf{p}_{Vf}^{(0)} + \mathbf{F}^{(0)},\ \dot{\mathbf{p}}_{\omega f}^{(0)} = -\tilde{V}_f^{(0)}\mathbf{p}_{Vf}^{(0)} - \tilde{\omega}_f^{(0)}\mathbf{p}_{\omega f}^{(0)} + \mathbf{M}^{(0)}\end{gathered} \tag{43}$$

in which $C_f^{(0)}$ and $E_f^{(0)}$ can be obtained from C_f and E_f, Eqs. (2), by replacing ψ, θ and ϕ by $\psi^{(0)}$, $\theta^{(0)}$ and $\phi^{(0)}$, respectively. Moreover, from Eqs. (28), the zero-order generalized force and moment are given by

$$
\begin{aligned}
\mathbf{F}^{(0)} &= \int_{D_f}[\mathbf{f}_f^{(0)} + \mathbf{F}_E^{(0)}\delta(\mathbf{r}-\mathbf{r}_E)]dD_f + C_w^T\int_{D_w}\mathbf{f}_w^{(0)}dD_w + C_e^T\int_{D_e}\mathbf{f}_e^{(0)}dD_e \\
\mathbf{M}^{(0)} &= \int_{D_f}\tilde{r}_f[\mathbf{f}_f^{(0)} + \mathbf{F}_E^{(0)}\delta(\mathbf{r}-\mathbf{r}_E)]dD_f + \int_{D_w}(\tilde{r}_{fw}C_w^T + C_w^T\tilde{r}_w)\mathbf{f}_w^{(0)}dD_w \\
&\quad + \int_{D_e}(\tilde{r}_{fe}C_e^T + C_e^T\tilde{r}_e)\mathbf{f}_e^{(0)}dD_e
\end{aligned}
\tag{44}
$$

where the zero-order parts of the aerodynamic force densities contributing to $\mathbf{f}_f^{(0)}$, $\mathbf{f}_w^{(0)}$ and $\mathbf{f}_e^{(0)}$ are

$$
\begin{aligned}
\mathbf{f}_{af}^{(0)} &= \begin{bmatrix} \ell_f^{(0)}\sin\alpha_f^{(0)} - d_f^{(0)}\cos\alpha_f^{(0)} \\ 0 \\ -\ell_f^{(0)}\cos\alpha_f^{(0)} - d_f^{(0)}\sin\alpha_f^{(0)} \end{bmatrix}, \ \mathbf{f}_{sf}^{(0)} = \begin{bmatrix} s_f^{(0)}\sin\beta_f^{(0)} \\ -s_f^{(0)}\cos\beta_f^{(0)} \\ 0 \end{bmatrix} \\
\mathbf{f}_{ai}^{(0)} &= \begin{bmatrix} 0 \\ \ell_i^{(0)}\sin\alpha_i^{(0)} - d_i^{(0)}\cos\alpha_i^{(0)} \\ -\ell_i^{(0)}\cos\alpha_i^{(0)} - d_i^{(0)}\sin\alpha_i^{(0)} \end{bmatrix}, \ i = w, e; \ \mathbf{f}_{se}^{(0)} = \begin{bmatrix} 0 \\ s_e^{(0)}\sin\beta_e^{(0)} \\ -s_e^{(0)}\cos\beta_e^{(0)} \end{bmatrix}
\end{aligned}
\tag{45}
$$

in which the zero-order parts of the lift, drag and lateral forces per unit area are

$$
\begin{aligned}
\ell_f^{(0)} &= q_f^{(0)}c_f C_{L\alpha f}\alpha_f^{(0)}, \ \ell_w^{(0)} = q_w^{(0)}c_w(C_{L\alpha w}\alpha_w^{(0)} + C_{L\delta a}\delta_a^{(0)}), \ \ell_e^{(0)} = q_e^{(0)}c_e(C_{L\alpha e}\alpha_e^{(0)} + C_{L\delta e}\delta_e^{(0)}) \\
s_f^{(0)} &= q_{sf}^{(0)}c_{sf}C_{s\beta f}\beta_f^{(0)}, \ s_e^{(0)} = q_{se}^{(0)}c_{se}(C_{s\beta e}\beta_e^{(0)} + C_{s\delta r}\delta_r^{(0)}) \\
d_i^{(0)} &= q_i^{(0)}c_i[C_{Di0} + k_i C_{L\alpha i}^2(\alpha_i^{(0)})^2], \ i = f, w, e
\end{aligned}
\tag{46}
$$

where

$$
\begin{aligned}
q_f^{(0)} &= \tfrac{1}{2}\rho[(\bar{V}_{fx}^{(0)})^2 + (\bar{V}_{fz}^{(0)})^2], \ \alpha_f^{(0)} = \tan^{-1}(\bar{V}_{fz}^{(0)}/\bar{V}_{fx}^{(0)}), \ \beta_f^{(0)} = \tan^{-1}(\bar{V}_{fy}^{(0)}/\bar{V}_{fx}^{(0)}) \\
q_i^{(0)} &= \tfrac{1}{2}\rho[(\bar{V}_{iy}^{(0)})^2 + (\bar{V}_{iz}^{(0)})^2], \ \alpha_i^{(0)} = \tan^{-1}(\bar{V}_{iz}^{(0)}/\bar{V}_{iy}^{(0)}), \ \beta_i^{(0)} = \tan^{-1}(\bar{V}_{iz}^{(0)}/\bar{V}_{iy}^{(0)}), \ i = w, e \\
q_{sf}^{(0)} &= \tfrac{1}{2}\rho[(\bar{V}_{fx}^{(0)})^2 + (\bar{V}_{fy}^{(0)})^2], \ q_{se}^{(0)} = \tfrac{1}{2}\rho[(\bar{V}_{ey}^{(0)})^2 + (\bar{V}_{ez}^{(0)})^2]
\end{aligned}
\tag{47}
$$

Moreover, the zero-order parts of the gravity force densities are

$$
\mathbf{f}_{gf}^{(0)} = C_f^{(0)}\left[0\ 0\ \rho_f g\right]^T; \ \mathbf{f}_{gi}^{(0)} = C_i C_f^{(0)}\left[0\ 0\ \rho_i g\right]^T, \ i = w, e \tag{48}
$$

The zero-order state is defined as $\mathbf{x}^{(0)} = [\mathbf{R}_f^{(0)T}\ \boldsymbol{\theta}_f^{(0)T}\ \mathbf{p}_{Vf}^{(0)T}\ \mathbf{p}_{\omega f}^{(0)T}]^T$, and Eqs. (43) contain in addition $\mathbf{V}_f^{(0)}$ and $\boldsymbol{\omega}_f^{(0)}$. However, $\mathbf{V}_f^{(0)}$ and $\boldsymbol{\omega}_f^{(0)}$ can be expresed in terms of $\mathbf{p}_{Vf}^{(0)}$ and $\mathbf{p}_{\omega f}^{(0)}$ by using Eqs. (21) and writing

$$
\mathbf{p}_{Vf}^{(0)} = m\mathbf{V}_f^{(0)} + \tilde{S}^{(0)T}\boldsymbol{\omega}_f^{(0)}, \ \mathbf{p}_{\omega f}^{(0)} = \tilde{S}^{(0)}\mathbf{V}_f^{(0)} + J^{(0)}\boldsymbol{\omega}_f^{(0)} \tag{49}
$$

The solution of Eqs. (43) in conjunction with Eqs. (44)-(49) consists of the state $\mathbf{x}^{(0)}$ and it represents a given maneuver of the aircraft.

Inserting Eqs. (42) into Eqs. (22) and retaining the first-order terms, we obtain the *extended aeroelasticity problem* defined by

$$
\begin{aligned}
&\dot{\mathbf{R}}_f^{(1)} = C_f^{(0)T}\mathbf{V}_f^{(1)} + C_f^{(1)T}\mathbf{V}_f^{(0)}, \ \dot{\boldsymbol{\theta}}_f^{(1)} = (E_f^{(0)})^{-1}\boldsymbol{\omega}_f^{(1)} - (E_f^{(0)})^{-1}E_f^{(1)}(E_f^{(0)})^{-1}\boldsymbol{\omega}_f^{(0)} \\
&\dot{\mathbf{q}}_{ui} = \mathbf{s}_{ui}, \ \dot{\mathbf{q}}_{\psi i} = \mathbf{s}_{\psi i}, \ i = f, w, e
\end{aligned}
$$

$$
\begin{aligned}
\dot{\mathbf{p}}_{Vf}^{(1)} &= -\tilde{\omega}_f^{(1)}\mathbf{p}_{Vf}^{(0)} - \tilde{\omega}_f^{(0)}\mathbf{p}_{Vf}^{(1)} + \mathbf{F}^{(1)} \\
\dot{\mathbf{p}}_{\omega f}^{(1)} &= -\tilde{V}_f^{(1)}\mathbf{p}_{Vf}^{(0)} - \tilde{V}_f^{(0)}\mathbf{p}_{Vf}^{(1)} - \tilde{\omega}_f^{(1)}\mathbf{p}_{\omega f}^{(0)} - \tilde{\omega}_f^{(0)}\mathbf{p}_{\omega f}^{(1)} + \mathbf{M}^{(1)} \\
\dot{\mathbf{p}}_{uf} &= \int\Phi_{uf}^T(\tilde{\omega}_f^{(0)T}\bar{\mathbf{V}}_f^{(1)} + \tilde{\omega}_f^{(1)T}\bar{\mathbf{V}}_f^{(0)})dm_f + \int\Phi_{ufw}^T(\tilde{\omega}_f^{(0)T}C_w^T\bar{\mathbf{V}}_w^{(1)} + \tilde{\omega}_f^{(1)T}C_w^T\bar{\mathbf{V}}_w^{(0)})dm_w \\
&\quad + \int\Phi_{ufe}^T(\tilde{\omega}_f^{(0)T}C_e^T\bar{\mathbf{V}}_e^{(1)} + \tilde{\omega}_f^{(1)T}C_e^T\bar{\mathbf{V}}_e^{(0)})dm_e - K_{uf}\mathbf{q}_{uf} - C_{uf}\mathbf{s}_{uf} + \mathbf{Q}_{uf} \\
&\quad + \int\Phi_{uf}^T\tilde{\omega}_f^{(0)T}\bar{\mathbf{V}}_f^{(0)}dm_f + \int\Phi_{ufw}^T\tilde{\omega}_f^{(0)T}C_w^T\bar{\mathbf{V}}_w^{(0)}dm_w + \int\Phi_{ufe}^T\tilde{\omega}_f^{(0)T}C_e^T\bar{\mathbf{V}}_e^{(0)}dm_e \\
\dot{\mathbf{p}}_{\psi f} &= -K_{\psi f}\mathbf{q}_{\psi f} - C_{\psi f}\mathbf{s}_{\psi f} + \mathbf{Q}_{\psi f} \\
\dot{\mathbf{p}}_{ui} &= \int\Phi_{ui}^T(\widetilde{C_i\boldsymbol{\omega}_f^{(0)}}^T\bar{\mathbf{V}}_i^{(1)} + \widetilde{C_i\boldsymbol{\omega}_f^{(1)}}^T\bar{\mathbf{V}}_i^{(0)})dm_i - K_{ui}\mathbf{q}_{ui} - C_{ui}\mathbf{s}_{ui} + \mathbf{Q}_{ui} \\
&\quad + \int\Phi_{ui}^T\widetilde{C_i\boldsymbol{\omega}_f^{(0)}}^T\bar{\mathbf{V}}_i^{(0)}dm_i,\ i=w,e \\
\dot{\mathbf{p}}_{\psi i} &= -K_{\psi i}\mathbf{q}_{\psi i} - C_{\psi i}\mathbf{s}_{\psi i} + \mathbf{Q}_{\psi i},\ i=w,e
\end{aligned} \tag{50}
$$

where

$$
C_f^{(1)} = C_{f\psi}^{(0)}\psi^{(1)} + C_{f\theta}^{(0)}\theta^{(1)} + C_{f\phi}^{(0)}\phi^{(1)},\ E_f^{(1)} = E_{f\theta}^{(0)}\theta^{(1)} + E_{f\phi}^{(0)}\phi^{(1)} \tag{51}
$$

in which

$$
\begin{aligned}
C_{f\psi}^{(0)} &= \left.\frac{\partial C_f}{\partial\psi}\right|_{\psi^{(0)},\theta^{(0)},\phi^{(0)}} \\
&= \begin{bmatrix} -\mathrm{s}\psi^{(0)}\mathrm{c}\theta^{(0)} & \mathrm{c}\psi^{(0)}\mathrm{c}\theta^{(0)} & 0 \\ -\mathrm{s}\psi^{(0)}\mathrm{s}\theta^{(0)}\mathrm{s}\phi^{(0)} - \mathrm{c}\psi^{(0)}\mathrm{c}\phi^{(0)} & \mathrm{c}\psi^{(0)}\mathrm{s}\theta^{(0)}\mathrm{s}\phi^{(0)} - \mathrm{s}\psi^{(0)}\mathrm{c}\phi^{(0)} & 0 \\ -\mathrm{s}\psi^{(0)}\mathrm{s}\theta^{(0)}\mathrm{c}\phi^{(0)} + \mathrm{c}\psi^{(0)}\mathrm{s}\phi^{(0)} & \mathrm{c}\psi^{(0)}\mathrm{s}\theta^{(0)}\mathrm{c}\phi^{(0)} + \mathrm{s}\psi^{(0)}\mathrm{s}\phi^{(0)} & 0 \end{bmatrix} \\
C_{f\theta}^{(0)} &= \left.\frac{\partial C_f}{\partial\theta}\right|_{\psi^{(0)},\theta^{(0)},\phi^{(0)}} \\
&= \begin{bmatrix} -\mathrm{c}\psi^{(0)}\mathrm{s}\theta^{(0)} & -\mathrm{s}\psi^{(0)}\mathrm{s}\theta^{(0)} & -\mathrm{c}\theta^{(0)} \\ \mathrm{c}\psi^{(0)}\mathrm{c}\theta^{(0)}\mathrm{s}\phi^{(0)} & \mathrm{s}\psi^{(0)}\mathrm{c}\theta^{(0)}\mathrm{s}\phi^{(0)} & -\mathrm{s}\theta^{(0)}\mathrm{s}\phi^{(0)} \\ \mathrm{c}\psi^{(0)}\mathrm{c}\theta^{(0)}\mathrm{c}\phi^{(0)} & \mathrm{s}\psi^{(0)}\mathrm{c}\theta^{(0)}\mathrm{c}\phi^{(0)} & -\mathrm{s}\theta^{(0)}\mathrm{c}\phi^{(0)} \end{bmatrix} \\
C_{f\phi}^{(0)} &= \left.\frac{\partial C_f}{\partial\phi}\right|_{\psi^{(0)},\theta^{(0)},\phi^{(0)}} \\
&= \begin{bmatrix} 0 & 0 & 0 \\ \mathrm{c}\psi^{(0)}\mathrm{s}\theta^{(0)}\mathrm{c}\phi^{(0)} + \mathrm{s}\psi^{(0)}\mathrm{s}\phi^{(0)} & \mathrm{s}\psi^{(0)}\mathrm{s}\theta^{(0)}\mathrm{c}\phi^{(0)} - \mathrm{c}\psi^{(0)}\mathrm{s}\phi^{(0)} & \mathrm{c}\theta^{(0)}\mathrm{c}\phi^{(0)} \\ -\mathrm{c}\psi^{(0)}\mathrm{s}\theta^{(0)}\mathrm{s}\phi^{(0)} + \mathrm{s}\psi^{(0)}\mathrm{c}\phi^{(0)} & -\mathrm{s}\psi^{(0)}\mathrm{s}\theta^{(0)}\mathrm{s}\phi^{(0)} - \mathrm{c}\psi^{(0)}\mathrm{c}\phi^{(0)} & -\mathrm{c}\theta^{(0)}\mathrm{s}\phi^{(0)} \end{bmatrix}
\end{aligned} \tag{52}
$$

$$
E_{f\theta}^{(0)} = \left.\frac{\partial E_f}{\partial\theta}\right|_{\theta^{(0)},\phi^{(0)}} = \begin{bmatrix} 0 & 0 & -\mathrm{c}\theta^{(0)} \\ 0 & 0 & -\mathrm{s}\theta^{(0)}\mathrm{s}\phi^{(0)} \\ 0 & 0 & -\mathrm{s}\theta^{(0)}\mathrm{c}\phi^{(0)} \end{bmatrix}
$$

$$
E_{f\phi}^{(0)} = \left.\frac{\partial E_f}{\partial\phi}\right|_{\theta^{(0)},\phi^{(0)}} = \begin{bmatrix} 0 & 0 & 0 \\ 0 & -\mathrm{s}\phi^{(0)} & \mathrm{c}\theta^{(0)}\mathrm{c}\phi^{(0)} \\ 0 & -\mathrm{c}\phi^{(0)} & -\mathrm{c}\theta^{(0)}\mathrm{s}\phi^{(0)} \end{bmatrix}
$$

and

$$
\begin{aligned}
\bar{\mathbf{V}}_f^{(0)} &= \mathbf{V}_f^{(0)} + \tilde{r}_f^T \boldsymbol{\omega}_f^{(0)}, \ \bar{\mathbf{V}}_f^{(1)} = \mathbf{V}_f^{(1)} + \tilde{r}_f^T \boldsymbol{\omega}_f^{(1)} + \widetilde{\Phi_{uf}\mathbf{q}_{uf}}^T \boldsymbol{\omega}_f^{(0)} + \Phi_{uf}\mathbf{s}_{uf} + \tilde{r}_f^T \Phi_{\psi f}\mathbf{s}_{\psi f} \\
\bar{\mathbf{V}}_w^{(0)} &= C_w \mathbf{V}_f^{(0)} + (C_w \tilde{r}_{fw}^T + \tilde{r}_w^T C_w)\boldsymbol{\omega}_f^{(0)} \\
\bar{\mathbf{V}}_w^{(1)} &= C_w \mathbf{V}_f^{(1)} + (C_w \tilde{r}_{fw}^T + \tilde{r}_w^T C_w)\boldsymbol{\omega}_f^{(1)} + (C_w \widetilde{\Phi_{ufw}\mathbf{q}_{uf}}^T + \widetilde{\Phi_{uw}\mathbf{q}_{uw}}^T C_w)\boldsymbol{\omega}_f^{(0)} \\
&\quad + (\tilde{r}_w^T C_w \Delta\Phi_{ufw} + C_w \Phi_{ufw})\mathbf{s}_{uf} + \Phi_{uw}\mathbf{s}_{uw} \\
&\quad + (\tilde{r}_w^T C_w \Phi_{\psi fw} + C_w \tilde{r}_{fw}^T \Phi_{\psi fw})\mathbf{s}_{\psi f} + \tilde{r}_w^T \Phi_{\psi w}\mathbf{s}_{\psi w}
\end{aligned} \tag{53}
$$

Then, from Eqs. (28), the first-order generalized forces are

$$
\begin{aligned}
\mathbf{F}^{(1)} &= \textstyle\int_{D_f} [\mathbf{f}_f^{(1)} + \mathbf{F}_E^{(1)}\delta(\mathbf{r}-\mathbf{r}_E)]dD_f + C_w^T \int_{D_w} \mathbf{f}_w^{(1)} dD_w + C_e^T \int_{D_e} \mathbf{f}_e^{(1)} dD_e \\
\mathbf{M}^{(1)} &= \textstyle\int_{D_f} \{\tilde{r}_f[\mathbf{f}_f^{(1)} + \mathbf{F}_E^{(1)}\delta(\mathbf{r}-\mathbf{r}_E)] + \widetilde{\Phi_{uf}\mathbf{q}_{uf}}[\mathbf{f}_f^{(0)} + \mathbf{F}_E^{(0)}\delta(\mathbf{r}-\mathbf{r}_E)]\}dD_f + \int_{D_w}[(\tilde{r}_{fw}C_w^T \\
&\quad + C_w^T \tilde{r}_w)\mathbf{f}_w^{(1)} + (\widetilde{\Phi_{ufw}\mathbf{q}_{uf}} C_w^T + C_w^T \widetilde{\Phi_{uw}\mathbf{q}_{uw}})\mathbf{f}_w^{(0)}]dD_w + \textstyle\int_{D_e}[(\tilde{r}_{fe}C_e^T + C_e^T \tilde{r}_e)\mathbf{f}_e^{(1)} \\
&\quad + (\widetilde{\Phi_{ufe}\mathbf{q}_{uf}} C_e^T + C_e^T \widetilde{\Phi_{ue}\mathbf{q}_{ue}})\mathbf{f}_e^{(0)}]dD_e
\end{aligned}
$$

$$
\begin{aligned}
\mathbf{Q}_{uf} &= \textstyle\int_{D_f} \Phi_{uf}^T [\mathbf{f}_f^{(0)} + \mathbf{f}_f^{(1)} + \mathbf{F}_E^{(0)}\delta(\mathbf{r}-\mathbf{r}_E) + \mathbf{F}_E^{(1)}\delta(\mathbf{r}-\mathbf{r}_E)]dD_f + \int_{D_w}(\tilde{r}_w^T C_w \Delta\Phi_{ufw} \\
&\quad + C_w \Phi_{ufw})^T (\mathbf{f}_w^{(0)} + \mathbf{f}_w^{(1)})dD_w + \textstyle\int_{D_e}(\tilde{r}_e^T C_e \Delta\Phi_{ufe} + C_e \Phi_{ufe})^T (\mathbf{f}_e^{(0)} + \mathbf{f}_e^{(1)})dD_e \\
\mathbf{Q}_{\psi f} &= \textstyle\int_{D_f} \Phi_{\psi f}^T \tilde{r}_f [\mathbf{f}_f^{(0)} + \mathbf{f}_f^{(1)} + \mathbf{F}_E^{(0)}\delta(\mathbf{r}-\mathbf{r}_E) + \mathbf{F}_E^{(1)}\delta(\mathbf{r}-\mathbf{r}_E)]dD_f + \int_{D_w}(\tilde{r}_w^T C_w \Phi_{\psi fw} \\
&\quad + C_w \tilde{r}_{fw}^T \Phi_{\psi fw})^T (\mathbf{f}_w^{(0)} + \mathbf{f}_w^{(1)})dD_w + \textstyle\int_{D_e}(\tilde{r}_e^T C_e \Phi_{\psi fe} + C_e \tilde{r}_{fe}^T \Phi_{\psi fe})^T (\mathbf{f}_e^{(0)} + \mathbf{f}_e^{(1)})dD_e \\
\mathbf{Q}_{ui} &= \textstyle\int_{D_i} \Phi_{ui}^T (\mathbf{f}_i^{(0)} + \mathbf{f}_i^{(1)})dD_i, \ \mathbf{Q}_{\psi i} = \int_{D_i} \Phi_{\psi i}^T \tilde{r}_i (\mathbf{f}_i^{(0)} + \mathbf{f}_i^{(1)})dD_i, \ i = w, e
\end{aligned} \tag{54}
$$

where the first-order parts of the aerodynamic force densities contributing to $\mathbf{f}_f^{(1)}$, $\mathbf{f}_w^{(1)}$ and $\mathbf{f}_e^{(1)}$ are

$$
\begin{aligned}
\mathbf{f}_{af}^{(1)} &= \begin{bmatrix} \ell_f^{(1)} \sin\alpha_f^{(0)} - d_f^{(1)} \cos\alpha_f^{(0)} + (\ell_f^{(0)} \cos\alpha_f^{(0)} + d_f^{(0)} \sin\alpha_f^{(0)})\alpha_f^{(1)} \\ 0 \\ -\ell_f^{(1)} \cos\alpha_f^{(0)} - d_f^{(1)} \sin\alpha_f^{(0)} + (\ell_f^{(0)} \sin\alpha_f^{(0)} - d_f^{(0)} \cos\alpha_f^{(0)})\alpha_f^{(1)} \end{bmatrix} \\
\mathbf{f}_{sf}^{(1)} &= \begin{bmatrix} s_f^{(1)} \sin\beta_f^{(0)} + s_f^{(0)}\beta_f^{(1)} \cos\beta_f^{(0)} \\ -s_f^{(1)} \cos\beta_f^{(0)} + s_f^{(0)}\beta_f^{(1)} \sin\beta_f^{(0)} \\ 0 \end{bmatrix} \\
\mathbf{f}_{ai}^{(1)} &= \begin{bmatrix} 0 \\ \ell_i^{(1)} \sin\alpha_i^{(0)} - d_i^{(1)} \cos\alpha_i^{(0)} + (\ell_i^{(0)} \cos\alpha_i^{(0)} + d_i^{(0)} \sin\alpha_i^{(0)})\alpha_i^{(1)} \\ -\ell_i^{(1)} \cos\alpha_i^{(0)} - d_i^{(1)} \sin\alpha_i^{(0)} + (\ell_i^{(0)} \sin\alpha_i^{(0)} - d_i^{(0)} \cos\alpha_i^{(0)})\alpha_i^{(1)} \end{bmatrix}, \quad i = w, e \\
\mathbf{f}_{se}^{(1)} &= \begin{bmatrix} 0 \\ s_e^{(1)} \sin\beta_e^{(0)} + s_e^{(0)}\beta_e^{(1)} \cos\beta_e^{(0)} \\ -s_e^{(1)} \cos\beta_e^{(0)} + s_e^{(0)}\beta_e^{(1)} \sin\beta_e^{(0)} \end{bmatrix}
\end{aligned} \tag{55}
$$

in which the first-order parts of the lift, drag and lateral forces per unit area are

$$
\begin{aligned}
\ell_f^{(1)} &= c_f C_{L\alpha f}(q_f^{(1)}\alpha_f^{(0)} + q_f^{(0)}\alpha_f^{(1)}) \\
\ell_w^{(1)} &= q_w^{(1)} c_w (C_{L\alpha w}\alpha_w^{(0)} + C_{L\delta a}\delta_a^{(0)}) + q_w^{(0)} c_w (C_{L\alpha w}\alpha_w^{(1)} + C_{L\delta a}\delta_a^{(1)}) \\
\ell_e^{(1)} &= q_e^{(1)} c_e (C_{L\alpha e}\alpha_e^{(0)} + C_{L\delta e}\delta_e^{(0)}) + q_e^{(0)} c_e (C_{L\alpha e}\alpha_e^{(1)} + C_{L\delta e}\delta_e^{(1)}) \\
s_f^{(1)} &= c_{sf} C_{s\beta f}(q_{sf}^{(1)}\beta_f^{(0)} + q_{sf}^{(0)}\beta_f^{(1)}) \\
s_e^{(1)} &= q_{se}^{(1)} c_{se} (C_{s\beta e}\beta_e^{(0)} + C_{s\delta r}\delta_r^{(0)}) + q_{se}^{(0)} c_{se} (C_{s\beta e}\beta_e^{(1)} + C_{s\delta r}\delta_r^{(1)}) \\
d_i^{(1)} &= q_i^{(1)} c_i [C_{Di0} + k_i C_{L\alpha i}^2 (\alpha_i^{(0)})^2] + 2 q_i^{(0)} c_i k_i C_{L\alpha i}^2 \alpha_i^{(0)} \alpha_i^{(1)}, \ i = f, w, e
\end{aligned} \tag{56}
$$

where

$$
\begin{aligned}
q_f^{(1)} &= \rho(\bar{V}_{fx}^{(0)}\bar{V}_{fx}^{(1)} + \bar{V}_{fz}^{(0)}\bar{V}_{fz}^{(1)}), \ \alpha_f^{(1)} = \tan^{-1}\left(\frac{\bar{V}_{fx}^{(0)}\bar{V}_{fz}^{(1)} - \bar{V}_{fx}^{(1)}\bar{V}_{fz}^{(0)}}{(\bar{V}_{fx}^{(0)})^2 + (\bar{V}_{fz}^{(0)})^2}\right) \\
q_{sf}^{(1)} &= \rho(\bar{V}_{fx}^{(0)}\bar{V}_{fx}^{(1)} + \bar{V}_{fy}^{(0)}\bar{V}_{fy}^{(1)}), \ \beta_f^{(1)} = \tan^{-1}\left(\frac{\bar{V}_{fx}^{(0)}\bar{V}_{fy}^{(1)} - \bar{V}_{fx}^{(1)}\bar{V}_{fy}^{(0)}}{(\bar{V}_{fx}^{(0)})^2 + (\bar{V}_{fy}^{(0)})^2}\right) \\
q_i^{(1)} &= \rho(\bar{V}_{iy}^{(0)}\bar{V}_{iy}^{(1)} + \bar{V}_{iz}^{(0)}\bar{V}_{iz}^{(1)}), \ \alpha_i^{(1)} = \tan^{-1}\left(\frac{\bar{V}_{iy}^{(0)}\bar{V}_{iz}^{(1)} - \bar{V}_{iy}^{(1)}\bar{V}_{iz}^{(0)}}{(\bar{V}_{iy}^{(0)})^2 + (\bar{V}_{iz}^{(0)})^2}\right) + \psi_{ix}, \ i = w, e \\
q_{se}^{(1)} &= \rho(\bar{V}_{ey}^{(0)}\bar{V}_{ey}^{(1)} + \bar{V}_{ez}^{(0)}\bar{V}_{ez}^{(1)}), \ \beta_e^{(1)} = \tan^{-1}\left(\frac{\bar{V}_{ey}^{(0)}\bar{V}_{ez}^{(1)} - \bar{V}_{ey}^{(1)}\bar{V}_{ez}^{(0)}}{(\bar{V}_{ey}^{(0)})^2 + (\bar{V}_{ez}^{(0)})^2}\right) + \psi_{ex}
\end{aligned} \tag{57}
$$

Moreover, the first-order parts of the gravity force densities are

$$
\mathbf{f}_{gf}^{(1)} = C_f^{(1)}\left[0\ 0\ \rho_f g\right]^T; \ \mathbf{f}_{gi}^{(1)} = C_i C_f^{(1)}\left[0\ 0\ \rho_i g\right]^T, \ i = w, e \tag{58}
$$

Equations (50)-(58) must be solved for the state $\mathbf{x}^{(1)} = [\mathbf{R}_f^{(1)T}\boldsymbol{\theta}_f^{(1)T}\mathbf{q}_{uf}^T\ \mathbf{q}_{uw}^T \cdots \mathbf{q}_{\psi e}^T\ \ \mathbf{p}_{Vf}^{(1)T}\mathbf{p}_{\omega f}^{(1)T}$ $\mathbf{p}_{uf}^T\ \mathbf{p}_{uw}^T \cdots \mathbf{p}_{\psi e}^T]^T$ in conjunction with

$$
\begin{aligned}
\mathbf{p}_{Vf}^{(1)} &= m\mathbf{V}_f^{(1)} + \tilde{S}^{(1)T}\boldsymbol{\omega}_f^{(0)} + \tilde{S}^{(0)T}\boldsymbol{\omega}_f^{(1)} + M_{13}^{(0)}\mathbf{s}_{uf} + M_{14}^{(0)}\mathbf{s}_{uw} + M_{15}^{(0)}\mathbf{s}_{ue} + M_{16}^{(0)}\mathbf{s}_{\psi f} \\
&\quad + M_{17}^{(0)}\mathbf{s}_{\psi w} + M_{18}^{(0)}\mathbf{s}_{\psi e} \\
\mathbf{p}_{\omega f}^{(1)} &= \tilde{S}^{(1)}\mathbf{V}_f^{(0)} + \tilde{S}^{(0)}\mathbf{V}_f^{(1)} + J^{(1)}\boldsymbol{\omega}_f^{(0)} + J^{(0)}\boldsymbol{\omega}_f^{(1)} + M_{23}^{(0)}\mathbf{s}_{uf} + M_{24}^{(0)}\mathbf{s}_{uw} + M_{25}^{(0)}\mathbf{s}_{ue} \\
&\quad + M_{26}^{(0)}\mathbf{s}_{\psi f} + M_{27}^{(0)}\mathbf{s}_{\psi w} + M_{28}^{(0)}\mathbf{s}_{\psi e} \\
\mathbf{p}_{uf} &= M_{31}^{(0)}\mathbf{V}_f^{(1)} + M_{31}^{(1)}\mathbf{V}_f^{(0)} + M_{32}^{(0)}\boldsymbol{\omega}_f^{(1)} + M_{32}^{(1)}\boldsymbol{\omega}_f^{(0)} + M_{33}^{(0)}\mathbf{s}_{uf} + M_{34}^{(0)}\mathbf{s}_{uw} + M_{35}^{(0)}\mathbf{s}_{ue} \\
&\quad + M_{36}^{(0)}\mathbf{s}_{\psi f} + M_{37}^{(0)}\mathbf{s}_{\psi w} + M_{38}^{(0)}\mathbf{s}_{\psi e} \\
\mathbf{p}_{uw} &= M_{41}^{(0)}\mathbf{V}_f^{(1)} + M_{41}^{(1)}\mathbf{V}_f^{(0)} + M_{42}^{(0)}\boldsymbol{\omega}_f^{(1)} + M_{42}^{(1)}\boldsymbol{\omega}_f^{(0)} + M_{43}^{(0)}\mathbf{s}_{uf} + M_{44}^{(0)}\mathbf{s}_{uw} + M_{45}^{(0)}\mathbf{s}_{ue} \\
&\quad + M_{46}^{(0)}\mathbf{s}_{\psi f} + M_{47}^{(0)}\mathbf{s}_{\psi w} + M_{48}^{(0)}\mathbf{s}_{\psi e} \\
\mathbf{p}_{ue} &= M_{51}^{(0)}\mathbf{V}_f^{(1)} + M_{51}^{(1)}\mathbf{V}_f^{(0)} + M_{52}^{(0)}\boldsymbol{\omega}_f^{(1)} + M_{52}^{(1)}\boldsymbol{\omega}_f^{(0)} + M_{53}^{(0)}\mathbf{s}_{uf} + M_{54}^{(0)}\mathbf{s}_{uw} + M_{55}^{(0)}\mathbf{s}_{ue} \\
&\quad + M_{56}^{(0)}\mathbf{s}_{\psi f} + M_{57}^{(0)}\mathbf{s}_{\psi w} + M_{58}^{(0)}\mathbf{s}_{\psi e}
\end{aligned} \tag{59}
$$

$$
\begin{aligned}
\mathbf{p}_{\psi f} &= M_{61}^{(0)}\mathbf{V}_f^{(1)} + M_{61}^{(1)}\mathbf{V}_f^{(0)} + M_{62}^{(0)}\boldsymbol{\omega}_f^{(1)} + M_{62}^{(1)}\boldsymbol{\omega}_f^{(0)} + M_{63}^{(0)}\mathbf{s}_{uf} + M_{64}^{(0)}\mathbf{s}_{uw} + M_{65}^{(0)}\mathbf{s}_{ue} \\
&\quad + M_{66}^{(0)}\mathbf{s}_{\psi f} + M_{67}^{(0)}\mathbf{s}_{\psi w} + M_{68}^{(0)}\mathbf{s}_{\psi e} \\
\mathbf{p}_{\psi w} &= M_{71}^{(0)}\mathbf{V}_f^{(1)} + M_{71}^{(1)}\mathbf{V}_f^{(0)} + M_{72}^{(0)}\boldsymbol{\omega}_f^{(1)} + M_{72}^{(1)}\boldsymbol{\omega}_f^{(0)} + M_{73}^{(0)}\mathbf{s}_{uf} + M_{74}^{(0)}\mathbf{s}_{uw} + M_{75}^{(0)}\mathbf{s}_{ue} \\
&\quad + M_{76}^{(0)}\mathbf{s}_{\psi f} + M_{77}^{(0)}\mathbf{s}_{\psi w} + M_{78}^{(0)}\mathbf{s}_{\psi e} \\
\mathbf{p}_{\psi e} &= M_{81}^{(0)}\mathbf{V}_f^{(1)} + M_{81}^{(1)}\mathbf{V}_f^{(0)} + M_{82}^{(0)}\boldsymbol{\omega}_f^{(1)} + M_{82}^{(1)}\boldsymbol{\omega}_f^{(0)} + M_{83}^{(0)}\mathbf{s}_{uf} + M_{84}^{(0)}\mathbf{s}_{uw} + M_{85}^{(0)}\mathbf{s}_{ue} \\
&\quad + M_{86}^{(0)}\mathbf{s}_{\psi f} + M_{87}^{(0)}\mathbf{s}_{\psi w} + M_{88}^{(0)}\mathbf{s}_{\psi e}
\end{aligned}
$$

where $M_{ij}^{(0)}$ and $M_{ij}^{(1)}$ are the zero-order part and first-order part of M_{ij}, Eqs. (15). Equations (59) are to be solved for $\mathbf{V}_f^{(1)}$, $\boldsymbol{\omega}_f^{(1)}$, $\mathbf{s}_{uf}$, $\mathbf{s}_{uw}$, $\ldots$, $\mathbf{s}_{\psi e}$ in terms of $\mathbf{p}_{Vf}^{(1)}$, $\mathbf{p}_{\omega f}^{(1)}$, $\mathbf{p}_{uf}$, $\mathbf{p}_{uw}$, $\ldots$, $\mathbf{p}_{\psi e}$, $\mathbf{V}_f^{(0)}$ and $\boldsymbol{\omega}^{(0)}$ and the result inserted in Eqs. (50).

The zero-order problem, or flight dynamics problem, represents an inverse problem, which amounts to determining the controls permitting realization of a given rigid body maneuver. The first-order equations representing the extended aeroelasticity problem are linear and tend to be of high order. Moreover, they contain the zero-order variables $\mathbf{V}_f^{(0)}$ and $\boldsymbol{\omega}_f^{(0)}$, representing a given maneuver, as coefficients and as an input. If $\mathbf{V}_f^{(0)}$ and $\boldsymbol{\omega}_f^{(0)}$ are constant, then the system is time-invariant, and if $\mathbf{V}_f^{(0)}$ and $\boldsymbol{\omega}_f^{(0)}$ depend on time, then the system is time-varying. In either case, controls can be designed by various methods. In the time-invariant case, a stability analysis for the closed-loop system can be carried out by solving an eigenvalue problem. Such a stability analysis is precluded in the time-varying case. Simulation of the response of the closed-loop system to external excitations, such as gusts, can be obtained in both the time-invariant case and time-varying case.

6. Control Design

Flying aircraft are subjected to various disturbances tending to drive them from the intended maneuver and to cause vibration. If the system is controllable, these effects can be suppressed through controls, which are carried out by means of actuators; in the case of aircraft they consist of the engine thrust and the control surfaces. A system is said to be controllable if there exists a piecewise continuous input that will drive the initial state to any final state within a finite time interval. System controllability can be determined by checking the rank of a so-called controllability matrix,[40] which may not be feasible if the system order is large. In practice, controllability can be ascertained on physical grounds by making sure that the input forces, namely, the forces due to the engine thrust and control surfaces, affect all the state variables.

As indicated in earlier sections, there are two types of controls, one type designed to permit the aircraft to execute a desired maneuver as if it were rigid and the other type to reduce any deviations from the rigid body maneuver to zero, which amounts to suppressing vibration and perturbations in the rigid body motions of the aircraft. The first is associated with the flight dynamics problem and the second with the extended aeroelasticity problem. In general, the engine thrust and control surfaces are designed so as to ensure that the aircraft is able to carry out the required maneuvers, as well as to suppress any undesirable disturbances, thus addressing the needs of both the flight dynamics problem and extended aeroelasticity problem.

Using Eqs. (43), we write the flight dynamics problem, or the zero-order problem, in the compact state form

$$\dot{\mathbf{x}}^{(0)}(t) = \mathbf{f}[\mathbf{x}^{(0)}(t),\ \mathbf{V}_{rb}^{(0)}(t)] + B^{(0)}[\mathbf{V}_{rb}^{(0)}(t)]\mathbf{u}^{(0)}(t) \tag{60}$$

which, from Eqs. (49), must be considered in conjunction with

$$\mathbf{p}_{rb}^{(0)}(t) = M_{rb}^{(0)}\mathbf{V}_{rb}^{(0)}(t) \tag{61}$$

where the zero-order quantities are identified as follows: $\mathbf{x}^{(0)} = [\mathbf{R}_f^{(0)^T}\ \ \boldsymbol{\theta}_f^{(0)^T}\ \ \mathbf{p}_{Vf}^{(0)^T}\ \ \mathbf{p}_{\omega f}^{(0)^T}]^T$ is the state vector, $\mathbf{f}$ is a nonlinear function of the state vector and the zero-order rigid body velocity vector $\mathbf{V}_{rb}^{(0)} = [\mathbf{V}_f^{(0)^T}\ \ \boldsymbol{\omega}_f^{(0)^T}]^T$, $B^{(0)}$ is a coefficient matrix, $\mathbf{u}^{(0)} = [F_E^{(0)}\ \ \delta_a^{(0)}\ \ \delta_e^{(0)}\ \ \delta_r^{(0)}]^T$ is the control vector, in which $F_E^{(0)}$, $\delta_a^{(0)}$, $\delta_e^{(0)}$ and $\delta_r^{(0)}$ are the engine thrust and control surfaces angles, $\mathbf{p}_{rb}^{(0)} = [\mathbf{p}_{Vf}^{(0)^T}\ \ \mathbf{p}_{\omega f}^{(0)^T}]^T$ is the rigid body momentum vector and

$$M_{rb}^{(0)} = \begin{bmatrix} mI & \tilde{S}^{(0)T} \\ \tilde{S}^{(0)} & J^{(0)} \end{bmatrix} \tag{62}$$

is the rigid-body mass matrix. In the context of the present integrated approach, Eqs. (60) and (61) represent an inverse problem, in the sense that a state vector $\mathbf{x}^{(0)}$ describing a desired maneuver is postulated and a force vector $\mathbf{u}^{(0)}$ permitting a realization of the given maneuver is determined.

Next, we assume that $\mathbf{x}^{(0)}(t)$ and $\mathbf{V}_{rb}^{(0)}(t)$ are known and use Eqs. (50) and (59) to express the extended aeroelasticity problem, or first-order problem, in the form

$$\dot{\mathbf{x}}^{(1)}(t) = A(t)\mathbf{x}^{(1)}(t) + B(t)\mathbf{u}^{(1)}(t) + [0\ \ I]^T\mathbf{F}_{\text{ext}}(t) \tag{63}$$

and

$$\mathbf{p}^{(1)}(t) = M^{(0)}\mathbf{V}^{(1)}(t) + M^{(1)}(t)\mathbf{V}^{(0)}(t) \tag{64}$$

respectively, in which $\mathbf{x}^{(1)} = [\mathbf{R}_f^{(1)T} \;\; \boldsymbol{\theta}_f^{(1)T} \;\; \mathbf{q}_{uf}^T \;\; \mathbf{q}_{uw}^T \cdots \mathbf{q}_{\psi e}^T \;\; \mathbf{p}_{Vf}^{(1)T} \;\; \mathbf{p}_{\omega f}^{(1)T} \;\; \mathbf{p}_{uf}^T \;\; \mathbf{p}_{uw}^T \cdots \mathbf{p}_{\psi e}^T]^T$ is the first-order state vector, $A(t) = A[\mathbf{x}^{(0)}(t), \; \mathbf{V}_{rb}^{(0)}(t)]$ and $B(t) = B\;[\mathbf{x}^{(0)}(t), \mathbf{V}_{rb}^{(0)}(t)]$ are coefficient matrices, $\mathbf{u}^{(1)}(t) = [F_E^{(1)} \;\; \delta_a^{(1)} \;\; \delta_e^{(1)} \;\; \delta_r^{(1)}]^T$ is a first-order control vector, $\mathbf{F}_{\text{ext}}$ is an external disturbing force vector, such as due to gusts, $\mathbf{p}^{(1)} = [\mathbf{p}_{Vf}^{(1)T} \;\; \mathbf{p}_{\omega f}^{(1)T} \;\; \mathbf{p}_{uf}^T \;\; \mathbf{p}_{uw}^T \cdots \mathbf{p}_{\psi e}^T]^T$ is the first-order momentum vector and

$$M^{(0)} = \begin{bmatrix} mI & \tilde{S}^{(0)T} & M_{13}^{(0)} & \dots & M_{18}^{(0)} \\ \tilde{S}^{(0)} & J^{(0)} & M_{23}^{(0)} & \dots & M_{28}^{(0)} \\ M_{31}^{(0)} & M_{32}^{(0)} & M_{33}^{(0)} & \dots & M_{38}^{(0)} \\ \dots & \dots & \dots & \dots & \dots \\ M_{81}^{(0)} & M_{82}^{(0)} & M_{83}^{(0)} & \dots & M_{88}^{(0)} \end{bmatrix}, \; M^{(1)} = \begin{bmatrix} 0 & \tilde{S}^{(1)T} & 0 & \dots & 0 \\ \tilde{S}^{(1)} & J^{(1)} & M_{23}^{(1)} & \dots & M_{28}^{(1)} \\ 0 & M_{32}^{(1)} & 0 & \dots & 0 \\ \dots & \dots & \dots & \dots & \dots \\ 0 & M_{82}^{(1)} & 0 & \dots & 0 \end{bmatrix} \tag{65}$$

are zero-order and first-order extended mass matrices. Note that $\mathbf{F}_{\text{ext}}$ is regarded as a disturbing force of a transient nature whose effects will be eventually suppressed by the controls.

Equation (63) represents a set of linear equations, and the objective is to find a control vector $\mathbf{u}^{(1)}(t)$ that drives the state vector $\mathbf{x}^{(1)}$ to zero. To this end, we consider a linear regulator whereby the control vector is a linear function of the state vector. In particular, we consider a linear quadratic regulator (LQR) in which the objective is to determine an optimal control vector minimizing the quadratic performance measure[40]

$$J = \tfrac{1}{2}\mathbf{x}^{(1)T}(t_f)H\mathbf{x}^{(1)}(t_f) + \tfrac{1}{2}\int_{t_0}^{t_f}[\mathbf{x}^{(1)T}(t)\mathbf{Q}(t)\mathbf{x}^{(1)}(t) + \mathbf{u}^{(1)T}(t)R(t)\mathbf{u}^{(1)}(t)]dt \tag{66}$$

where H and Q are real symmetric positive semidefinite matrices R is a real symmetric positive definite matrix, t_0 is the initial time (commonly assumed to be zero) and t_f is the final time. It is shown in Ref. 40 that the optimal feedback control vector is given by

$$\mathbf{u}^{(1)}(t) = -R^{-1}(t)B^T(t)K(t)\mathbf{x}^{(1)}(t) = -G(t)\mathbf{x}^{(1)}(t) \tag{67}$$

where

$$G(t) = R^{-1}(t)B^T(t)K(t) \tag{68}$$

is a control gain matrix, in which $K(t)$ is a real symmetric matrix satisfying the transient matrix Riccati equation

$$\dot{K} = -Q - A^TK - KA + KBR^{-1}B^TK, \quad K(t_f) = H(t_f) = H \tag{69}$$

a nonlinear equation which must be integrated backward in time from t_f to t_0. Rather than integrating a nonlinear matrix equation, it is advisable to transform the problem into a linear one. To this end, we consider the transformation

$$K(t) = E(t)F^{-1}(t) \tag{70}$$

where $E(t)$ and $F(t)$ can be obtained by solving the linear equation

$$\begin{bmatrix} \dot{E}(t) \\ \dot{F}(t) \end{bmatrix} = \begin{bmatrix} -A^T(t) & -Q(t) \\ -B(t)R^{-1}(t)B^T(t) & A(t) \end{bmatrix} \begin{bmatrix} E(t) \\ F(t) \end{bmatrix}, \quad \begin{bmatrix} E(t_f) \\ F(t_f) \end{bmatrix} = \begin{bmatrix} H \\ I \end{bmatrix} \tag{71}$$

which again must be integrated backward in time. Inserting Eq. (67) into Eq. (63), we obtain the closed-loop equation

$$\dot{\mathbf{x}}^{(1)}(t) = [A(t) - B(t)G(t)]\mathbf{x}^{(1)}(t) + [0 \;\; I]^T\mathbf{F}_{\text{ext}}(t) \tag{72}$$

which can be integrated to simulate the system response.

The problem is considerably simpler when the zero-order solution is constant, such as in steady level flight, as in this case the coefficient matrix A is constant. Then, if the system is controllable, $H = 0$ and Q and R are constant, the Riccati matrix K approaches a constant value as t_f increases without bounds. In this case, Eq. (69) reduces to the steady-state matrix Riccati equation

$$-Q - A^T K - KA + KBR^{-1}B^T K = 0 \tag{73}$$

a nonlinear algebraic matrix equation, which can be solved by means of Potter's algorithm,[40] and the gain matrix G becomes constant. The closed-loop equation reduces to one with constant coefficients, or

$$\dot{\mathbf{x}}^{(1)}(t) = (A - BG)\mathbf{x}^{(1)}(t) + [0 \;\; I]^T \mathbf{F}_{\text{ext}}(t) \tag{74}$$

which can be used for response simulation. For a stability analysis, we solve the associated eigenvalue problem

$$(A - BG - \lambda I)\mathbf{x} = \mathbf{0} \tag{75}$$

The closed-loop system is stable if all the eigenvalues are pure imaginary and/or complex with negative real part.

The control vector $\mathbf{u}^{(1)}$ is optimal in the sense that it minimizes the performance index J, but the physical merit of this optimality is debatable. In fact, it is often necessary to adjust the otherwise arbitrary weighting matrices Q and R to achieve a desirable system performance. The real value of the LQR algorithm is that it guarantees a stable closed-loop system.

7. Optimal State Observer

In Sec. 6, we carried out the control design in two stages. In the first stage, we postulated a desired aircraft maneuver $\mathbf{x}^{(0)}$ and used an inverse approach to determine the control vector $\mathbf{u}^{(0)}$ permitting realization of the maneuver. In the second stage, we designed a feedback control vector $\mathbf{u}^{(1)}$ ensuring stability of the maneuver, which amounts to driving the perturbation vector $\mathbf{x}^{(1)}$ to zero. The control vector is given by Eq. (67), in which G is the control gain matrix.

Implementation of the control law, Eq. (67), requires knowledge of the state vector $\mathbf{x}^{(1)}$, which can be obtained through measurement. This creates somewhat of a problem, as measurements represent real quantities and our state vector consists of abstract generalized coordinates rather than real coordinates. Moreover, we feed back only perturbations from the maneuver variables. In the absence of external forces, the state equations describing the extended aeroelasticity problem have the vector form

$$\dot{\mathbf{x}}^{(1)}(t) = A\mathbf{x}^{(1)}(t) + B\mathbf{u}^{(1)}(t) \tag{76}$$

where the coefficient matrices A and B were defined in Sec. 6. Moreover, denoting the measurement vector by $\mathbf{y}(t)$, we can write

$$\mathbf{y}(t) = \mathbf{y}^{(0)}(t) + \mathbf{y}^{(1)}(t) \tag{77}$$

where $\mathbf{y}^{(0)}(t)$ is the contribution from the maneuver variables and $\mathbf{y}^{(1)}(t)$ is the contribution from the perturbations in the maneuver variables. We express the latter in the form

$$\mathbf{y}^{(1)}(t) = C\mathbf{x}^{(1)}(t) \tag{78}$$

and refer to $\mathbf{y}^{(1)}(t)$ as the output vector. The assumption is made here that the system is observable,[40] which implies that the initial state $\mathbf{x}^{(1)}(0)$ can be deduced from the outputs within a finite time period. Observability can be established by checking the rank of a so-called observability matrix,[40] a matrix involving the matrices A and C. For large-order systems, working with the observability matrix may not be feasible, and in practice the choice of sensors ensuring observability must be made on physical grounds. In particular, the choice must be such that the sensors signals permit reconstruction of the state at all times. The task of determining the matrix C relating the output vector to the state vector is discussed later in this section.

In reality, the state vector cannot be determined exactly from the output vector and must be estimated. A device permitting an estimate of the state vector is known as an observer[40] and can be expressed in the form

$$\dot{\hat{\mathbf{x}}}^{(1)}(t) = A\hat{\mathbf{x}}^{(1)}(t) + B\mathbf{u}^{(1)}(t) + K_o[\mathbf{y}^{(1)}(t) - C\hat{\mathbf{x}}^{(1)}(t)] \tag{79}$$

where K_o is an observer gain matrix. Subtracting Eq. (79) from Eq. (76), we obtain

$$\dot{\mathbf{e}}(t) = [A - K_oC]\mathbf{e}(t) \tag{80}$$

in which

$$\mathbf{e}(t) = \mathbf{x}^{(1)}(t) - \hat{\mathbf{x}}^{(1)}(t) \tag{81}$$

represents the observer error vector. The objective is to find a matrix K_o such that the vector $\mathbf{e}(t)$ approaches zero as t increases. In this case, $\hat{\mathbf{x}}(t) \to \mathbf{x}(t)$ with time. For a time-invariant system, this amounts to determining K_o so that all the eigenvalues of the matrix $A - K_oC$, known as the observer poles, lie in the left half of the complex plane. In implementing feedback controls, we must use the estimated state $\hat{\mathbf{x}}^{(1)}(t)$, because the actual state $\mathbf{x}^{(1)}(t)$ is not available. Hence, Eq. (67) must be replaced by

$$\mathbf{u}^{(1)}(t) = -G\hat{\mathbf{x}}^{(1)}(t) \tag{82}$$

One question of interest is how the choice of observer poles affect the choice of controller poles. To answer this question, we use Eqs. (81) and (82) and rewrite Eq. (76) in the form

$$\dot{\mathbf{x}}^{(1)}(t) = [A - BG]\mathbf{x}^{(1)}(t) + BG\mathbf{e}(t) \tag{83}$$

Equations (80) and (83) can be combined into

$$\begin{bmatrix} \dot{\mathbf{x}}^{(1)}(t) \\ \dot{\mathbf{e}}(t) \end{bmatrix} = \begin{bmatrix} A - BG & BG \\ 0 & A - K_oC \end{bmatrix} \begin{bmatrix} \mathbf{x}^{(1)}(t) \\ \mathbf{e}(t) \end{bmatrix} \tag{84}$$

Because the coefficient matrix in Eq. (84) is block-triangular, the poles of the combined system consist of the sum of the poles of $A - BG$ and the poles of $A - K_oC$, so that the observer poles can be chosen independently of the controller poles.

An optimal observer gain matrix can be obtained by adopting a stochastic approach, leading to the so-called Kalman-Bucy filter, in contrast to a deterministic observer known as a Luenberger observer. To this end, we rewrite Eqs. (76) and (78) in the form

$$\dot{\mathbf{x}}^{(1)}(t) = A\mathbf{x}^{(1)}(t) + B\mathbf{u}^{(1)}(t) + \mathbf{v}(t) \tag{85}$$

and

$$\mathbf{y}^{(1)}(t) = C\mathbf{x}^{(1)}(t) + \mathbf{w}(t) \tag{86}$$

where $\mathbf{v}(t)$ is known as the state excitation noise and $\mathbf{w}(t)$ as the observation noise, or sensor noise. It is customary to assume that $\mathbf{v}(t)$ and $\mathbf{w}(t)$ are white noise processes, with intensities $V(t)$ and $W(t)$, respectively, so that the correlation matrices have the form

$$E\{\mathbf{v}(t_1)\mathbf{v}^T(t_2)\} = V(t_1)\delta(t_2 - t_1),\ E\{\mathbf{w}(t_1)\mathbf{w}^T(t_2)\} = W(t_1)\delta(t_2 - t_1) \tag{87}$$

and that they are uncorrelated, so that

$$E\{\mathbf{v}(t_1)\mathbf{w}^T(t_2)\} = E\{\mathbf{w}(t_1)\mathbf{v}^T(t_2)\} = 0 \tag{88}$$

in which $E\{\cdot\}$ denotes the expected value.

The stochastic observer has the same form as that given by Eq. (79) in which the optimal gain matrix is determined by minimizing the performance measure

$$J_o = E\{\mathbf{e}^T(t)U(t)\mathbf{e}(t)\} \tag{89}$$

where $U(t)$ is a symmetric positive definite weighting matrix. From Ref. 40, the optimal observer gain matrix is given by

$$K_o^*(t) = Q(t)C^TW^{-1}(t) \tag{90}$$

where $Q(t)$ is the variance matrix of $\mathbf{e}(t)$ satisfying the transient matrix Riccati equation

$$\dot{Q}(t) = AQ(t) + Q(t)A^T + V(t) - Q(t)C^TW^{-1}(t)CQ(t),\ Q(0) = Q_0 \tag{91}$$

In the time-invariant case, Eq. (91) reduces to an algebraic matrix Riccati equation yielding a steady-state optimal observer gain matrix. The main problem in implementing a Kalman-Bucy filter lies in the selection of the noise intensities $V(t)$ and $W(t)$.

At this point, we turn our attention to the determination of the matrix C defined by Eq. (78). To this end, we must first specify the measurement vector $\mathbf{y}^{(1)}(t)$, which in turn depends on the sensors used. In inertial navigation[41], which represents the process of determining the position and attitude of a moving vehicle from self-contained inertial measurements made on board of the vehicle, the system consists of a platform containing accelerometers sensing translational motions, gyroscopes sensing angular motions and a computer capable of integrating the sensors signals to generate the state. Inertial navigation is widely used for aircraft, in which case there are two accelerometers aligned with the North and East directions and three rate gyroscopes with the spin axes aligned with the North, East and zenith directions. To ensure that gravity does not contaminate the accelerometers signals, the platform is made to rotate continuously so as to remain normal to the local vertical. The vertical position of the aircraft is measured by means of an altimeter. In view of this, we can assume that the system measures the vectors $\mathbf{R}_f$ and $\boldsymbol{\theta}_f$ giving the position and attitude relative to axes XYZ. In this regard, it should be mentioned that we referred to axes XYZ as inertial, but in reality they represent earth-fixed axes. If the current formulation is used to describe relatively long flights, then proper allowance must be made for the rotation of the earth. Because the same process can be used to determine the zero-order position vectors $\mathbf{R}^{(0)}$ and $\boldsymbol{\theta}^{(0)}$, we can assume that the measurement system is capable of yielding $\mathbf{R}_f^{(1)}$ and $\boldsymbol{\theta}_f^{(1)}$.

The above process can be used to measure the perturbations in the rigid-body motions of the aircraft and the question remains as to how to measure the balance of the variables, namely, the elastic variables. To this end, we assume that there are N_i $(i = f, w, e)$ sensors measuring velocities at the points P_k $(k = 1, 2, \dots, N_i)$ of the aircraft components and express the output vector in the form

$$\mathbf{y}^{(1)}(t) = [\mathbf{R}_f^{(1)T} \ \boldsymbol{\theta}_f^{(1)T} \ \mathbf{0}^T \ \mathbf{0}^T \dots \mathbf{0}^T]^T + [\mathbf{y}_f^{(1)T}(t) \ \mathbf{y}_w^{(1)T}(t) \ \mathbf{y}_e^{(1)T}(t)]^T \tag{92}$$

where

$$\mathbf{y}_i^{(1)T} = [\bar{\mathbf{V}}_i^{(1)T}(P_1, t) \ \bar{\mathbf{V}}_i^{(1)T}(P_2, t) \ \dots \ \bar{\mathbf{V}}_i^{(1)T}(P_{N_i}, t)]^T, \ i = f, w, e \tag{93}$$

in which $\bar{\mathbf{V}}_i^{(1)}(P_k, t)$ are vectors of velocity measurements. From Eqs. (12) and (53), we can write

$$\begin{aligned} \bar{\mathbf{V}}_f^{(1)}(P_k, t) &= \mathbf{V}_f^{(1)}(t) + \tilde{r}_f^T(P_k)\boldsymbol{\omega}_f^{(1)}(t) + \tilde{\omega}_f^{(0)}(t)\Phi_{uf}(P_k)\mathbf{q}_{uf}(t) \\ &\quad + \Phi_{uf}(P_k)\mathbf{s}_{uf}(t) + \tilde{r}_f^T(P_k)\Phi_{\psi f}(P_k)\mathbf{s}_{\psi f}(t) \\ &= \text{block-diag } C_{fk} \begin{bmatrix} \mathbf{d}^{(1)}(t) \\ \mathbf{V}^{(1)}(t) \end{bmatrix}, \ k = 1, 2, \dots, N_f \end{aligned} \tag{94}$$

where

$$\begin{aligned} \text{block-diag } C_{fk} = \text{block-diag}[&0 \ \ 0 \ \ \tilde{\omega}_f^{(0)}\Phi_{uf}(P_k) \ \ 0 \ \ 0 \ \ 0 \ \ 0 \ \ 0 \\ &I \ \ \tilde{r}_f^T(P_k) \ \ \Phi_{uf}(P_k) \ \ 0 \ \ 0 \ \ \tilde{r}_f^T(P_k)\Phi_{\psi f}(P_k) \ \ 0 \ \ 0] \end{aligned} \tag{95}$$

and $\mathbf{d}^{(1)} = [\mathbf{R}_f^{(1)T} \ \boldsymbol{\theta}_f^{(1)T} \ \mathbf{q}_{uf}^T \ \mathbf{q}_{uw}^T \ \mathbf{q}_{ue}^T \ \mathbf{q}_{\psi f}^T \ \mathbf{q}_{\psi w}^T \ \mathbf{q}_{\psi e}^T]^T$, $\mathbf{V}^{(1)} = [\mathbf{V}_f^{(1)T} \ \boldsymbol{\omega}_f^{(1)T} \ \mathbf{s}_{uf}^T \ \mathbf{s}_{uw}^T \ \mathbf{s}_{ue}^T \ \mathbf{s}_{\psi f}^T$

$\mathbf{s}_{\psi w}^T \;\; \mathbf{s}_{\psi e}^T]^T$. Also from Eqs. (12) and (53), we can write

$$\begin{aligned}
\bar{\mathbf{V}}_w^{(1)}(P_k,t) &= C_w \mathbf{V}_f^{(1)} + (C_w \tilde{r}_{fw}^T + \tilde{r}_w^T(P_k) C_w) \boldsymbol{\omega}_f^{(1)} + C_w \tilde{\omega}_f^{(0)} \Phi_{ufw} \mathbf{q}_{uf} \\
&\quad + \widetilde{C_w \boldsymbol{\omega}_f^{(0)}} \Phi_{uw}(P_k) \mathbf{q}_{uw} + (\tilde{r}_w^T(P_k) C_w \Delta\Phi_{ufw} + C_w \Phi_{ufw}) \mathbf{s}_{uf} \\
&\quad + \Phi_{uw}(P_k) \mathbf{s}_{uw} + (\tilde{r}_w^T(P_k) C_w \Phi_{\psi fw} + C_w \tilde{r}_{fw}^T \Phi_{\psi fw}) \mathbf{s}_{\psi f} \\
&\quad + \tilde{r}_w^T(P_k) \Phi_{\psi w}(P_k) \mathbf{s}_{\psi w} \\
&= \text{block-diag}\, C_{wk} \begin{bmatrix} \mathbf{d}^{(1)}(t) \\ \mathbf{V}^{(1)}(t) \end{bmatrix}, \quad k = 1, 2, \ldots, N_w
\end{aligned} \tag{96}$$

where

$$\begin{aligned}
\text{block-diag}\, C_{wk} = \text{block-diag}[0 \;\; 0 \;\; & C_w \tilde{\omega}_f^{(0)} \Phi_{ufw} \;\; \widetilde{C_w \boldsymbol{\omega}_f^{(0)}} \Phi_{uw}(P_k) \;\; 0 \;\; 0 \;\; 0 \;\; 0 \\
& C_w \;\; (C_w \tilde{r}_{fw}^T + \tilde{r}_w^T(P_k) C_w) \;\; (\tilde{r}_w^T(P_k) C_w \Delta\Phi_{ufw} + C_w \Phi_{ufw}) \\
& \Phi_{uw}(P_k) \;\; 0 \;\; (\tilde{r}_w^T(P_k) C_w \Phi_{\psi fw} + C_w \tilde{r}_{fw}^T \Phi_{\psi fw}) \\
& \tilde{r}_w^T(P_k) \Phi_{\psi w}(P_k) \;\; 0]
\end{aligned} \tag{97}$$

In a similar fashion, we can write

$$\bar{\mathbf{V}}_e^{(1)}(P_k,t) = \text{block-diag}\, C_{ek} \begin{bmatrix} \mathbf{d}^{(1)}(t) \\ \mathbf{V}^{(1)}(t) \end{bmatrix}, \quad k = 1, 2, \ldots, N_e \tag{98}$$

where

$$\begin{aligned}
\text{block-diag}\, C_{ek} = [0 \;\; 0 \;\; & C_e \tilde{\omega}_f^{(0)} \Phi_{ufe} \;\; 0 \;\; \widetilde{C_e \omega_f^{(0)}} \Phi_{ue}(P_k) \;\; 0 \;\; 0 \;\; 0 \\
& C_e \;\; (C_e \tilde{r}_{fe}^T + \tilde{r}_e^T(P_k) C_e) \;\; (\tilde{r}_e^T(P_k) C_e \Delta\Phi_{ufe} + C_e \Phi_{ufe}) \;\; 0 \;\; \Phi_{ue}(P_k) \\
& (\tilde{r}_e^T(P_k) C_e \Phi_{\psi fe} + C_e \tilde{r}_{fe}^T \Phi_{\psi fe}) \;\; 0 \;\; \tilde{r}_e^T(P_k) \Phi_{\psi e}(P_k)]
\end{aligned} \tag{99}$$

Equations (94), (96) and (98) are in terms of $\mathbf{d}^{(1)}$ and $\mathbf{V}^{(1)}$. They can be transformed into expressions in terms of the state $\mathbf{x}^{(1)} = [\mathbf{d}^{(1)T} \mathbf{p}^{(1)T}]^T$ by considering Eq. (64). To this end, we observe that $M^{(1)} = M^{(1)}(\mathbf{q}_{uf},\; \mathbf{q}_{uw},\; \mathbf{q}_{ue})$, so that we can write

$$M^{(1)} \mathbf{V}^{(0)} = M_V \mathbf{d}^{(1)} \tag{100}$$

where M_V is a matrix depending on $\mathbf{V}^{(0)}$. Hence, using Eq. (64), we obtain

$$\mathbf{V}^{(1)} = (M^{(0)})^{-1} (\mathbf{p}^{(1)} - M_V \mathbf{d}^{(1)}) \tag{101}$$

so that

$$\begin{bmatrix} \mathbf{d}^{(1)} \\ \mathbf{V}^{(1)} \end{bmatrix} = \begin{bmatrix} I & 0 \\ -(M^{(0)})^{-1} M_V & (M^{(0)})^{-1} \end{bmatrix} \mathbf{x}^{(1)} \tag{102}$$

Finally, using Eqs. (92), (93), (94), (96), (98) and (102), we conclude that

$$C = \begin{bmatrix} I \;\; 0 \;\; 0 \;\; \ldots \;\; 0 \\ 0 \;\; I \;\; 0 \;\; \ldots \;\; 0 \\ \text{block-diag } C_{f1} \\ \text{block-diag } C_{f2} \\ \cdots\cdots\cdots\cdots\cdots \\ \text{block-diag } C_{fN_f} \\ \text{block-diag } C_{w1} \\ \text{block-diag } C_{w2} \\ \cdots\cdots\cdots\cdots\cdots \\ \text{block-diag } C_{wN_w} \\ \text{block-diag } C_{e1} \\ \text{block-diag } C_{e2} \\ \cdots\cdots\cdots\cdots\cdots \\ \text{block-diag } C_{eN_e} \end{bmatrix} \begin{bmatrix} I & 0 \\ -(M^{(0)})^{-1} M_V & (M^{(0)})^{-1} \end{bmatrix} \tag{103}$$

8. Numerical Example

The flight of a flexible aircraft is fully described by Eqs. (43), (49), (50) and (59). A solution of these equations requires the aircraft geometry, the mass and stiffness distributions and the aerodynamic coefficients. Information pertaining to an actual aircraft was made available by an aircraft manufacturer and is listed in the **Appendix**.

The solution of the flight dynamics equations, Eqs. (43) and (49), requires the matrices $C_f^{(0)}$, $E_f^{(0)}$, the total aircraft mass m, the matrix $\tilde{S}^{(0)}$ of the first moments of inertia of the undeformed aircraft and the inertia matrix $J^{(0)}$ of the undeformed aircraft. The matrices $C_f^{(0)}$ and $E_f^{(0)}$ can be obtained from C_f and E_f, Eqs. (2), by simply replacing ψ, θ and ϕ by $\psi^{(0)}$, $\theta^{(0)}$ and $\phi^{(0)}$, respectively. The aerodynamic forces are given by Eqs. (45) and the required coefficients are given in the **Appendix**. Other data required is as follows: engines locations, $\mathbf{r}_{E1} = [-108.62 \;\; 37.0 \;\; -13.96]^T$ in, $\mathbf{r}_{E2} = [-108.62 \;\; -37.0 \;\; -13.96]^T$ in; total aircraft mass, $m = 33.5896$ lb $\cdot$ s^2/in; matrix of first moments of inertia and inertia matrix

$$\tilde{S}^{(0)} = \begin{bmatrix} 0 & -134.6827 & 0 \\ 134.6827 & 0 & 0 \\ 0 & 0 & 0 \end{bmatrix} \text{lb} \cdot \text{s}^2$$
$$J^{(0)} = \begin{bmatrix} 183183.4257 & 4.7745 & -37624.9453 \\ & 566328.8970 & 81.1583 \\ \text{symm} & & 704218.5794 \end{bmatrix} \text{lb} \cdot \text{in} \cdot \text{s}^2 \qquad (104)$$

Some of the above quantities involve the matrices of direction cosines between the various components body axes and the fuselage body axes. These matrices are listed in the **Appendix**. The flight dynamics problem essentially consists of setting the control surfaces and the engine thrust for a given aircraft maneuver, of which the steady cruise is a special case. It essentially amounts to the problem of "trimming" the aircraft. As far as this paper is concerned, it provides the input $\mathbf{V}_f^{(0)}$, $\boldsymbol{\omega}_f^{(0)}$, $\mathbf{p}_{Vf}^{(0)}$ and $\mathbf{p}_{\omega f}^{(0)}$ to the extended aeroelasticity problem.

The solution of the extended aeroelasticity equations, Eqs. (50) and (59), requires an explicit choice of the structural model for the aircraft of Fig. 1. As a first approximation, the fuselage, wing, and both the horizontal and vertical stabilizers in the empennage are modeled as beams clamped at the origin of the respective body axes and undergoing bending and torsion. The fuselage undergoes the bending displacements u_{fy} and u_{fz} and the torsional displacement ψ_{fx}, as shown in Fig. 2, so that $\mathbf{u}_f = [0 \;\; u_{fy} \;\; u_{fz}]^T$ and $\boldsymbol{\psi}_f = [\psi_{fx} \;\; 0 \;\; 0]^T$. On the other hand, the wing and the stabilizers undergo only one bending and one torsional displacement each. Note that, as customary, displacements are measured relative to the elastic axis (Fig. 2). Each clamped beam is assumed to be discretized by the Galerkin method in conjunction with two shape functions per displacement component. For bending, the shape functions are chosen as the eigenfunctions of a

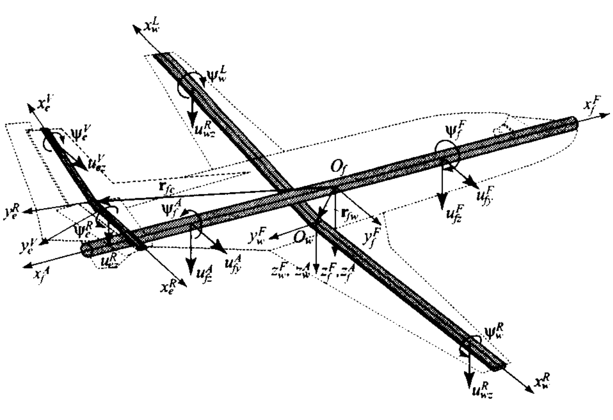

Figure 2. Aircraft Components Undergoing Bending and Torsion

uniform cantilever beam

$$\phi_{uir} = \sin\beta_r x_i - \sinh\beta_r x_i - \frac{\sin\beta_r L_i + \sinh\beta_r L_i}{\cos\beta_r L_i + \cosh\beta_r L_i}(\cos\beta_r x_i - \cosh\beta_r x_i),\ r = 1,2;\ i = f, w, e \tag{105}$$

and for torsion, the eigenfunctions of a uniform clampe-free shaft

$$\phi_{\psi ir} = \sin(2r-1)\pi x_i/2L_i,\ r = 1,2;\ i = f, w, e \tag{106}$$

where L_i is the length of the cantilever beam. In this regard, we note from Fig. 2 that the fuselage is modeled as two cantilever beams clamped at O_f, one pointing to the aircraft nose and the other to the tail. New quantities entering into the first-order equation are $C_f^{(1)}$ and $E_f^{(1)}$, which can be obtained from C_f and E_f by using $\boldsymbol{\theta}_f = \boldsymbol{\theta}_f^{(0)} + \boldsymbol{\theta}_f^{(1)}$ and letting the components of $\boldsymbol{\theta}_f^{(1)}$ be small, $\mathbf{F}^{(1)}$, $\mathbf{M}^{(1)}$, $\mathbf{Q}_{ui}$ and $\mathbf{Q}_{\psi i}$ $(i = f, w, e)$, which are given by Eqs. (54), and Φ_{ui} and $\Phi_{\psi i}$, which contain ϕ_{uir} and $\phi_{\psi ir}$ as given above. Moreover, the stiffness matrices are obtained from the potential energy as follows:

$$\begin{aligned} V = \tfrac{1}{2}\textstyle\int_{D_f} &\left[EI_{fz}\left(\partial^2 u_{fy}/\partial x_f^2\right)^2 + EI_{fy}\left(\partial^2 u_{fz}/\partial x_f^2\right)^2 + GJ_{fx}\left(\partial\psi_{fx}/\partial x_f\right)^2\right] dD_f \\ &+ \textstyle\int_{D_w}\left[EI_w\left(\partial^2 u_{wz}/\partial x_w^2\right)^2 + GJ_w\left(\partial\psi_{wx}/\partial x_w\right)^2\right] dD_w + \int_{D_e}\Big[EI_e\left(\partial^2 u_{ez}/\partial x_e^2\right)^2 \\ &+ GJ_e\left(\partial\psi_{ex}/\partial x_e\right)^2\Big] dD_e = \tfrac{1}{2}\textstyle\sum_i(\mathbf{q}_{ui}^T K_{ui}\mathbf{q}_{ui} + \mathbf{q}_{\psi i}^T K_{\psi i}\mathbf{q}_{\psi i}) \end{aligned} \tag{107}$$

where

$$\begin{aligned} &K_{uf} = \textstyle\int_{D_f}(\Phi_{uf}'')^T \mathrm{diag}[EI_{fz}\ \ EI_{fy}]\Phi_{uf}'' dD_f,\ K_{ui} = \int_{D_i} EI_i(\Phi_{ui}'')^T\Phi_{ui}'' dD_i \\ &K_{\psi i} = \textstyle\int_{D_i} GJ_i(\Phi_{\psi i}')^T\Phi_{\psi i}' dD_i,\ i = f, w, e \end{aligned} \tag{108}$$

are the desired stiffness matrices, in which primes denote differentiations with respect to x_i.

Equations (63) for the model in question are of order 76, but the equations are linear. However, in the case of certain aircraft maneuvers, the systems is time-varying.

To demonstrate the ideas, we consider two cases, steady level flight and steady level turn maneuver.

i. Steady level flight

For steady level flight, the zero-order velocities are defined by

$$\mathbf{V}_f^{(0)} = C_f^{(0)}[V^{(0)}\ \ 0\ \ 0]^T = \text{constant},\ \boldsymbol{\omega}_f^{(0)} = \mathbf{0} \tag{109}$$

where $V^{(0)}$ is the aircraft forward velocity. From Eqs. (49), we conclude that the zero-order momenta are

$$\mathbf{p}_{Vf}^{(0)} = m\mathbf{V}_f^{(0)} = \text{constant},\ \mathbf{p}_{\omega f}^{(0)} = \tilde{S}^{(0)}\mathbf{V}_f^{(0)} = \text{constant} \tag{110}$$

Hence, from the second line of Eqs. (43), we have

$$\mathbf{F}^{(0)} = \mathbf{0},\ \mathbf{M}^{(0)} = \mathbf{0} \tag{111}$$

The implication of Eqs. (111) is that, for steady level flight, the forces and moments due to the engine thrust, aerodynamic forces, gravitational forces and control forces balance out to zero. The angle of attack can be expressed as

$$\alpha_f^{(0)} = \tan^{-1}(V_{fz}^{(0)}/V_{fx}^{(0)}) = \alpha_0 = \text{constant} \tag{112}$$

For level flight, we have $\psi^{(0)} = \phi^{(0)} = 0$, so that the pitch angle is equal to the angle of attack, or

$$\theta^{(0)} = \alpha_f^{(0)} \tag{113}$$

Moreover, because $V_{fy}^{(0)} = 0$, the sideslip angle is zero,

$$\beta_f^{(0)} = \tan^{-1}(V_{fy}^{(0)}/V_{fx}^{(0)}) = 0 \tag{114}$$

In view of this, and due to the symmetry of the gravitational and aerodynamic forces, the side force $F_y^{(0)}$ and the roll and yaw moments, $M_x^{(0)}$ and $M_z^{(0)}$, are automatically zero. We assume that $V^{(0)} = 5000$ in/s and consider a flight at a 25000 ft altitude, so that the speed of sound is 1016.1 ft/s and, hence, the Mach number is $5000/(1016.1 \times 12) = 0.41$. From Eq. (109), we have $\mathbf{V}_f^{(0)} = 5000[\cos\theta^{(0)} \;\; 0 \;\; \sin\theta^{(0)}]^T$. Then, using Eqs. (44) in conjunction with Eqs. (45)-(48), Eqs. (111) yield

$$\begin{aligned}
F_x^{(0)} &= 2F_E^{(0)} - 695.3237\cos^2\theta^{(0)} - 12973\sin\theta^{(0)} + 2149.5358\delta_e^{(0)}\cos\theta^{(0)}\sin\theta^{(0)} \\
&\quad + \sin^2\theta^{(0)}(164224.6592 + 2149.5358\delta_e^{(0)}\tan\theta^{(0)} + 164919.9829\tan^2\theta^{(0)}) = 0 \\
F_z^{(0)} &= -2149.5358\delta_e^{(0)}\cos^2\theta^{(0)} + \cos\theta^{(0)}(12973 - 202450.4921\sin\theta^{(0)}) \\
&\quad + \sin^2\theta^{(0)}(-2149.5358\delta_e^{(0)} - 239285.6777\tan\theta^{(0)} - 36835.1856\tan^3\theta^{(0)}) = 0 \\
M_y^{(0)} &= -27.92F_E^{(0)} + (-16069.8929 - 553904.5798\delta_e^{(0)})\cos^2\theta^{(0)} \\
&\quad -52019.1354\sin\theta^{(0)} + (-2.0058\times 10^6 - 116986.5503\delta_e^{(0)})\cos\theta^{(0)}\sin\theta^{(0)} \\
&\quad + \sin^2\theta^{(0)}(3.0203\times 10^6 - 553904.5798\delta_e^{(0)} + (-1.6634\times 10^6 \\
&\quad - 116986.5503\delta_e^{(0)})\tan\theta^{(0)} + 3.0364\times 10^6\tan^2\theta^{(0)} + 342353.8625\tan^3\theta^{(0)}) = 0
\end{aligned} \tag{115}$$

which can be solved for the pitch angle $\theta^{(0)}$, the engine thrust $F_E^{(0)}$ and the elevator angle $\delta_e^{(0)}$. Solving the nonlinear equations (115), we obtain $\theta^{(0)} = 0.0667$ rad, $F_E^{(0)} = 431.6465$ lb and $\delta_e^{(0)} = -0.2703$ rad, so that the zero-order control vector is given by $\mathbf{u}^{(0)} = [F_E^{(0)} \;\; 0 \;\; \delta_e^{(0)} \;\; 0]^T = [431.6465 \;\; 0 \;\; -0.2703 \;\; 0]^T$. Hence, the control force vector can be written in the matrix form

$$\begin{aligned}
\mathbf{F}_c^{(0)} = B^{(0)}\mathbf{u}^{(0)} &= \begin{bmatrix}
0 & 0 & 0 & 0 \\
0 & 0 & 0 & 0 \\
0 & 0 & 0 & 0 \\
0 & 0 & 0 & 0 \\
0 & 0 & 0 & 0 \\
0 & 0 & 0 & 0 \\
2 & 0 & 143.4894 & 0 \\
0 & 0 & 0 & -1905.7803 \\
0 & 0 & -2149.5358 & 0 \\
0 & 803506.9168 & 0 & -153855.5426 \\
-27.92 & 0 & -561713.8624 & 0 \\
0 & 53637.0429 & 0 & 529190.6764
\end{bmatrix}
\begin{bmatrix} 431.6465 \\ 0 \\ -0.2703 \\ 0 \end{bmatrix} \\
&= [0 \; 0 \; 0 \; 0 \; 0 \; 0 \; 824.5038 \; 0 \; 581.0801 \; 0 \; 139795.5057 \; 0]^T
\end{aligned} \tag{116}$$

In the case of steady level flight, the aircraft experiences static deformations due to zero-order forces. Because static deformations are constant and deformations are first-order quantities, we denote all quantities involved by a subscript c and a superscript (1). Consistent with the zero-order results and using the first of Eqs. (50), we write

$$\mathbf{V}_{fc}^{(1)} = C_f^{(0)}\{[V^{(1)}0\ \ 0]^T - C_f^{(1)}\mathbf{V}_f^{(0)}\},\ \boldsymbol{\omega}_{fc}^{(1)} = \mathbf{0};\ \mathbf{s}_{uic} = \mathbf{0},\ \mathbf{s}_{\psi ic} = \mathbf{0},\ i = f, w, e \tag{117}$$

where $V^{(1)}$ is the first-order forward velocity. Then, from Eqs. (59), the corresponding momenta are

$$\mathbf{p}_{Vfc}^{(1)} = m\mathbf{V}_{fc}^{(1)},\ \mathbf{p}_{\omega fc}^{(1)} = \tilde{S}_c^{(1)}\mathbf{V}_f^{(0)} + \tilde{S}^{(0)}\mathbf{V}_f^{(1)} \tag{118}$$

and, from Eqs. (50), we conclude that

$$\begin{aligned} &\mathbf{F}_c^{(1)} = \mathbf{0},\ \mathbf{M}_c^{(1)} = \mathbf{0} \\ &-K_{ui}\mathbf{q}_{uic} + \mathbf{Q}_{uic} = \mathbf{0},\ -K_{\psi i}\mathbf{q}_{\psi ic} + \mathbf{Q}_{\psi ic} = \mathbf{0},\ i = f, w, e \end{aligned} \tag{119}$$

which represent algebraic equations to be solved for the first-order pitch angle, the first-order elevator incident angle, the first-order engine thrust and the static generalized displacements $\mathbf{q}_{uic}$ and $\mathbf{q}_{\psi ic}$. We note that $\mathbf{F}_c^{(1)} = [F_{xc}^{(1)}\ \ 0\ \ F_{zc}^{(1)}]^T$, $\mathbf{M}_c^{(1)} = [0\ \ M_{yc}^{(1)}\ \ 0]^T$, $\mathbf{Q}_{uic}$ and $\mathbf{Q}_{\psi ic}$ are all functions of $\mathbf{q}_{uic}$ and $\mathbf{q}_{\psi ic}$ $(i = f, w, e)$.

The stiffness matrices are as follows:

$$\begin{aligned}
K_{uf}^F &= \begin{bmatrix} 8687.0713 & -3181.9271 & 0 & 0 \\ -3181.9271 & 293633.2239 & 0 & 0 \\ 0 & 0 & 12883.4627 & -4643.2903 \\ 0 & 0 & -4643.2903 & 419984.1291 \end{bmatrix} \\
K_{uf}^A &= \begin{bmatrix} 8891.2109 & -28248.0864 & 0 & 0 \\ -28248.0864 & 231517.6212 & 0 & 0 \\ 0 & 0 & 13097.4380 & -36822.7531 \\ 0 & 0 & -36822.7531 & 363078.6024 \end{bmatrix} \\
K_{\psi f}^F &= \begin{bmatrix} 1.5462 & 1.0134 \\ 1.0134 & 9.0414 \end{bmatrix} \times 10^8,\ K_{\psi f}^A = \begin{bmatrix} 1.0781 & 1.9339 \\ 1.9339 & 6.7838 \end{bmatrix} \times 10^8 \\
K_{uw}^R = K_{uw}^L &= \begin{bmatrix} 581.3939 & -1488.0598 \\ -1488.0598 & 13050.3375 \end{bmatrix},\ K_{\psi w}^R = K_{\psi w}^L = \begin{bmatrix} 2.2974 & 3.6438 \\ 3.6438 & 13.5871 \end{bmatrix} \times 10^7 \\
K_{ue}^R = K_{ue}^L &= \begin{bmatrix} 406.2228 & -696.8287 \\ -696.8287 & 10685.4900 \end{bmatrix},\ K_{\psi e}^R = K_{\psi e}^L = \begin{bmatrix} 1.5455 & 1.4924 \\ 1.4924 & 10.0858 \end{bmatrix} \times 10^6 \\
K_{ue}^V &= \begin{bmatrix} 2126.9677 & -4303.4586 \\ -4303.4586 & 52929.3173 \end{bmatrix},\ K_{\psi e}^V = \begin{bmatrix} 5.0679 & 5.3834 \\ 5.3834 & 31.9145 \end{bmatrix} \times 10^6
\end{aligned} \tag{120}$$

where the superscripts F, A, R, L and V denote the fore part, aft part, right half, left half and vertical (stabilizer), respectively. Assuming that $V^{(1)} = -5$ in/s, so that $\mathbf{V}_{fc}^{(1)} = V^{(1)}[\cos\theta^{(0)}\ \ 0\ \ \sin\theta^{(0)}]^T + V^{(0)}[-\theta^{(1)}s\theta^{(0)}\ \ 0\ \ \theta^{(1)}c\theta^{(0)}]^T = [-4.6953 - 333.02727\theta^{(1)}\ \ 0\ \ -4.7316 + 4988.89707\theta^{(1)}]^T$, we can solve Eqs. (119) and obtain

$$\begin{aligned}
&\theta^{(1)} = -0.00088 \text{ rad},\ F_E^{(1)} = -3.1169 \text{ lb},\ \delta_e^{(1)} = -0.0047 \text{ rad} \\
&\mathbf{q}_{ufc}^F = [0\ \ 0\ \ 0.1206\ \ -0.0015]^T \text{ in},\ \mathbf{q}_{\psi fc}^F = [0\ \ 0]^T \text{ rad} \\
&\mathbf{q}_{ufc}^A = [0\ \ 0\ \ 0.0585\ \ 0.0038]^T \text{ in},\ \mathbf{q}_{\psi fc}^A = [0\ \ 0]^T \text{ rad}
\end{aligned} \tag{121}$$

$\mathbf{q}_{uwc}^R = \mathbf{q}_{uwc}^L = [-3.4537 \quad -0.2918]^T$ in, $\mathbf{q}_{\psi wc}^R = \mathbf{q}_{\psi wc}^L = [0.0021 \quad -0.0002]^T$ rad
$\mathbf{q}_{uec}^R = \mathbf{q}_{uec}^L = [-0.0279 \;\; 0.0006]^T$ in, $\mathbf{q}_{\psi ec}^R = \mathbf{q}_{\psi ec}^L = [0.0024 \quad -0.0002]^T$ rad
$\mathbf{q}_{uec}^V = [0 \;\; 0]^T$ in, $\mathbf{q}_{\psi ec}^V = [0 \;\; 0]^T$ rad

Assuming that the first-order state $\mathbf{x}^{(1)}$ is measured from the static elastic displacements position, the first-order state equations for steady level flight can be written in the customary form, Eq. (63), where A and B are constant coefficient matrices. This requires the mass matrices, defined by Eqs. (15). They can be computed as follows:

$$
\begin{aligned}
M_{11} &= mI, \\
M_{12} &= \tilde{S}^T = \begin{bmatrix} 0 & 131.1002 & 0 \\ -131.1002 & 0 & 0 \\ 0 & 0 & 0 \end{bmatrix} + \begin{bmatrix} 0 & 0 & -4.2385 \\ 0 & 0 & 0 \\ 4.2385 & 0 & 0 \end{bmatrix} q_{ufy1}^F \\
&\quad + \begin{bmatrix} 0 & 0 & 3.2026 \\ 0 & 0 & 0 \\ -3.2026 & 0 & 0 \end{bmatrix} q_{ufy2}^F + \begin{bmatrix} 0 & 4.2385 & 0 \\ -4.2385 & 0 & 0 \\ 0 & 0 & 0 \end{bmatrix} q_{ufz1}^F + \dots \\
&\quad + \begin{bmatrix} 0 & -0.0807 & -0.0128 \\ 0.0807 & 0 & 0 \\ 0.0128 & 0 & 0 \end{bmatrix} q_{ue2}^L + \begin{bmatrix} 0 & 0 & -0.1252 \\ 0 & 0 & 0 \\ 0.1252 & 0 & 0 \end{bmatrix} q_{ue1}^V \\
&\quad + \begin{bmatrix} 0 & 0 & 0.0219 \\ 0 & 0 & 0 \\ -0.0219 & 0 & 0 \end{bmatrix} q_{ue2}^V, \\
M_{13}^F &= \begin{bmatrix} 0 & 0 & 0 & 0 \\ 4.2385 & -3.2026 & 0 & 0 \\ 0 & 0 & 4.2385 & -3.2026 \end{bmatrix}, \dots, \\
M_{22} &= J = \begin{bmatrix} 182862.0586 & 4.7745 & -37732.0967 \\ 4.7745 & 566132.2704 & 81.1583 \\ -37732.0967 & 81.1583 & 704093.8389 \end{bmatrix} + \begin{bmatrix} 0 & -863.2814 & 0 \\ -863.2814 & 0 & -21.0393 \\ 0 & -21.0393 & 0 \end{bmatrix} q_{ufy1}^F \\
&\quad + \begin{bmatrix} 0 & 367.2116 & 0 \\ 367.2116 & 0 & 7.3021 \\ 0 & 7.3021 & 0 \end{bmatrix} q_{ufy2}^F + \begin{bmatrix} 42.0786 & 0 & -863.2814 \\ 0 & 42.0786 & 0 \\ -863.2814 & 0 & 0 \end{bmatrix} q_{ufz1}^F + \dots \qquad (122) \\
&\quad + \begin{bmatrix} 6.9600 & 3.2162 & -20.3065 \\ 3.2162 & 7.5428 & -1.2425 \\ -20.3065 & -1.2425 & -0.5828 \end{bmatrix} q_{ue2}^L + \begin{bmatrix} 0 & 35.9911 & 0 \\ 35.9911 & 0 & 12.8989 \\ 0 & 12.8989 & 0 \end{bmatrix} q_{ue1}^V \\
&\quad + \begin{bmatrix} 0 & -4.0598 & 0 \\ -4.0598 & 0 & 4.0183 \\ 0 & 4.0183 & 0 \end{bmatrix} q_{ue2}^V, \\
M_{23}^F &= \begin{bmatrix} -21.0393 & 7.3021 & 0 & 0 \\ 0 & 0 & -863.2814 & 367.2116 \\ 863.2814 & -367.2116 & 0 & 0 \end{bmatrix} + \begin{bmatrix} 0 & 0 & 2.4862 & -0.7090 \\ 0 & 0 & 0 & 0 \\ 0 & 0 & 0 & 0 \end{bmatrix} q_{ufy1}^F + \dots \\
&\quad + \begin{bmatrix} 0.7090 & -2.3655 & 0 & 0 \\ 0 & 0 & 0 & 0 \\ 0 & 0 & 0 & 0 \end{bmatrix} q_{ufz2}^F, \dots, \; M_{28}^V = \begin{bmatrix} 68.4129 & 72.7595 \\ 0 & 0 \\ -344.8056 & -402.1912 \end{bmatrix}, \dots, \\
M_{33}^A &= \begin{bmatrix} 2.2363 & -1.5318 & 0 & 0 \\ -1.5318 & 8.4942 & 0 & 0 \\ 0 & 0 & 2.0922 & -1.5310 \\ 0 & 0 & -1.5310 & 7.9257 \end{bmatrix}, \dots,
\end{aligned}
$$

$$M_{88}^{L} = \begin{bmatrix} 17.3669 & 10.8317 \\ 10.8317 & 32.5338 \end{bmatrix}, \; M_{88}^{V} = \begin{bmatrix} 34.1002 & 32.0129 \\ 32.0129 & 65.4667 \end{bmatrix}$$

Before we can compute A and B, we must still generate the damping matrices C_{ui} and $C_{\psi i}$ $(i = f, w, e)$. To this end, we assume that the damping functions c_{ui} and $c_{\psi i}$ $(i = f, w, e)$ are all constant, so that the damping matrices, Eqs. (19), reduce to

$$C_{ui} = c_{ui} K_{ui}, \; C_{\psi i} = c_{\psi i} K_{\psi i}, \; i = f, w, e \tag{123}$$

Equations (123) state that the damping matrices are proportional to the stiffness matrices, which permits us to write the relations[37]

$$c_{ui} = 2\zeta / \Lambda_{ui}^{1/2}, \; c_{\psi i} = 2\zeta / \Lambda_{\psi i}^{1/2}, \; i = f, w, e \tag{124}$$

where ζ is a structural damping factor and $\Lambda_{ui}^{1/2}$ and $\Lambda_{\psi i}^{1/2}$ $(i = f, w, e)$ are the lowest natural frequencies of the respective components. We assume that $\zeta = 0.03$. Moreover, we obtain the component natural frequencies by solving the eigenvalue problems

$$\begin{gathered} \det[K_{uf}^{F} - \Lambda_{uf}^{F} M_{33}^{F}] = 0, \; \det[K_{uf}^{A} - \Lambda_{uf}^{A} M_{33}^{A}] = 0, \; \det[K_{uw}^{R} - \Lambda_{uw}^{R} M_{44}^{R}] = 0 \\ \det[K_{uw}^{L} - \Lambda_{uw}^{L} M_{44}^{L}] = 0, \; \ldots, \; \det[K_{\psi e}^{L} - \Lambda_{\psi e}^{L} M_{88}^{L}] = 0, \; \det[K_{\psi e}^{V} - \Lambda_{\psi e}^{V} M_{88}^{V}] = 0 \end{gathered} \tag{125}$$

with the results

$$\begin{gathered} \sqrt{\Lambda_{uf}^{F}} = 59.1046 \text{ rad/s}, \; \sqrt{\Lambda_{uf}^{A}} = 54.1788 \text{ rad/s}, \; \sqrt{\Lambda_{uw}^{R}} = \sqrt{\Lambda_{uw}^{L}} = 36.2911 \text{ rad/s} \\ \sqrt{\Lambda_{ue}^{R}} = \sqrt{\Lambda_{ue}^{L}} = 72.1276 \text{ rad/s}, \; \sqrt{\Lambda_{ue}^{V}} = 131.9557 \text{ rad/s}, \\ \sqrt{\Lambda_{\psi f}^{F}} = 221.8479 \text{ rad/s}, \; \sqrt{\Lambda_{\psi f}^{A}} = 61.9940 \text{ rad/s}, \; \sqrt{\Lambda_{\psi w}^{R}} = \sqrt{\Lambda_{\psi w}^{L}} = 253.9293 \text{ rad/s} \\ \sqrt{\Lambda_{\psi e}^{R}} = \sqrt{\Lambda_{\psi e}^{L}} = 294.1938 \text{ rad/s} \sqrt{\Lambda_{\psi e}^{V}} = 384.8014 \text{ rad/s} \end{gathered} \tag{126}$$

Hence, using Eqs. (120), (123), (124) and (126), the damping matrices are

$$\begin{gathered} C_{uf}^{F} = \begin{bmatrix} 8.8187 & -3.2301 & 0 & 0 \\ -3.2301 & 298.0817 & 0 & 0 \\ 0 & 0 & 13.0786 & -4.7136 \\ 0 & 0 & -4.7136 & 426.3467 \end{bmatrix} \\ C_{uf}^{A} = \begin{bmatrix} 9.8465 & -31.2832 & 0 & 0 \\ -31.2832 & 256.3929 & 0 & 0 \\ 0 & 0 & 14.5047 & -40.7792 \\ 0 & 0 & -40.7792 & 402.0894 \end{bmatrix} \\ C_{\psi f}^{F} = \begin{bmatrix} 41818.3661 & 27408.5814 \\ 27408.5814 & 244530.1083 \end{bmatrix}, \; C_{\psi f}^{A} = \begin{bmatrix} 104342.4068 & 187172.4172 \\ 187172.4172 & 656562.6583 \end{bmatrix} \\ C_{uw}^{R} = C_{uw}^{L} = \begin{bmatrix} 0.9612 & -2.4602 \\ -2.4602 & 21.5761 \end{bmatrix}, \; C_{\psi w}^{R} = C_{\psi w}^{L} = \begin{bmatrix} 5428.3762 & 8609.7859 \\ 8609.7859 & 32104.4936 \end{bmatrix} \\ C_{ue}^{R} = C_{ue}^{L} = \begin{bmatrix} 0.3379 & -0.5797 \\ -0.5797 & 8.8888 \end{bmatrix}, \; C_{\psi e}^{R} = C_{\psi e}^{L} = \begin{bmatrix} 315.1931 & 304.3728 \\ 304.3728 & 2056.9682 \end{bmatrix} \\ C_{ue}^{V} = \begin{bmatrix} 0.9671 & -1.9568 \\ -1.9568 & 24.0669 \end{bmatrix}, \; C_{\psi e}^{V} = \begin{bmatrix} 790.2110 & 839.4058 \\ 839.4058 & 4976.2592 \end{bmatrix} \end{gathered} \tag{127}$$

Then, the coefficient matrices in Eq. (63) can be shown to be

$$
\begin{aligned}
A &= \begin{bmatrix}
0 & 0 & 0 & 0 & 0 & 0 & \cdots & 0 & 0 \\
0 & 0 & 0 & -333.0272 & 0 & 5000 & \cdots & -0.0014 & -0.0001 \\
0 & 0 & 0 & 0 & -5000 & 0 & \cdots & 0 & 0 \\
0 & 0 & 0 & 0 & 0 & 0 & \cdots & 0 & 0 \\
\cdots & \cdots & \cdots & \cdots & \cdots & \cdots & \cdots & \cdots & \cdots \\
0 & 0 & 0 & 36.3883 & 19.0770 & 0 & \cdots & -0.0212 & -0.0020 \\
0 & 0 & 0 & 40.8390 & 41.4025 & 0 & \cdots & 0.1414 & 0.0257 \\
0 & 0 & 0 & 455.5429 & 0 & 0 & \cdots & -31.2223 & -9.6060 \\
0 & 0 & 0 & 538.2891 & 0 & 0 & \cdots & 63.7274 & -136.8998
\end{bmatrix} \\
B &= \begin{bmatrix}
0 & 0 & 0 & 0 \\
0 & 0 & 0 & 0 \\
\cdots & \cdots & \cdots & \cdots \\
0 & 0 & 0 & 0 \\
2 & 0 & 143.4894 & 0 \\
0 & 0 & 0 & -1905.7803 \\
\cdots & \cdots & \cdots & \cdots \\
0 & 0 & 0 & -3097.7273
\end{bmatrix}
\end{aligned}
\tag{128}
$$

Moreover, the feedback control vector is

$$
\mathbf{u}^{(1)} = [F_E^{(1)} \ \ \delta_a^{(1)} \ \ \delta_e^{(1)} \ \ \delta_r^{(1)}]^T \tag{129}
$$

in which it is assumed that the right and the left ailerons rotate by angles of the same magnitude $\delta_a^{(1)}$ but of opposite sense and that the right and left elevators rotate by angles of the same magnitude and sense.

Choosing the weighting matrices Q and R in the performance index, Eq. (66), as follows

$$
Q = \begin{bmatrix}
1 & 0 & 0 & 0 & 0 & 0 & 0 & \cdots & 0 \\
0 & 1 & 0 & 0 & 0 & 0 & 0 & \cdots & 0 \\
0 & 0 & 1 & 0 & 0 & 0 & 0 & \cdots & 0 \\
0 & 0 & 0 & 1 & 0 & 0 & 0 & \cdots & 0 \\
0 & 0 & 0 & 0 & 1 & 0 & 0 & \cdots & 0 \\
0 & 0 & 0 & 0 & 0 & 1 & 0 & \cdots & 0 \\
0 & 0 & 0 & 0 & 0 & 0 & 0 & \cdots & 0 \\
\cdots & \cdots & \cdots & \cdots & \cdots & \cdots & \cdots & \cdots & \cdots \\
0 & 0 & 0 & 0 & 0 & 0 & 0 & \cdots & 0
\end{bmatrix}
\qquad
R = \begin{bmatrix}
10 & 0 & 0 & 0 \\
0 & 5 \times 10^8 & 0 & 0 \\
0 & 0 & 10^8 & 0 \\
0 & 0 & 0 & 10^8
\end{bmatrix}
\tag{130}
$$

solving the steady-state Riccati equation, Eq. (73), and using Eq. (68), we obtain the gain matrix

$$
G = \begin{bmatrix}
0.2994 & 0 & 0 & 0 \\
0 & 0 & 0 & 0 \\
-0.1016 & 0 & 0.0001 & 0 \\
0.0003 & 0.5222 & 0 & 0.1024 \\
-1112.0150 & 0 & -1.8943 & 0 \\
-0.0187 & 1.9350 & 0 & 0.5103 \\
\cdots & \cdots & \cdots & \cdots \\
-0.0006 & 0 & 0 & 0 \\
0.0001 & 0 & 0 & 0 \\
0 & 0 & 0 & 0 \\
0 & 0 & 0 & 0
\end{bmatrix}^T
\tag{131}
$$

Then, solving the closed-loop eigenvalue problem, Eq. (75), we obtain the closed-loop eigenvalues

$$
\begin{aligned}
&\lambda_{1,2} = -0.1038 \pm 0.0868\, i,\ \lambda_{3,4} = -0.1174 \pm 0.2033\, i,\ \lambda_5 = -0.2349,\\
&\lambda_{6,7} = -0.2918 \pm 0.3064\, i,\ \dots,\ \lambda_{69,70} = -40.5617 \pm 599.4532\, i,\\
&\lambda_{71,72} = -40.7342 \pm 604.4685\, i,\ \lambda_{73,74} = -79.0030 \pm 791.6011 i,\\
&\lambda_{75,76} = -211.4842 \pm 1063.7436\, i
\end{aligned}
\tag{132}
$$

Clearly, all the eigenvalues are real and negative or complex with negative real part, so that the closed-loop first-order system is asymptotically stable. The implication is that any disturbances from the steady level flight are driven to zero. This is in contrast with the open-loop eigenvalues, the eigenvalues of A, the first four of which are zero and the fifth is real and positive.

Finally we consider the response of a closed-loop system to a gust acting on the wing and having the linearly distributed form

$$
\begin{aligned}
\mathbf{f}_w^R(x_w^R, t) &= [0\ \ 0\ \ -0.5(3 + x_w^R/L_w)\sin \pi t \sqcap (1-t)]^T,\ 0 < x_w^R < L_w\\
\mathbf{f}_w^L(x_w^L, t) &= [0\ \ 0\ \ -0.5(3 - x_w^L/L_w)\sin \pi t \sqcap (1-t)]^T,\ 0 < x_w^L < L_w
\end{aligned}
\tag{133}
$$

where $\sin \pi t \sqcap (1-t)$ represents a half-sine pulse, in which $\sqcap(1-t)$ is a rectangular function of unit amplitude and unit length. Inserting Eq. (133) into Eqs. (54), we obtain the generalized force components of the disturbance vector $\mathbf{F}_{\text{ext}}$ entering into Eq. (74), which can be integrated to obtain the system response. Figures 3-5 show the response for the rigid body variables and a selected number of elastic variables, and Fig. 6 shows the control inputs.

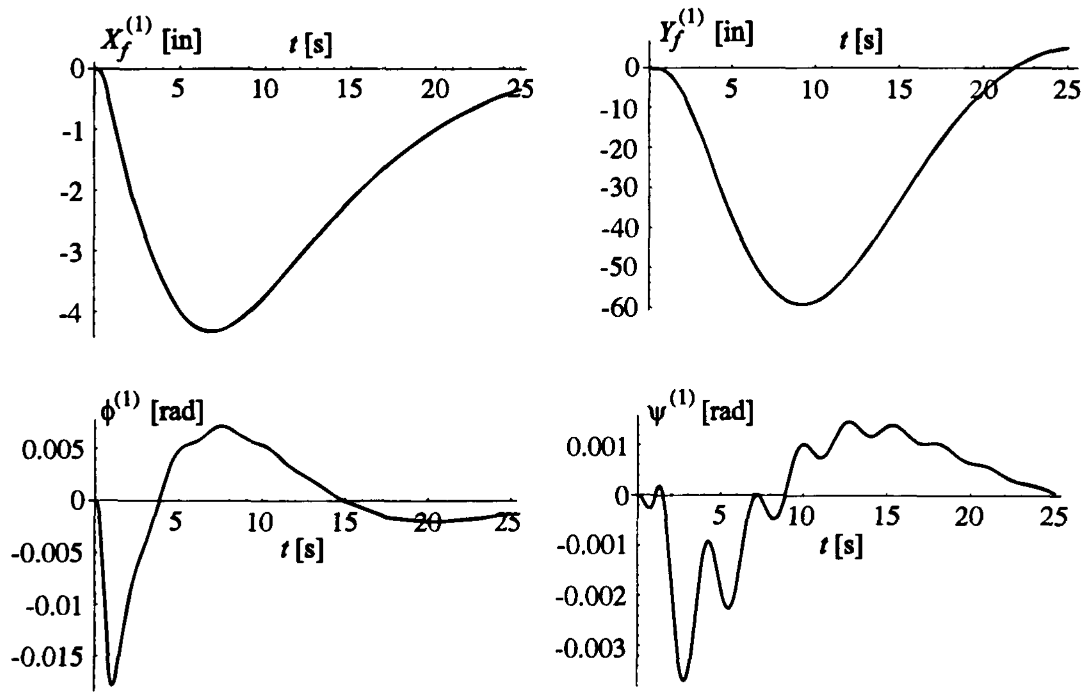

Figure 3. Rigid Body Displacements

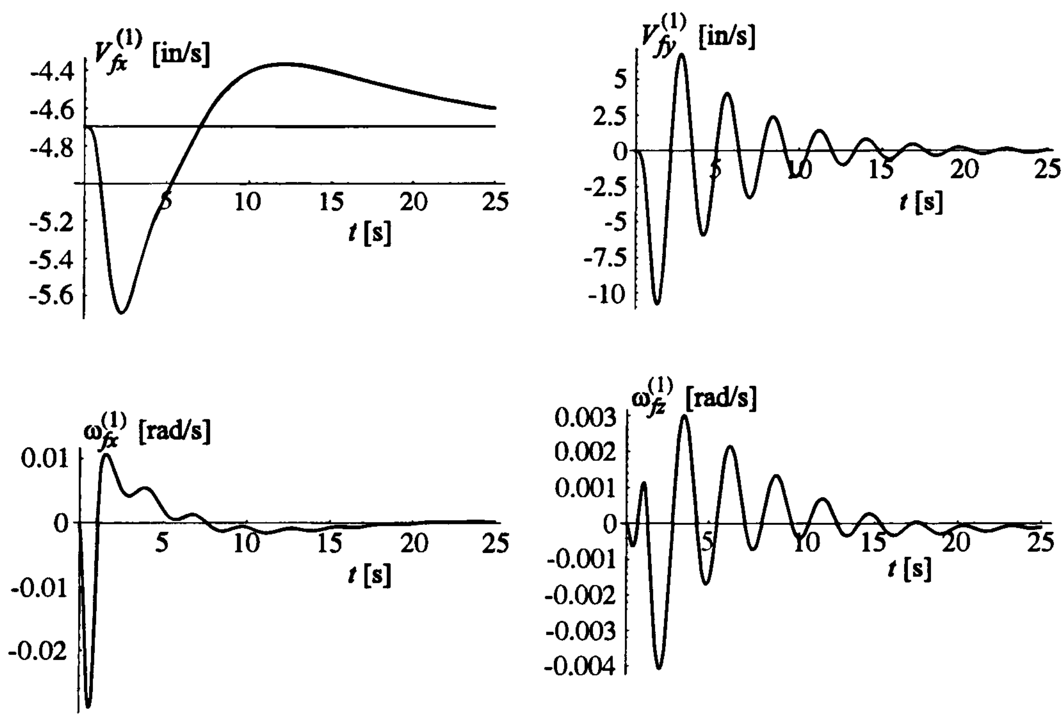

Figure 4. Rigid Body Velocities

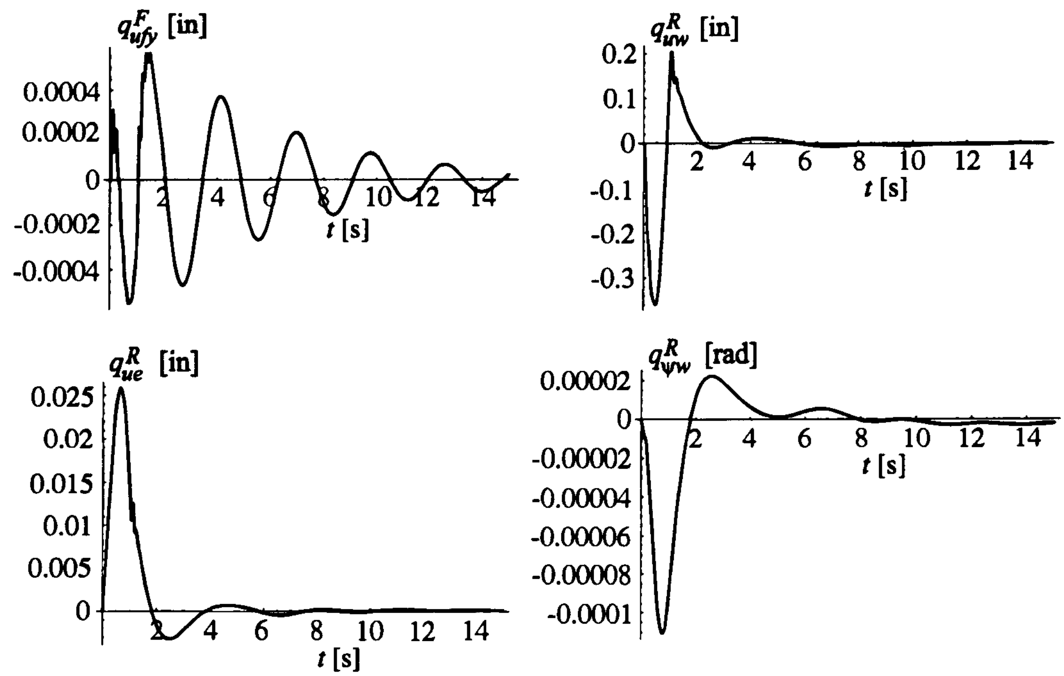

Figure 5. Generalized Elastic Displacements

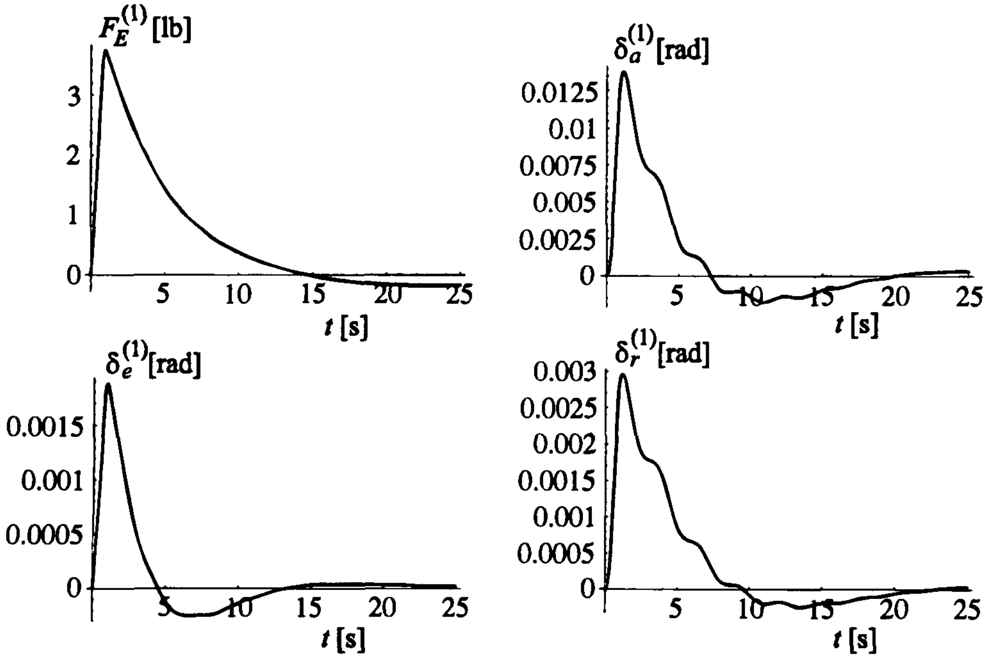

Figure 6. Control Inputs

Next, we turn our attention to the observer. To this end, we assume that $\mathbf{R}_f^{(1)}$ and $\boldsymbol{\theta}_f^{(1)}$ are available as part of the output of an inertial navigation system and that there are four sensors measuring velocities at the points P_k $(k = 1, 2, 3, 4)$ of each aircraft component. The coordinates x_k, y_k of P_k in component body axes, together with the type of velocities measured, are listed in Table 1. Moreover, the sensors locations are shown in Fig. A.

Table 1

	Fore Fuselage	Aft Fuselage	Right Wing	Left Wing	Right Horizontal Stabilizer	Left Horizontal Stabilizer	Vertical Stabilizer
$P_1 : x_1, y_1$	111.21, 36.25	111.92, 35.0	120.35, 58.23	120.35, −58.23	50.54, 32.0	50.54, −32.0	50.0, 42.0
Velocities	$\bar{V}_{fy}^{(1)}$ and $\bar{V}_{fz}^{(1)}$	$\bar{V}_{fy}^{(1)}$ and $\bar{V}_{fz}^{(1)}$	$\bar{V}_{wz}^{(1)}$	$\bar{V}_{wz}^{(1)}$	$\bar{V}_{ez}^{(1)}$	$\bar{V}_{ez}^{(1)}$	$\bar{V}_{ez}^{(1)}$
$P_2 : x_2, y_2$	111.21, −36.25	111.92, −35.0	120.35, −28.0	120.35, 28.0	46.6, −20.0	46.6, 20.0	41.0, −28.0
Velocities	$\bar{V}_{fz}^{(1)}$	$\bar{V}_{fz}^{(1)}$	$\bar{V}_{wz}^{(1)}$	$\bar{V}_{wz}^{(1)}$	$\bar{V}_{ez}^{(1)}$	$\bar{V}_{ez}^{(1)}$	$\bar{V}_{ez}^{(1)}$
$P_3 : x_3, y_3$	277.21, 24.0	279.79, 25.0	327.66, 25.07	327.66, −25.07	127.0, 19.0	127.0, −19.0	112.0, 27.0
Velocities	$\bar{V}_{fy}^{(1)}$ and $\bar{V}_{fz}^{(1)}$	$\bar{V}_{fy}^{(1)}$ and $\bar{V}_{fz}^{(1)}$	$\bar{V}_{wz}^{(1)}$	$\bar{V}_{wz}^{(1)}$	$\bar{V}_{ez}^{(1)}$	$\bar{V}_{ez}^{(1)}$	$\bar{V}_{ez}^{(1)}$
$P_4 : x_4, y_4$	277.21, −24.0	279.79, −25.0	327.66, −10.0	327.66, 10.0	127.0, −12.0	127.0, 12.0	113.0, −16.0
Velocities	$\bar{V}_{fz}^{(1)}$	$\bar{V}_{fz}^{(1)}$	$\bar{V}_{wz}^{(1)}$	$\bar{V}_{wz}^{(1)}$	$\bar{V}_{ez}^{(1)}$	$\bar{V}_{ez}^{(1)}$	$\bar{V}_{ez}^{(1)}$

To compute the matrix C, Eq. (103), relating the output vector to the state vector, we use Eq. (100) and write

$$M_V = \left[\begin{array}{ccccc} 0 \;\ldots & 0 & 0 & 0 & 0 \\ 0 \;\ldots & 0 & 0 & 0 & 0 \\ 0 \;\ldots & 0 & 0 & 0 & 0 \\ 0 \;\ldots & 0 & 1411.5402 & -1066.5377 & 0 \\ 0 \;\ldots & 0 & 0 & 0 & 21145.5039 \\ 0 \;\ldots & 0 & -21145.5039 & 15977.2118 & 0 \\ 0 \;\ldots & 0 & 0 & 0 & 0 \\ \cdots & \cdots & \cdots & \cdots & \cdots \\ 0 \;\ldots & 0 & 0 & 0 & 0 \end{array}\right]$$

$$
\begin{matrix}
\cdots & 0 & 0 & 0 & 0 & \cdots & 0 \\
\cdots & 0 & 0 & 0 & 0 & \cdots & 0 \\
\cdots & 0 & 0 & 0 & 0 & \cdots & 0 \\
\cdots & 4.2544 & 41.7049 & -7.3013 & 0 & \cdots & 0 \\
\cdots & -402.3892 & 0 & 0 & 0 & \cdots & 0 \\
\cdots & -63.7322 & -624.7574 & 109.3773 & 0 & \cdots & 0 \\
\cdots & 0 & 0 & 0 & 0 & \cdots & 0 \\
\cdots & \cdots & \cdots & \cdots & \cdots & \cdots & \cdots \\
\cdots & 0 & 0 & 0 & 0 & \cdots & 0
\end{matrix}
\Bigg] \tag{134}
$$

Then, inserting Eq. (134) into Eq. (103), we obtain

$$
C = \Bigg[
\begin{matrix}
1 & 0 & 0 & 0 & 0 & 0 & 0 & 0 & 0 & \cdots \\
\cdots & \cdots & \cdots & \cdots & \cdots & \cdots & \cdots & \cdots & \cdots & \cdots \\
0 & 0 & 0 & 0 & 0 & 1 & 0 & 0 & 0 & 0 \\
0 & 0 & 0 & 0 & 0 & 0 & 0.6890 & -0.5206 & 0.0026 & 0.0019 \\
0 & 0 & 0 & 0 & 0 & 0 & -1.8548 & 1.4015 & 4.1411 & -3.1290 \\
0 & 0 & 0 & 0 & 0 & 0 & 1.8590 & -1.4046 & 4.1328 & -3.1227 \\
\cdots & \cdots & \cdots & \cdots & \cdots & \cdots & \cdots & \cdots & \cdots & \cdots \\
0 & 0 & 0 & 0 & 0 & 0 & 1.5244 & -1.1518 & -0.0066 & 0.0050 \\
0 & 0 & 0 & 0 & 0 & 0 & -2.4135 & 1.8236 & -0.1611 & 0.1217 \\
0 & 0 & 0 & 0 & 0 & 0 & 1.8189 & -1.3970 & 0.1101 & -0.0832
\end{matrix}
$$

$$
\begin{matrix}
0 & 0 & \cdots & 0 & 0 \\
\cdots & \cdots & \cdots & \cdots & \cdots \\
0 & 0 & \cdots & 0 & 0 \\
-0.00003 & 0.0123 & \cdots & -0.0002 & 0 \\
0.0008 & 0.0320 & \cdots & -0.0004 & 0 \\
0.0011 & -0.0373 & \cdots & 0.0004 & 0 \\
\cdots & \cdots & \cdots & \cdots & \cdots \\
-0.0015 & 0.0871 & \cdots & -0.4412 & -0.6612 \\
0.0002 & -0.0260 & \cdots & 2.1761 & -1.4006 \\
0.0009 & -0.0385 & \cdots & -1.4522 & 0.9932
\end{matrix}
\Bigg] \tag{135}
$$

We assume that the excitation noise $\mathbf{v}(t)$ and observation noise $\mathbf{w}(t)$ represent white noise processes with intensities V and W, respectively, and choose

$$
\begin{aligned}
V = \mathrm{diag}[&100000\ 100000\ 100000\ 100000\ 100000\ 100000\ 10^{-9}\ 10^{-9} \\
&10^{-9}\ 10^{-9}\ 10^{-9}\ 10^{-9}\ 10^{-9}\ 10^{-9}\ 10^{-9}\ 10^{-9}\ 10^{-9}\ 10^{-9}10^{-9}\ 10^{-9}\ 10^{-9}\ 10^{-9}\ 10^{-9}\ 10^{-9} \\
&10^{-9}\ 10^{-9}\ 10^{-9}\ 10^{-9}\ 10^{-9}\ 10^{-9}\ 10^{-9}\ 10^{-9}\ 10^{-9}\ 10^{-9}10^{-9}\ 10^{-9}\ 10^{-9}\ 10^{-9}\ 0\ \ldots\ 0]
\end{aligned} \tag{136}
$$

and

$$
W = \mathrm{diag}[10^{-12}\ 10^{-12}\ 10^{-12}\ 10^{-6}\ 10^{-6}\ 10^{-6}\ 1\ \ldots\ 1] \tag{137}
$$

so that, from Eq. (91), the steady-state Riccati equation

$$
AQ + QA^T + V - QC^TW^{-1}CQ = 0 \tag{138}
$$

yields

$$
Q = \mathrm{diag}\left[\ 0.0003\quad 0.0003\quad 0.0003\quad 0.3162\quad 0.3162\quad 0.3162\quad \ldots\quad 0\quad 0\ \right] \tag{139}
$$

Hence, from Eq. (90), the optimal observer gain matrix is

$$K_o = QC^T W^{-1}$$

$$= \begin{bmatrix} 3.1623 \times 10^8 & 0 & 0 & 0 & 0 & 0 & \dots & 0 \\ 0 & 3.1623 \times 10^8 & 0 & -0.0003 & 0 & 0.0050 & \dots & 0 \\ 0 & 0 & 3.1623 \times 10^8 & 0 & -0.0050 & 0 & \dots & 0 \\ 0 & -332.6945 & 0 & 316227.7660 & 0 & 0 & \dots & 0 \\ 0 & 0 & -4995.0051 & 0 & 316227.7661 & 0 & \dots & 0 \\ 0 & 4995.0050 & 0 & 0 & 0 & 316227.7661 & \dots & 0 \\ 0.0018 & -0.6163 & 0.0023 & -0.0471 & -0.0003 & 0.1358 & \dots & 0 \\ -0.0013 & 0.4656 & -0.0018 & 0.0348 & 0.0002 & -0.1029 & \dots & 0 \\ 3.4719 & 0.0042 & 4.5563 & 0.0001 & -0.5724 & 0.0003 & \dots & 0 \\ -2.6233 & -0.0032 & -3.4428 & -0.0001 & 0.4346 & -0.0002 & \dots & 0 \\ 0.0016 & -0.5422 & 0.0021 & -0.0414 & -0.0003 & 0.1193 & \dots & 0 \\ \dots & \dots & \dots & \dots & \dots & \dots & \dots & \dots \\ 0 & -0.0014 & 0 & 0 & 0 & 0 & \dots & 0 \\ 0 & -0.0001 & 0 & 0 & 0 & 0 & \dots & 0 \end{bmatrix} \tag{140}$$

Finally, solving the eigenvalue problem for $A - K_0C$, we obtain the observer eigenvalues

$$\begin{aligned} &\lambda_1 = -0.0103,\ \lambda_{2,3} = -0.7807 \pm 1.6618i,\ \lambda_{4,5} = -0.1874 \pm 2.2166i, \\ &\lambda_6 = -5.7278,\ \lambda_{7,8} = -5.7237 \pm 36.9798i,\ \lambda_{9,10} = -3.7696 \pm 45.6080i, \\ &\lambda_{11,12} = -4.6367 \pm 62.6348i,\ \lambda_{13,14} = -4.2692 \pm 68.7929i, \dots, \\ &\lambda_{63,64} = -40.5621 \pm 599.4494i,\ \lambda_{65,66} = -40.7343 \pm 604.4687i, \\ &\lambda_{67,68} = -79.0066 \pm 791.5821i,\ \lambda_{69,70} = -211.4807 \pm 1063.7432i, \\ &\lambda_{71,72,73} = -316228,\ \lambda_{74,75,76} = -3.1623 \times 10^8 \end{aligned} \tag{141}$$

The performance of the observer design can be demonstrated by simulating the response of the combined system, defined by Eq. (84), to an initial state and initial observer error. To this end, we choose the values

$$\begin{aligned} \mathbf{x}^{(1)}(0) = [&5\ 5\ 5\ 0.005\ 0.005\ 0.005\ 0.2\ 0.1\ 0.2\ 0.1\ 0.2\ 0.1\ -0.2\ -0.1\ -0.2 \\ &-0.1\ -0.2\ -0.1\ -0.2\ -0.1\ -0.2\ -0.1\ -0.2\ -0.1\ 0.05\ 0.01\ -0.05 \\ &-0.01\ 0.05\ 0.01\ -0.05\ -0.01\ 0.05\ 0.01\ -0.05\ -0.01\ 0.05\ 0.01\ 0 \dots\ 0]^T \\ \mathbf{e}(0) = &-0.15\mathbf{x}^{(1)}(0) \end{aligned} \tag{142}$$

Figures 7-9 show the response for a selected number of rigid body and elastic variables and their observer estimates. Figure 10 shows the control inputs as given by Eq. (82).

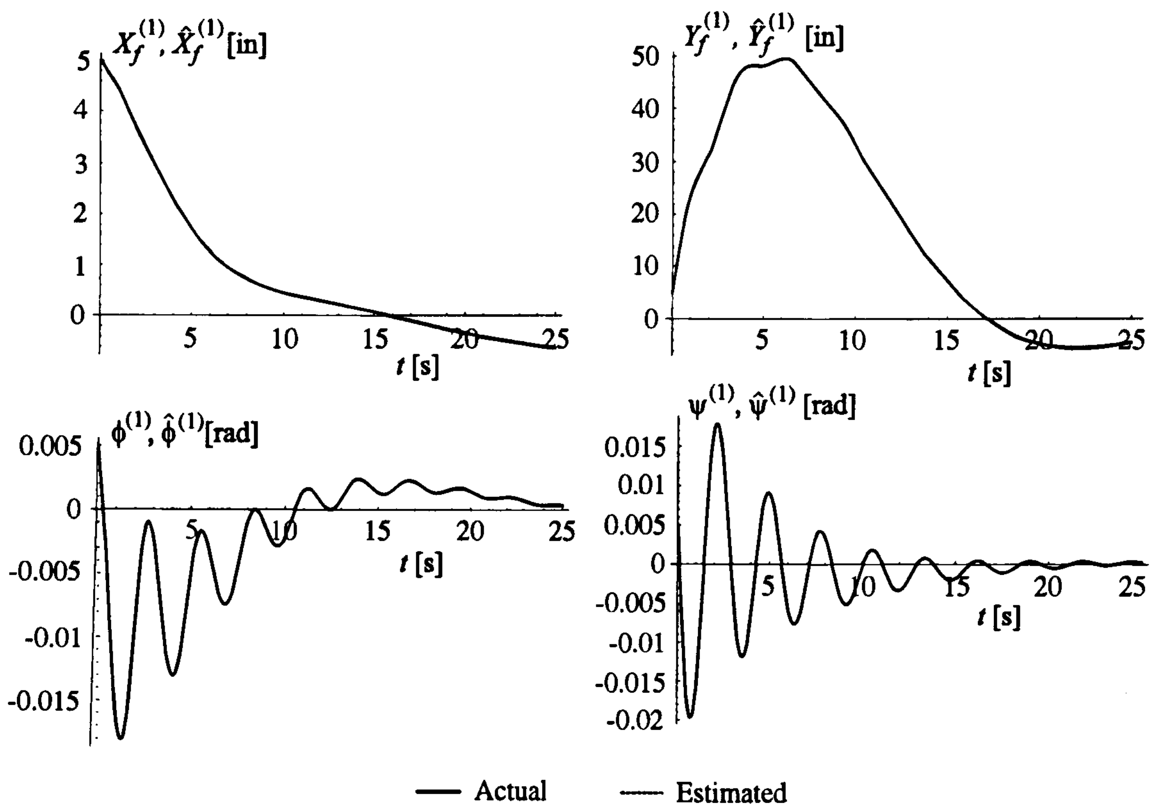

Figure 7. Rigid Body Displacements

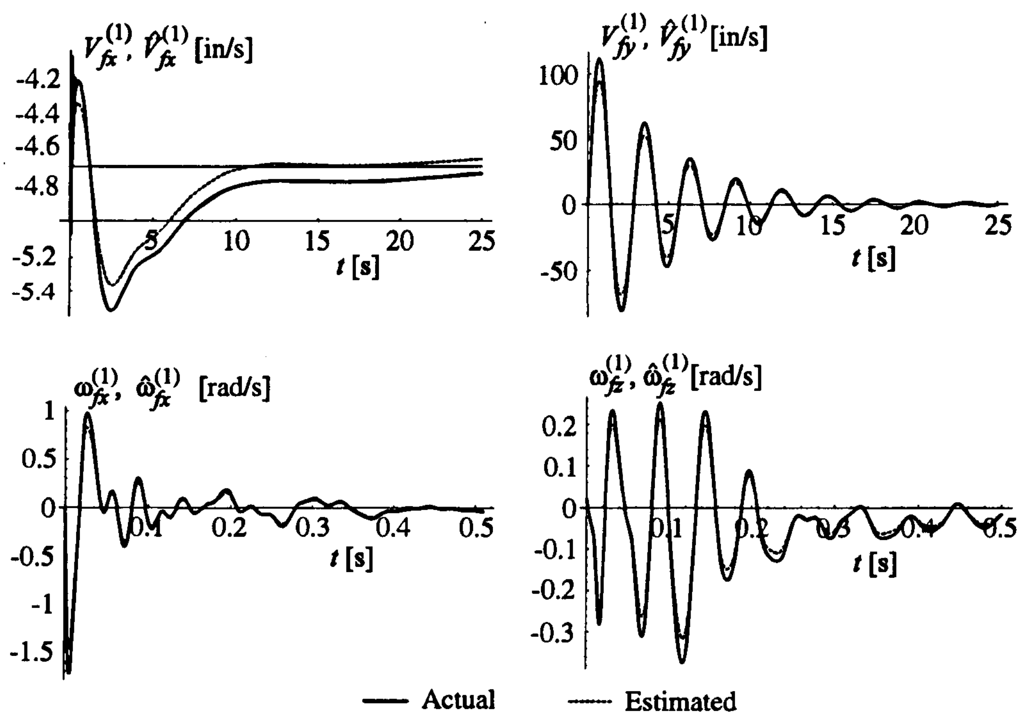

Figure 8. Rigid Body Velocities

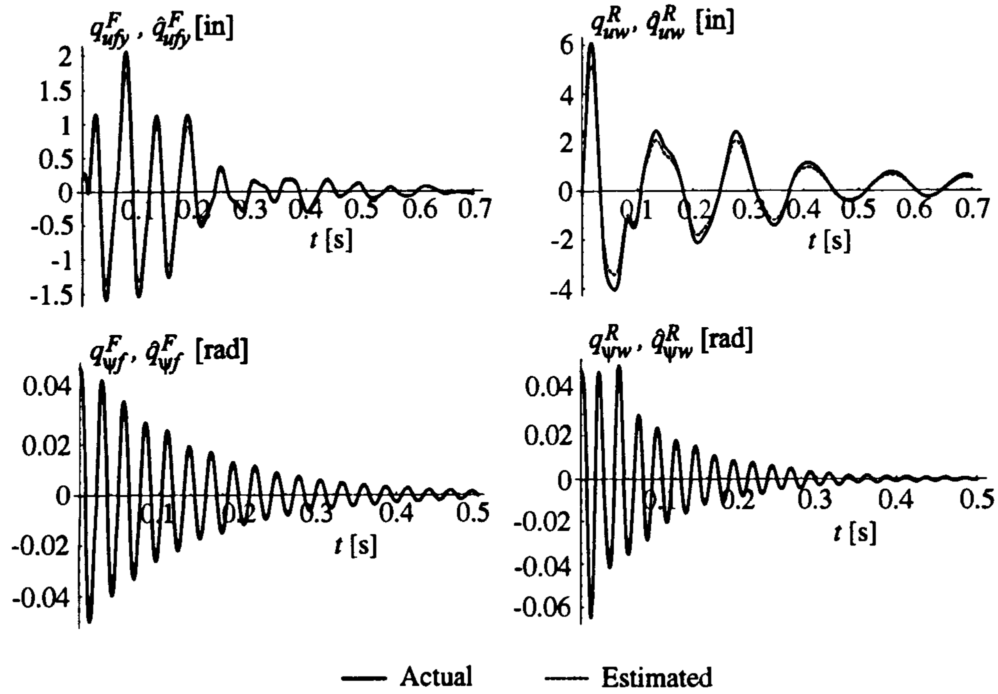

Figure 9. Generalized Elastic Displacements

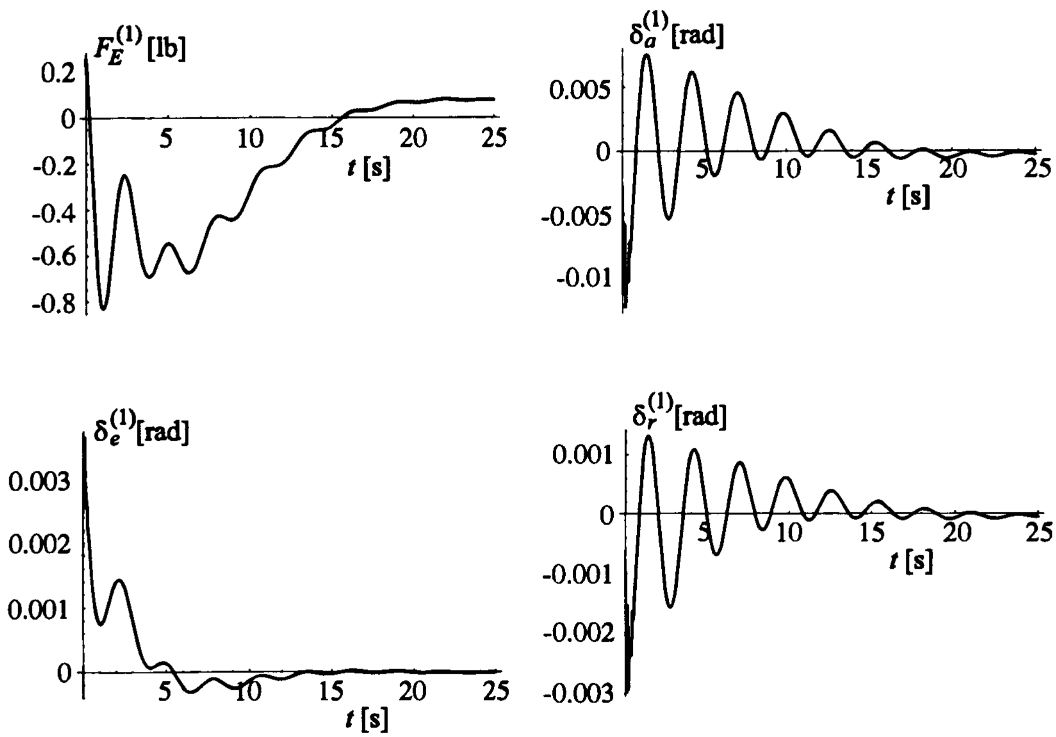

Figure 10. Control Inputs

ii. Level steady turn maneuver

We consider the case in which in the zero-order problem the aircraft flies at a constant velocity around a circular path of radius R in the horizontal X, Y-plane. In this case, it is convenient to refer the rigid body motions to a set of axes $x_1y_1z_1$ obtained through a rotation $\psi^{(0)}$ about Z, where $\dot{\psi}^{(0)} = \Omega =$ constant. It is not difficult to see that axes x_1, y_1 and z_1 represent a set of cylindrical axes t, n and Z, where t is tangent to the circle and n is normal to it. Denoting by $\dot{\bar{\mathbf{R}}}_f^{(0)}$ the velocity of O_f in terms of cylindrical components, the kinematical relation corresponding to the first of Eqs. (43) can be written as

$$\dot{\bar{\mathbf{R}}}_f^{(0)} = [\dot{R}_{ft}^{(0)} \ \ \dot{R}_{fn}^{(0)} \ \ \dot{Z}^{(0)}]^T = [R\Omega \ \ 0 \ \ 0]^T = \bar{C}_f^{(0)^T}\mathbf{V}_f^{(0)} \tag{143}$$

where

$$\bar{C}_f^{(0)} = \begin{bmatrix} c\theta^{(0)} & 0 & -s\theta^{(0)} \\ s\theta^{(0)}s\phi^{(0)} & c\phi^{(0)} & c\theta^{(0)}s\phi^{(0)} \\ s\theta^{(0)}c\phi^{(0)} & -s\phi^{(0)} & c\theta^{(0)}c\phi^{(0)} \end{bmatrix} \tag{144}$$

is the matrix of direction cosines between tnZ and the fuselage body axes $x_fy_fz_f$, obtained from C_f, the first of Eqs. (2), by letting $\psi = 0$ and replacing θ and ϕ by $\theta^{(0)}$ and $\psi^{(0)}$, respectively. Similarly, the second of Eqs. (43) can be written as

$$\dot{\boldsymbol{\theta}}_f^{(0)} = [\dot{\phi}^{(0)} \ \ \dot{\theta}^{(0)} \ \ \dot{\psi}^{(0)}] = [0 \ \ 0 \ \ \Omega]^T = (E_f^{(0)})^{-1}\boldsymbol{\omega}_f^{(0)} \tag{145}$$

where $E_f^{(0)}$ can be obtained from E_f, the second of Eqs. (2), by replacing θ and ϕ by $\theta^{(0)}$ and $\psi^{(0)}$, respectively. Equations (143) and (145) yield

$$\mathbf{V}_f^{(0)} = [V_{fx}^{(0)} \ \ V_{fy}^{(0)} \ \ V_{fz}^{(0)}]^T = \bar{C}_f^{(0)}\dot{\bar{\mathbf{R}}}_f^{(0)} = R\Omega[c\theta^{(0)} \ \ s\theta^{(0)}s\phi^{(0)} \ \ s\theta^{(0)}c\phi^{(0)}]^T = \text{constant} \tag{146}$$

and

$$\boldsymbol{\omega}_f^{(0)} = [\omega_{fx}^{(0)} \ \ \omega_{fy}^{(0)} \ \ \omega_{fz}^{(0)}]^T = E_f^{(0)}\dot{\boldsymbol{\theta}}_f^{(0)} = \Omega[-s\theta^{(0)} \ \ c\theta^{(0)}s\phi^{(0)} \ \ c\theta^{(0)}s\phi^{(0)}]^T = \text{constant} \tag{147}$$

so that, from Eqs. (49), we have

$$\mathbf{p}_{Vf}^{(0)} = m\mathbf{V}_f^{(0)} + \tilde{S}^{(0)^T}\boldsymbol{\omega}_f^{(0)} = \text{constant}, \ \ \mathbf{p}_{\omega f}^{(0)} = \tilde{S}^{(0)}\mathbf{V}_f^{(0)} + J^{(0)}\boldsymbol{\omega}_f^{(0)} = \text{constant} \tag{148}$$

It follows that the equations of motion, the last two of Eqs. (43), reduce to

$$-\tilde{\omega}_f^{(0)}\mathbf{p}_{Vf}^{(0)} + \mathbf{F}^{(0)} = \mathbf{0}, \ \ -\tilde{V}_f^{(0)}\mathbf{p}_{Vf}^{(0)} - \tilde{\omega}_f^{(0)}\mathbf{p}_{\omega f}^{(0)} + \mathbf{M}^{(0)} = \mathbf{0} \tag{149}$$

which are independent of time.

To determine the parameters defining the steady level turn maneuver, we choose the turn radius R and angular velocity Ω and solve Eqs. (149) for the bank angle $\phi^{(0)}$, pitch angle $\theta^{(0)}$ and control vector $\mathbf{u}^{(0)} = [F_e^{(0)} \ \ \delta_a^{(0)} \ \ \delta_e^{(0)} \ \ \delta_r^{(0)}]^T$. Hence, assuming the values $R = 1.5\,\text{mi} = 95037\,\text{in}$ and $\Omega = 0.0526\,\text{rad/s}$, so that $R\Omega = 5000\,\text{in/s}$, and using Eqs. (146) and (147), we have

$$\mathbf{V}_f^{(0)} = 5000\begin{bmatrix} c\theta^{(0)} \\ s\theta^{(0)}s\phi^{(0)} \\ s\theta^{(0)}c\phi^{(0)} \end{bmatrix}, \ \ \boldsymbol{\omega}_f^{(0)} = 0.0526\begin{bmatrix} -s\theta^{(0)} \\ c\theta^{(0)}s\phi^{(0)} \\ c\theta^{(0)}c\phi^{(0)} \end{bmatrix} \tag{150}$$

We consider a flight at a 25000 ft altitude, so that the speed of sound is 1016.1 ft/s and, hence, the Mach number for the flight is $5000/(1016.1 \times 12) = 0.41$. Inserting Eqs. (150) into Eqs. (149) in conjunction with Eqs. (148) and solving the resulting transcendental equations, we obtain

$$\begin{aligned} &\theta^{(0)} = 0.0986\,\text{rad}, \ \ \phi^{(0)} = 0.6160\,\text{rad} \\ &F_E^{(0)} = 468.7429\,\text{lb}, \ \ \delta_a^{(0)} = -0.0028\,\text{rad}, \ \ \delta_e^{(0)} = -0.3233\,\text{rad}, \ \ \delta_r^{(0)} = -0.3445\,\text{rad} \end{aligned} \tag{151}$$

Then, the zero-order control force vector can be written as

$$\mathbf{F}_c^{(0)} = B^{(0)}\mathbf{u}^{(0)} =$$

$$\begin{bmatrix} 0 & 0 & 0 & 0 \\ 0 & 0 & 0 & 0 \\ 0 & 0 & 0 & 0 \\ 0 & 0 & 0 & 0 \\ 0 & 0 & 0 & 0 \\ 0 & 0 & 0 & 0 \\ 2 & 1.0370 & 178.2611 & 77.3023 \\ 0 & 0 & 0 & -1916.1116 \\ 0 & -13.7394 & -2875.1495 & 0 \\ 0 & 1.0746\times10^6 & 1.4415 & -154689.6019 \\ -27.92 & -164.5690 & -750586.5476 & -6240.6944 \\ 0 & 65027.5713 & 11.7592 & 532059.4480 \end{bmatrix} \begin{bmatrix} 468.7429 \\ -0.0028 \\ -0.3233 \\ -0.3445 \end{bmatrix} = \begin{bmatrix} 0 \\ 0 \\ 0 \\ 0 \\ 0 \\ 0 \\ 844.5606 \\ 654.9960 \\ 692.9931 \\ 50641.1455 \\ 171482.9784 \\ -182061.4664 \end{bmatrix} \tag{152}$$

As in the case of steady level flight, the aircraft experiences static deformations in the steady level turn maneuver as well. Denoting the corresponding constant quantities by the superscript (1) and subscript c, using the first of Eqs. (50) and letting $\mathbf{V}^{(1)}$ be the cylindrical coordinates counterpart of $\dot{\mathbf{R}}_f^{(1)}$, we can write

$$\begin{gathered} \mathbf{V}_{fc}^{(1)} = \bar{C}_f^{(0)}[\mathbf{V}^{(1)} - \bar{C}_f^{(1)T}\mathbf{V}_f^{(0)}] = \text{constant}, \ \boldsymbol{\omega}_{fc}^{(1)} = \mathbf{0} \\ \mathbf{s}_{uic} = \mathbf{0}, \ \mathbf{s}_{\psi ic} = \mathbf{0}, \ i = f, w, e \end{gathered} \tag{153}$$

The momenta are all constant and can be expressed in terms of the zero-order and first-order velocities and the static deformations using Eqs. (59).

A constant solution of the first-order equations, Eqs. (50), can be obtained by letting the left sides be equal to zero and solving for $\phi_c^{(1)}$, $\theta_c^{(1)}$, $\mathbf{u}_c^{(1)} = [F_{Ec}^{(1)} \ \delta_{ac}^{(1)} \ \delta_{ec}^{(1)} \ \delta_{rc}^{(1)}]^T$ and the static deformations $\mathbf{q}_{uic}$ and $\mathbf{q}_{\psi ic}$ $(i = f, w, e)$. Assuming that $\mathbf{V}^{(1)} = [-5 \ 0 \ 0]^T$ in/s and using the first of Eqs. (153), we obtain

$$\mathbf{V}_{fc}^{(1)} = \begin{bmatrix} -4.9754 - 492.1217\theta_c^{(1)} \\ -0.2843 + 2874.8121\theta_c^{(1)} + 486.4652\phi_c^{(1)} \\ -0.4017 + 4061.1909\theta_c^{(1)} - 344.3562\phi_c^{(1)} \end{bmatrix} \tag{154}$$

so that Eqs. (50) yield

$$\begin{aligned} \phi_c^{(1)} &= -0.0011\,\text{rad},\ \theta_c^{(1)} = -0.0013\,\text{rad} \\ \mathbf{u}_c^{(1)} &= [-4.0727 \ -0.0002 \ -0.0063 \ 0.0001]^T \\ \mathbf{q}_{ufc}^F &= [-0.0005 \ 0.0001 \ 0.1458 \ -0.0019]^T,\ \mathbf{q}_{\psi fc}^F = [-0.0001 \ 0]^T \\ \mathbf{q}_{ufc}^A &= [-0.0408 \ -0.0008 \ 0.0827 \ 0.0039]^T,\ \mathbf{q}_{\psi fc}^A = [0.0003 \ -0.0001]^T \\ \mathbf{q}_{uwc}^R &= [-4.1523 \ -0.3511]^T,\ \mathbf{q}_{\psi wc}^R = [0.0025 \ -0.0003]^T \\ \mathbf{q}_{uwc}^L &= [-4.1765 \ -0.3526]^T,\ \mathbf{q}_{\psi wc}^L = [-0.0025 \ 0.0003]^T \\ \mathbf{q}_{uec}^R &= [-0.0473 \ 0.0001]^T,\ \mathbf{q}_{\psi ec}^R = [0.0029 \ -0.0002]^T \\ \mathbf{q}_{uec}^L &= [-0.0489 \ 0.00008]^T,\ \mathbf{q}_{\psi ec}^L = [-0.0029 \ 0.0002]^T \\ \mathbf{q}_{uec}^V &= [0.0032 \ 0.0014]^T,\ \mathbf{q}_{\psi ec}^V = [0.0017 \ -0.0001]^T \end{aligned} \tag{155}$$

The mass matrices, Eqs. (15), for the steady turn case are as follows:

$$
\begin{aligned}
M_{12} = \tilde{S}^T &= \begin{bmatrix} 0 & 130.4114 & 0.1477 \\ -130.4114 & 0 & 0 \\ -0.1477 & 0 & 0 \end{bmatrix} + \begin{bmatrix} 0 & 0 & -4.2385 \\ 0 & 0 & 0 \\ 4.2385 & 0 & 0 \end{bmatrix} q^F_{ufy1} \\
&+ \begin{bmatrix} 0 & 0 & 3.2026 \\ 0 & 0 & 0 \\ -3.2026 & 0 & 0 \end{bmatrix} q^F_{ufy2} + \begin{bmatrix} 0 & 4.2385 & 0 \\ 0 & 0 & 0 \\ -4.2385 & 0 & 0 \end{bmatrix} q^F_{ufz1} + \dots \\
&+ \begin{bmatrix} 0 & 0.1095 & 0.0173 \\ -0.1095 & 0 & 0 \\ -0.0173 & 0 & 0 \end{bmatrix} q^L_{ue2} + \begin{bmatrix} 0 & 0 & -0.1252 \\ 0 & 0 & 0 \\ 0.1252 & 0 & 0 \end{bmatrix} q^V_{ue1} \\
&+ \begin{bmatrix} 0 & 0 & 0.0219 \\ 0 & 0 & 0 \\ -0.0219 & 0 & 0 \end{bmatrix} q^V_{ue2}, \; M^F_{13} = \begin{bmatrix} 0 & 0 & 0 & 0 \\ 4.2385 & -3.2026 & 0 & 0 \\ 0 & 0 & 4.2385 & -3.2026 \end{bmatrix}, \dots, \\
M_{22} = J &= \begin{bmatrix} 182795.8456 & -18.6695 & -37747.5473 \\ -18.6695 & 566091.8052 & 74.4042 \\ -37747.5473 & 74.4042 & 704068.0911 \end{bmatrix} + \begin{bmatrix} -0.0025 & -863.2814 & 0 \\ -863.2814 & 0 & -21.1022 \\ 0 & -21.1022 & -0.0025 \end{bmatrix} q^F_{ufy1} \\
&+ \begin{bmatrix} 0.0010 & 367.2116 & 0 \\ 367.2116 & 0 & 7.3208 \\ 0 & 7.3208 & 0.0010 \end{bmatrix} q^F_{ufy2} + \begin{bmatrix} 42.2044 & 0 & -863.2814 \\ 0 & 42.2044 & 0.0012 \\ -863.2814 & 0.0012 & 0 \end{bmatrix} q^F_{ufz1} + \dots \\
&+ \begin{bmatrix} 6.9557 & 3.2162 & -20.3065 \\ 3.2162 & 7.5394 & -1.2456 \\ -20.3065 & -1.2456 & -0.5837 \end{bmatrix} q^L_{ue2} + \begin{bmatrix} -0.0075 & 35.9911 & 0 \\ 35.9911 & 0 & 12.8965 \\ 0 & 12.8965 & -0.0075 \end{bmatrix} q^V_{ue1} \\
&+ \begin{bmatrix} 0.0022 & -4.0598 & 0 \\ -4.0598 & 0 & 4.0187 \\ 0 & 4.0187 & 0.0022 \end{bmatrix} q^V_{ue2}, \dots, \\
M^F_{23} &= \begin{bmatrix} -21.1022 & 7.3208 & -0.0012 & 0.0005 \\ 0 & 0 & -863.2814 & 367.2116 \\ 863.2814 & -367.2116 & 0 & 0 \end{bmatrix} + \begin{bmatrix} 0 & 0 & 2.4362 & -0.7090 \\ 0 & 0 & 0 & 0 \\ 0 & 0 & 0 & 0 \end{bmatrix} q^F_{ufy1} + \dots \\
&+ \begin{bmatrix} 0.7090 & -2.3655 & 0 & 0 \\ 0 & 0 & 0 & 0 \\ 0 & 0 & 0 & 0 \end{bmatrix} q^F_{ufz2}, \dots, \; M^V_{28} = \begin{bmatrix} 68.3900 & 72.7325 \\ 0 & 0 \\ -344.8056 & -402.1912 \end{bmatrix}, \dots, \\
M^A_{33} &= \begin{bmatrix} 2.4862 & -0.7090 & 0 & 0 \\ -0.7090 & 2.3655 & 0 & 0 \\ 0 & 0 & 2.4862 & -0.7090 \\ 0 & 0 & -0.7090 & 2.3655 \end{bmatrix}, \dots, \\
M^L_{88} &= \begin{bmatrix} 17.3669 & 10.8317 \\ 10.8317 & 32.5338 \end{bmatrix}, \; M^V_{88} = \begin{bmatrix} 34.1002 & 32.0129 \\ 32.0129 & 65.4667 \end{bmatrix}
\end{aligned}
\tag{156}
$$

Next, we consider the time-varying part of the first-order problem, Eqs. (50) with all quantities measured from the constant static solution. To this end, we use Eq. (63) in which the coefficient matrices are given by

$$
A = \begin{bmatrix}
0 & 0 & 0 & 0 & 0 & 0 & \dots & 0.0004 & -0.0001 & 0 \\
0 & 0 & 0 & -596.0114 & 0 & 5000 & \dots & -0.0008 & -0.0012 & -0.0001 \\
0 & 0 & 0 & 0 & -5000 & 0 & \dots & 0.0010 & -0.0008 & 0 \\
0 & 0 & 0 & 0 & 0.0529 & 0 & \dots & 0 & 0 & 0 \\
0 & 0 & 0 & -0.0524 & 0 & 0 & \dots & 0 & 0 & 0 \\
\hdotsfor{10} \\
0 & 0 & 0 & 174.9021 & 42.3914 & 0 & \dots & -76.1004 & 0.1415 & 0.0257 \\
0 & 0 & 0 & 370.8328 & -25.9627 & 0 & \dots & 0.0604 & -31.2428 & -9.6184 \\
0 & 0 & 0 & 438.1920 & -30.6787 & 0 & \dots & 0.1026 & 63.7171 & -136.9109
\end{bmatrix}
$$

$$
B = \begin{bmatrix}
0 & 0 & 0 & 0 \\
\hdotsfor{4} \\
0 & 0 & 0 & 0 \\
2 & 1.0326 & 176.1982 & 104.3594 \\
0 & 0 & 0 & -1901.4388 \\
0 & -10.2357 & -2143.1016 & 0 \\
0 & 800910.3941 & 1.8988 & -153505.0524 \\
-27.92 & -116.9527 & -561836.0209 & -8425.0411 \\
0 & 64654.3829 & 11.7819 & 527985.1550 \\
\hdotsfor{4} \\
0 & 0 & 0 & -7461.0801 \\
0 & 0 & 0 & -3090.6705
\end{bmatrix} \tag{157}
$$

and in which the feedback control vector has the form $\mathbf{u}^{(1)} = [F_E^{(1)} \;\; \delta_a^{(1)} \;\; \delta_e^{(1)} \;\; \delta_r^{(1)}]^T$. In the case in which $\mathbf{u}^{(1)} = \mathbf{0}$ and $\mathbf{F}_{\text{ext}} = \mathbf{0}$, the state equations admit an exponential solution yielding an eigenvalue problem. Solving the eigenvalue problem, we conclude that the system is unstable, with four eigenvalues being equal to zero and one being real and positive. Using a linear quadratic regulator in conjunction with the weighting matrices

$$
Q = \begin{bmatrix}
1 & 0 & 0 & 0 & 0 & 0 & \dots & 0 \\
0 & 1 & 0 & 0 & 0 & 0 & \dots & 0 \\
0 & 0 & 1 & 0 & 0 & 0 & \dots & 0 \\
0 & 0 & 0 & 1 & 0 & 0 & \dots & 0 \\
0 & 0 & 0 & 0 & 1 & 0 & \dots & 0 \\
0 & 0 & 0 & 0 & 0 & 1 & \dots & 0 \\
\hdotsfor{8} \\
0 & 0 & 0 & 0 & 0 & 0 & \dots & 0
\end{bmatrix}, \quad
R = \begin{bmatrix}
10 & 0 & 0 & 0 \\
0 & 6 \times 10^8 & 0 & 0 \\
0 & 0 & 10^8 & 0 \\
0 & 0 & 0 & 10^8
\end{bmatrix} \tag{158}
$$

solving the corresponding steady-state Riccati equation, Eq. (73), and using Eq. (68), we obtain the gain matrix

$$
G = \begin{bmatrix}
0.2974 & 0 & 0 & 0 \\
-0.0163 & 0 & -0.0001 & 0 \\
-0.1062 & 0 & 0.0001 & 0 \\
12.4530 & 0.5355 & 0.0531 & 0.1015 \\
-1022.6944 & -1.0086 & -1.2660 & -0.2651 \\
-71.9234 & 1.3797 & -1.4307 & 0.3965 \\
\hdotsfor{4} \\
-0.0006 & 0 & 0 & 0 \\
0.0001 & 0 & 0 & 0 \\
0 & 0 & 0 & 0 \\
0 & 0 & 0 & 0
\end{bmatrix}^T \tag{159}
$$

Then, solving the closed-loop eigenvalue problem, Eq. (75), we obtain the closed-loop eigenvalues

$$\begin{aligned}
&\lambda_{1,2} = -0.1031 \pm 0.0870i,\ \lambda_3 = -0.2342,\ \lambda_{4,5} = -0.1194 \pm 0.2172i, \\
&\lambda_{6,7} = -0.2998 \pm 0.3089i,\ \lambda_{8,9} = -0.7842 \pm 1.6226i,\ \dots, \\
&\lambda_{69,70} = -40.5623 \pm 599.4558i,\ \lambda_{71,72} = -40.7352 \pm 604.4713i \\
&\lambda_{73,74} = -79.0053 \pm 791.6059i,\ \lambda_{75,76} = -211.4850 \pm 1063.7465i
\end{aligned} \tag{160}$$

Clearly, all the closed-loop eigenvalues are either real and negative or complex with negative real part, so that the closed-loop first-order system is asymptotically stable. Hence, any disturbances from the steady level turn maneuver will be driven to zero.

Finally, we compute the response of the closed-loop system to the gust given by Eqs. (133). Figures 11-13 show a selected number of rigid body and elastic variables, and Fig. 14 shows the control inputs.

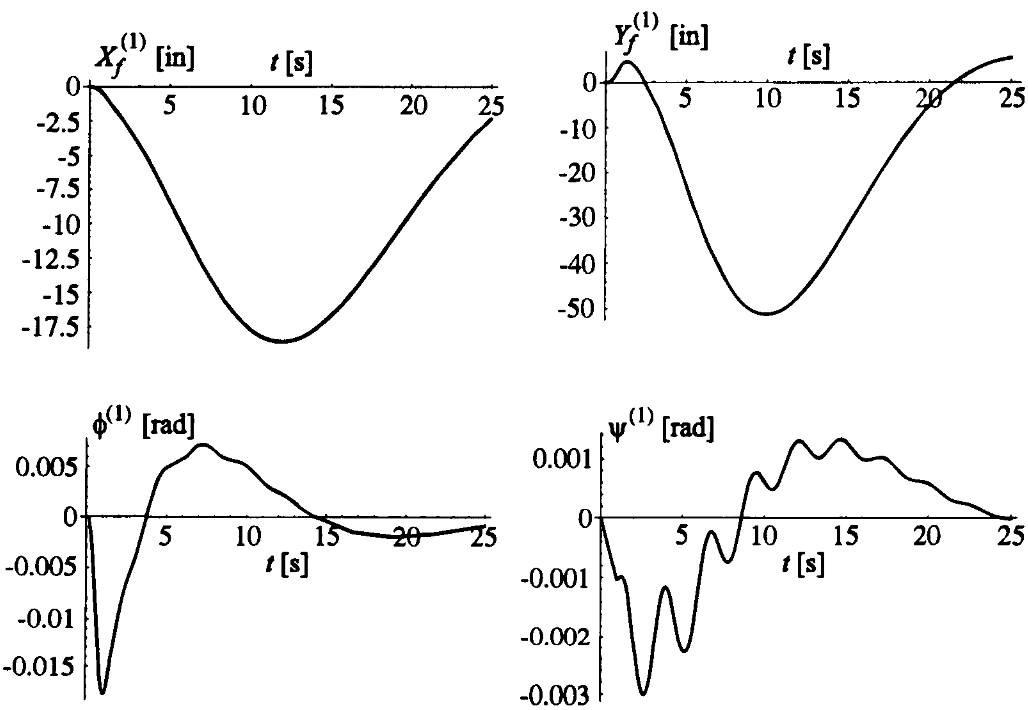

Figure 11. Rigid Body Displacements

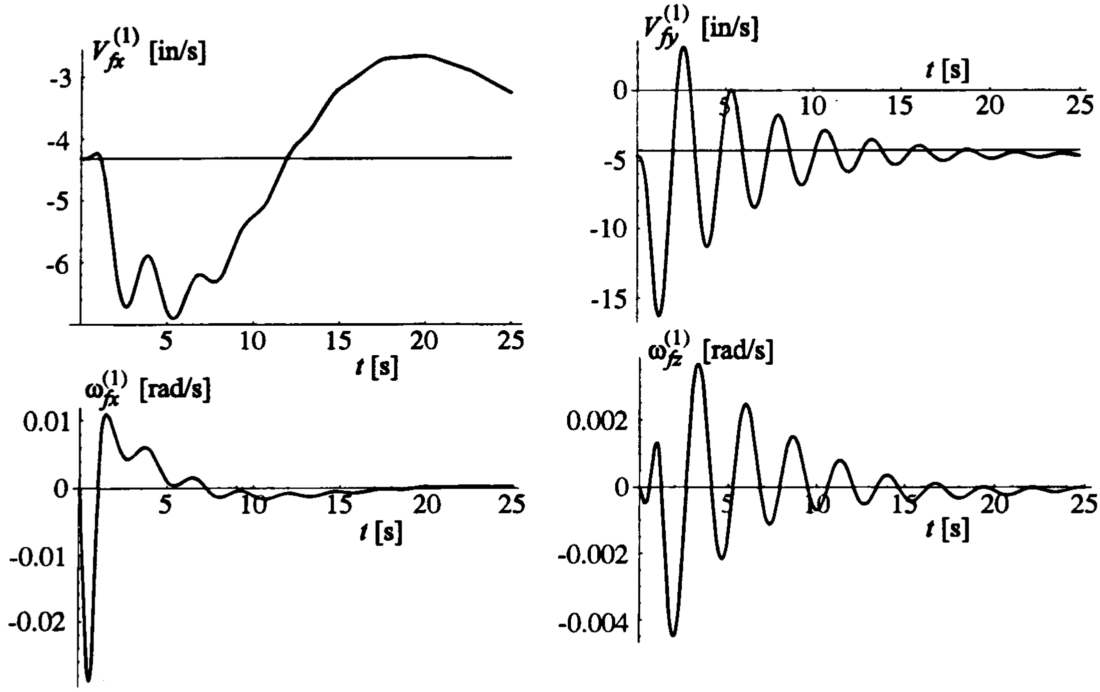

Figure 12. Rigid Body Velocities

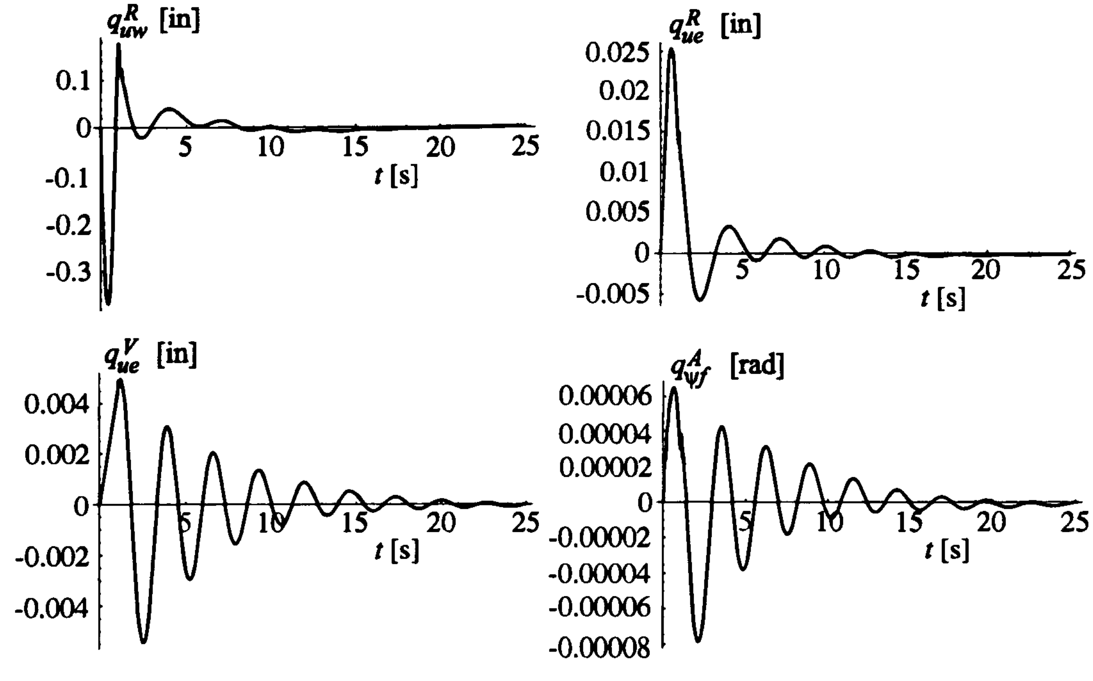

Figure 13. Generalized Elastic Displacements

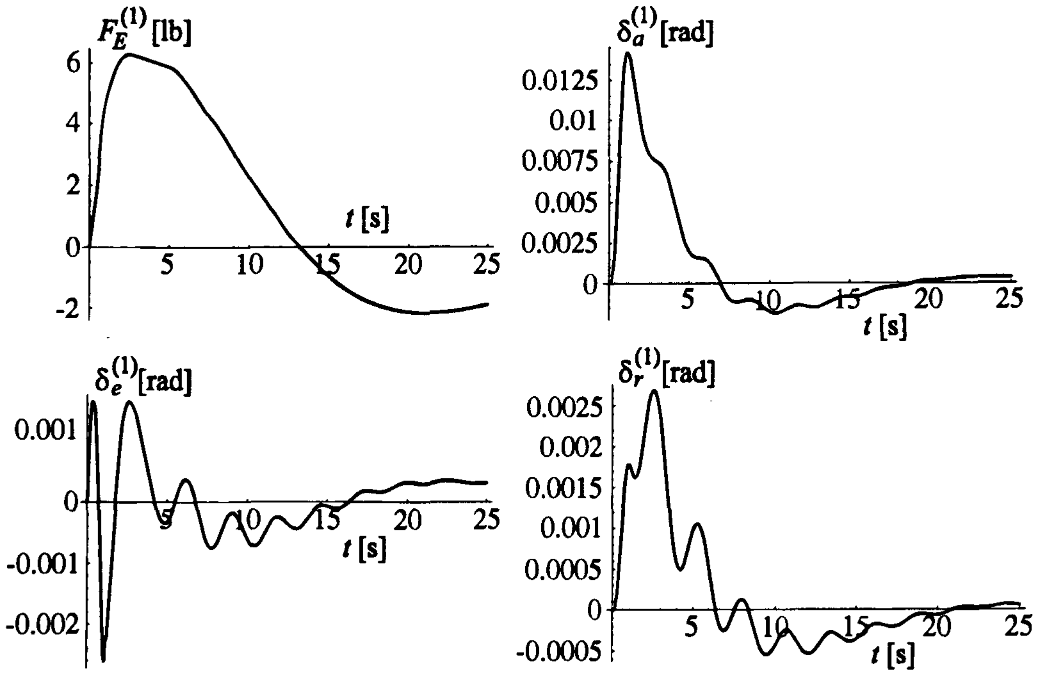

Figure 14. Control Inputs

Next, we turn our attention to the observer. To this end, we must compute the matrix C, Eq. (103), relating the output vector to the state vector. First, we use Eq. (100) and write

$$
M_V = \begin{bmatrix}
0 & \cdots & 0 & -0.1811 & 0.1369 & 0.1282 & -0.0030 & -0.0054 & 0.0009 & 0 & \cdots & 0 \\
0 & \cdots & 0 & 0 & 0 & 0.0219 & -0.0004 & 0 & 0 & 0 & \cdots & 0 \\
0 & \cdots & 0 & -0.0219 & 0.0166 & 0 & -0.0001 & -0.0006 & 0.0001 & 0 & \cdots & 0 \\
0 & \cdots & 0 & 1676.3711 & -1275.2629 & -1242.2537 & 27.2581 & 51.3897 & -8.9291 & 0 & \cdots & 0 \\
0 & \cdots & 0 & 3.5685 & -1.5887 & 21090.9413 & -401.1684 & 0.3647 & 0.1928 & 0 & \cdots & 0 \\
0 & \cdots & 0 & -21090.3030 & 15935.2420 & 0 & -63.5214 & -622.7178 & 109.2101 & 0 & \cdots & 0 \\
\cdots & \cdots & \cdots & \cdots & \cdots & \cdots & \cdots & \cdots & \cdots & \cdots & \cdots & \cdots \\
0 & \cdots & 0 & 0 & 0 & 0 & 0 & 0 & 0 & 0 & \cdots & 0
\end{bmatrix} \tag{161}
$$

Then, inserting Eq. (161) into Eq. (103), we obtain

$$
C = \begin{bmatrix}
1 & 0 & 0 & 0 & 0 & 0 & 0 & 0 & 0 & \cdots & 0 & \cdots & 0 & 0 \\
\cdots & \cdots & \cdots & \cdots & \cdots & \cdots & \cdots & \cdots & \cdots & \cdots & \cdots & \cdots & \cdots & \cdots \\
0 & 0 & 0 & 0 & 0 & 1 & 0 & 0 & 0 & 0 & 0 & \cdots & 0 & 0 \\
0 & 0 & 0 & 0 & 0 & 0 & 0.6400 & -0.4820 & 0.2213 & -0.1651 & 0 & \cdots & 0 & 0 \\
0 & 0 & 0 & 0 & 0 & 0 & -2.2285 & 1.6958 & 5.8787 & -4.4245 & 0 & \cdots & 0 & 0.0010 \\
0 & 0 & 0 & 0 & 0 & 0 & 2.2323 & -1.6989 & 2.3810 & -1.8161 & 0 & \cdots & 0 & 0.0011 \\
\cdots & \cdots & \cdots & \cdots & \cdots & \cdots & \cdots & \cdots & \cdots & \cdots & \cdots & \cdots & \cdots & \cdots \\
0 & 0 & 0 & 0 & 0 & 0 & 1.4370 & -1.0831 & 0.3731 & -0.2782 & 0 & \cdots & 0 & -0.0015 \\
0 & 0 & 0 & 0 & 0 & 0 & -2.3298 & 1.7578 & -0.5259 & 0.3938 & 0 & \cdots & 0 & 0.0002 \\
0 & 0 & 0 & 0 & 0 & 0 & 1.8150 & -1.3705 & 0.2414 & -0.1811 & 0 & \cdots & 0 & 0.0009
\end{bmatrix}
$$

$$
\left.\begin{array}{cccc}
0 & \cdots & 0 & 0 \\
\cdots & \cdots & \cdots & \cdots \\
0 & \cdots & 0 & 0 \\
0.0122 & \cdots & -0.0002 & 0 \\
0.0374 & \cdots & -0.0004 & 0 \\
-0.0372 & \cdots & 0.0004 & 0 \\
\cdots & \cdots & \cdots & \cdots \\
0.0871 & \cdots & -0.4412 & -0.6612 \\
-0.0259 & \cdots & 2.1761 & -1.4006 \\
-0.0384 & \cdots & -1.4522 & 0.9932
\end{array}\right] \tag{162}
$$

We assume that the excitation noise $\mathbf{v}(t)$ and observation noise $\mathbf{w}(t)$ represent white noise processes with intensities V and W, respectively, and choose

$$
\begin{aligned}
V = \mathrm{diag}[&100000\ 100000\ 100000\ 100000\ 100000\ 100000\ 10^{-9}\ 10^{-9}\ 10^{-9}\ 10^{-9}\ 10^{-9}\ 10^{-9}\ 10^{-9} \\
&10^{-9}\ 10^{-9}\ 10^{-9}\ 10^{-9}\ 10^{-9}\ 10^{-9}\ 10^{-9}\ 10^{-9}\ 10^{-9}\ 10^{-9}\ 10^{-9}\ 10^{-9}\ 10^{-9}\ 10^{-9}\ 10^{-9}\ 10^{-9} \\
&10^{-9}\ 10^{-9}\ 10^{-9}\ 10^{-9}\ 10^{-9}\ 10^{-9}\ 10^{-9}\ 10^{-9}\ 10^{-9}\ 0 \ldots 0]
\end{aligned} \tag{163}
$$

and

$$
W = \mathrm{diag}[10^{-12}\ 10^{-12}\ 10^{-12}\ 10^{-6}\ 10^{-6}\ 10^{-6}\ 1 \ldots 1] \tag{164}
$$

so that, from Eq. (91), the steady-state Riccati equation

$$
AQ + QA^T + V - QC^T W^{-1} CQ = 0 \tag{165}
$$

yields

$$
Q = \left[\begin{array}{cccccccccccc}
0.00032 & 0 & 0 & 0 & 0 & 0 & \cdots & 0 & 0 & \cdots & 0 \\
0 & 0.00032 & 0 & 0 & 0 & 0 & \cdots & 0 & 0 & \cdots & 0 \\
0 & 0 & 0.00032 & 0 & 0 & 0 & \cdots & 0 & 0 & \cdots & 0 \\
0 & 0 & 0 & 0.3162 & 0 & 0 & \cdots & 0 & 0 & \cdots & 0 \\
0 & 0 & 0 & 0 & 0.3162 & 0 & \cdots & 0 & 0 & \cdots & 0 \\
0 & 0 & 0 & 0 & 0 & 0.3162 & \cdots & 0 & 0 & \cdots & 0 \\
0 & 0 & 0 & 0 & 0 & 0 & \cdots & 0.0001 & 0 & \cdots & 0 \\
0 & 0 & 0 & 0 & 0 & 0 & \cdots & -0.0001 & -0.0001 & \cdots & 0 \\
\cdots & \cdots & \cdots & \cdots & \cdots & \cdots & \cdots & \cdots & \cdots & \cdots & \cdots \\
0 & 0 & 0 & 0 & 0 & 0 & \cdots & 0 & 0 & \cdots & 0 \\
0 & 0 & 0 & 0 & 0 & 0 & \cdots & 0.0705 & 0.0288 & \cdots & 0 \\
0 & 0 & 0 & 0 & 0 & 0 & \cdots & 0.0288 & 0.0133 & \cdots & 0 \\
\cdots & \cdots & \cdots & \cdots & \cdots & \cdots & \cdots & \cdots & \cdots & \cdots & \cdots \\
0 & 0 & 0 & 0 & 0 & 0 & \cdots & 0 & 0 & \cdots & 0 \\
0 & 0 & 0 & 0 & 0 & 0 & \cdots & 0 & 0 & \cdots & 0
\end{array}\right] \tag{166}
$$

Hence, from Eq. (90), the optimal observer gain matrix is

$$K_o = QC^TW^{-1}$$

$$= \begin{bmatrix} 3.1623\times10^8 & 0 & 0 & 0 & 0 & 0 & \dots & 0 \\ 0 & 3.1623\times10^8 & 0 & -0.0006 & 0 & 0.0050 & \dots & 0 \\ 0 & 0 & 3.1623\times10^8 & 0 & 0.0050 & 0 & \dots & 0 \\ 0 & -595.4161 & 0 & 316227.7660 & 0.0003 & 0 & \dots & 0 \\ 0 & 0.0001 & -4995.0050 & 0.0003 & 316227.7661 & 0.0026 & \dots & 0 \\ 0 & 4995.0050 & 0 & 0 & 0.0026 & 316227.7661 & \dots & 0 \\ -0.0427 & -0.7057 & -0.4951 & -0.0554 & -0.0783 & 0.1107 & \dots & 0 \\ 0.0326 & 0.5398 & 0.3786 & 0.0414 & 0.0594 & -0.0839 & \dots & 0 \\ 3.5739 & -1.8039 & 4.2355 & 0.0150 & -0.4665 & -0.3316 & \dots & 0 \\ -2.6997 & 1.3723 & -3.1937 & -0.0107 & 0.3542 & 0.2518 & \dots & 0 \\ \cdots & \cdots & \cdots & \cdots & \cdots & \cdots & \cdots & \cdots \\ 0.0003 & -0.0009 & 0.0010 & 0 & 0 & 0 & \dots & 0 \\ 0.0004 & -0.0008 & 0.0010 & 0 & 0 & 0 & \dots & 0 \\ -0.0001 & -0.0012 & -0.0008 & 0 & 0 & 0 & \dots & 0 \\ 0 & -0.0001 & 0 & 0 & 0 & 0 & \dots & 0 \end{bmatrix} \quad (167)$$

Finally, solving the eigenvalue problem for $A - K_oC$, we obtain the observer eigenvalues

$$\begin{aligned} &\lambda_1 = -0.0111,\ \lambda_{2,3} = -0.7858 \pm 1.6291i,\ \lambda_{4,5} = -0.1935 \pm 2.2231i, \\ &\lambda_6 = -5.7234,\ \lambda_{7,8} = -5.7294 \pm 36.9785i,\ \lambda_{9,10} = -3.7702 \pm 45.6096i, \\ &\lambda_{11,12} = -4.6312 \pm 62.6280i, \dots,\ \lambda_{63,64} = -40.5646 \pm 599.4514i, \\ &\lambda_{65,66} = -40.7353 \pm 604.4719i,\ \lambda_{67,68} = -79.0086 \pm 791.5892i, \\ &\lambda_{69,70} = -211.4819 \pm 1063.7463i,\ \lambda_{71,72} = -316227.8058 \pm 0.0346i, \\ &\lambda_{73} = -316227.8459,\ \lambda_{74,75,76} = -3.1623 \times 10^8 \end{aligned} \quad (168)$$

To check the performance of the observer just designed, we simulate the response of the combined system, Eq. (84) to the initial conditions

$$\begin{aligned} \mathbf{x}^{(1)}(0) = [&5\ 5\ 5\ 0.02\ 0.005\ 0.001\ 0.2\ 0.1\ 0.2\ 0.1\ 0.2\ 0.1\ -0.2\ -0.1 \\ &-0.2\ -0.1\ -0.2\ -0.1\ -0.2\ -0.1\ -0.2\ -0.1\ -0.2 \\ &-0.1\ 0.05\ 0.01\ -0.05\ -0.01\ 0.05\ 0.01\ -0.05\ -0.01 \\ &0.05\ 0.01\ -0.05\ -0.01\ 0.05\ 0.01\ 0 \dots 0] \\ \mathbf{e}(0) = {}&0.15\mathbf{x}^{(1)}(0) \end{aligned} \quad (169)$$

Figures 15-17 show a selected number of rigid body and elastic variables and Fig. 18 shows the control inputs as given by Eq. (82).

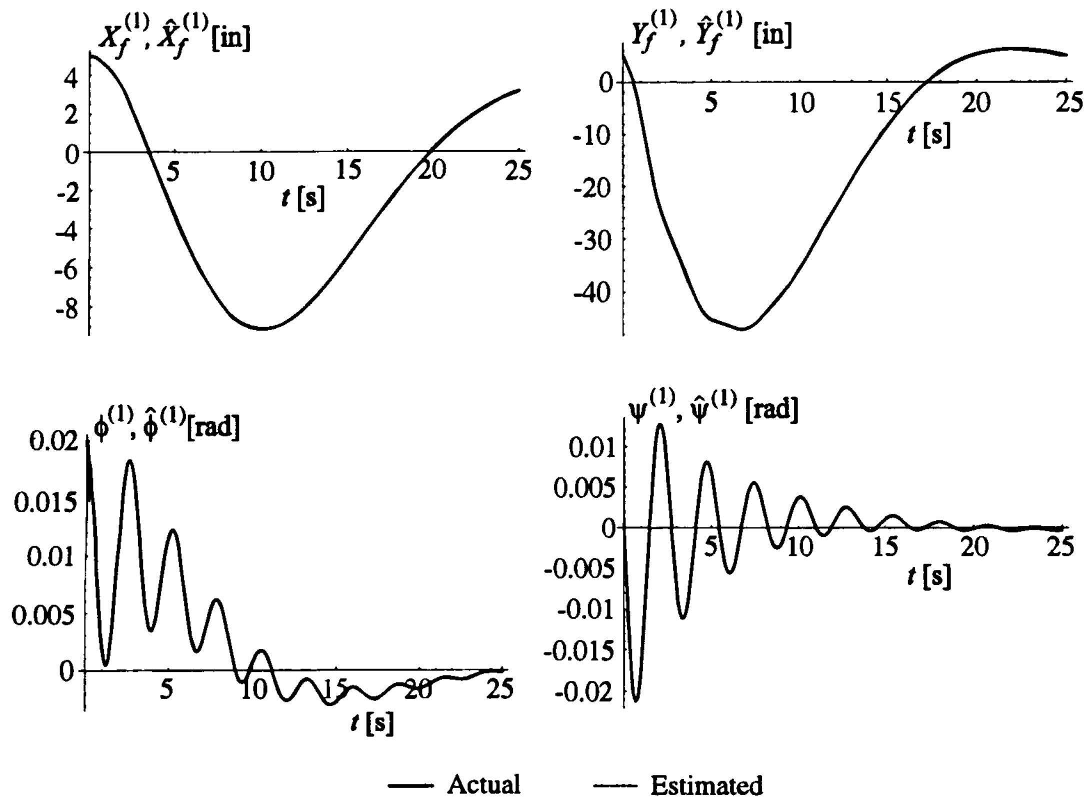

Figure 15. Rigid Body Displacements

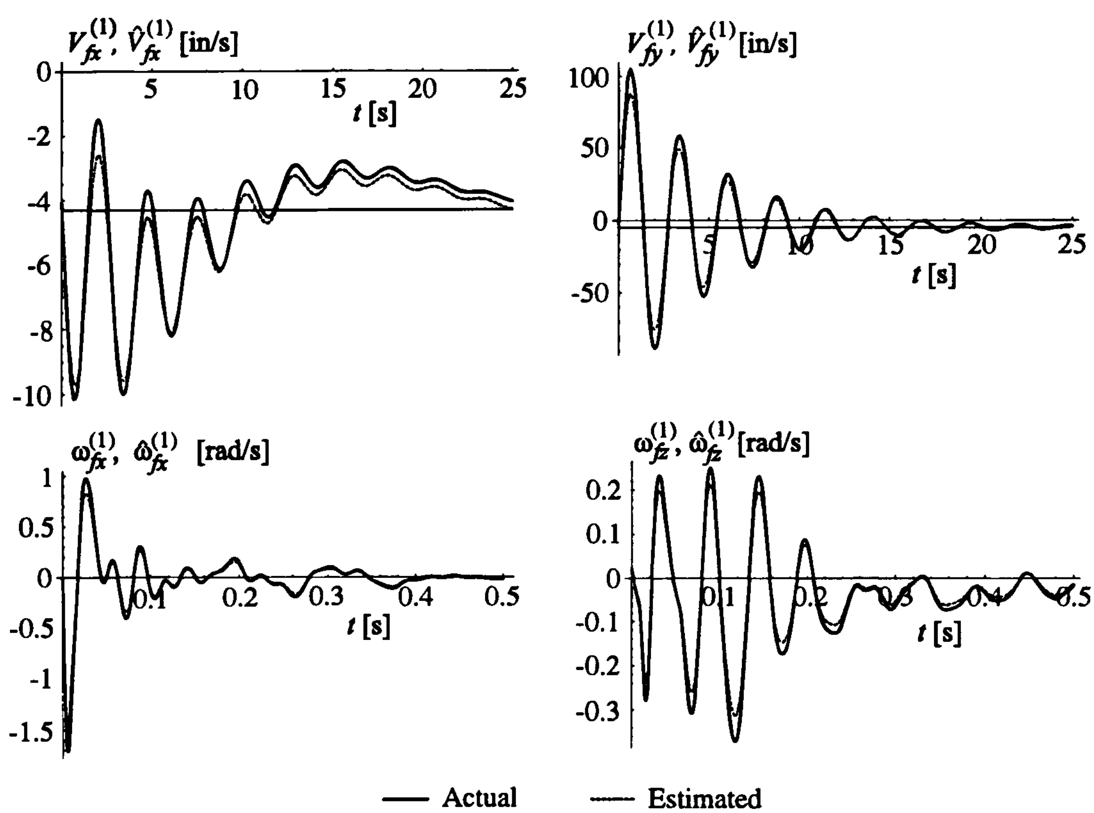

Figure 16. Rigid Body Velocities

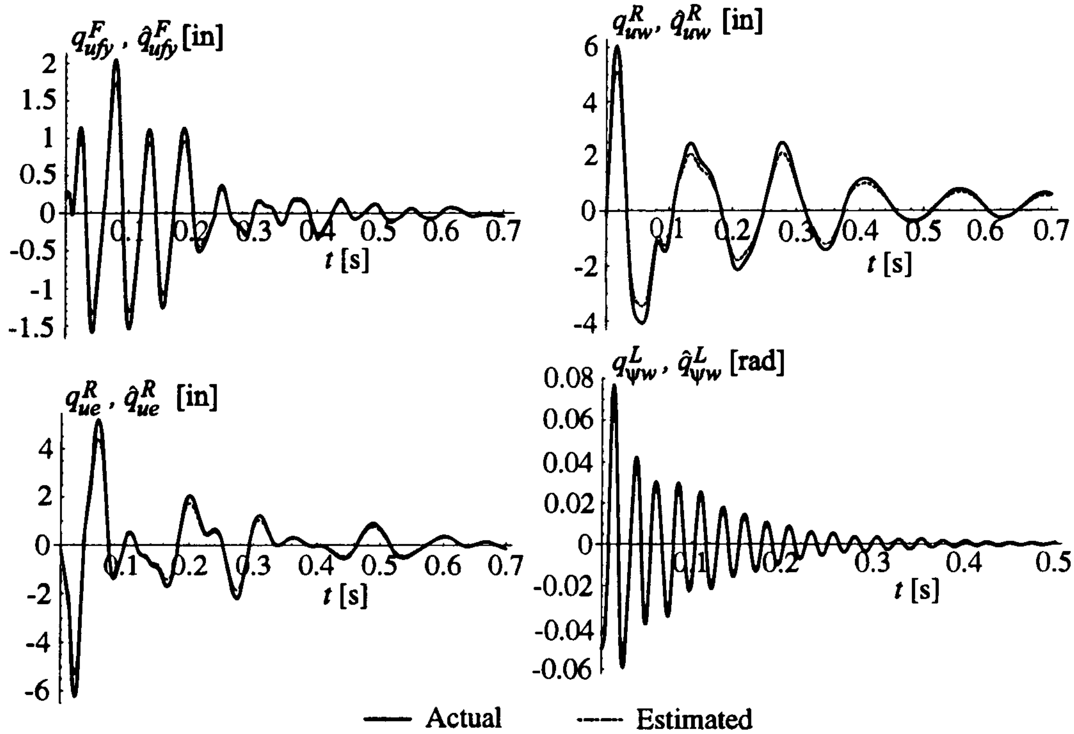

Figure 17. Generalized Elastic Displacements

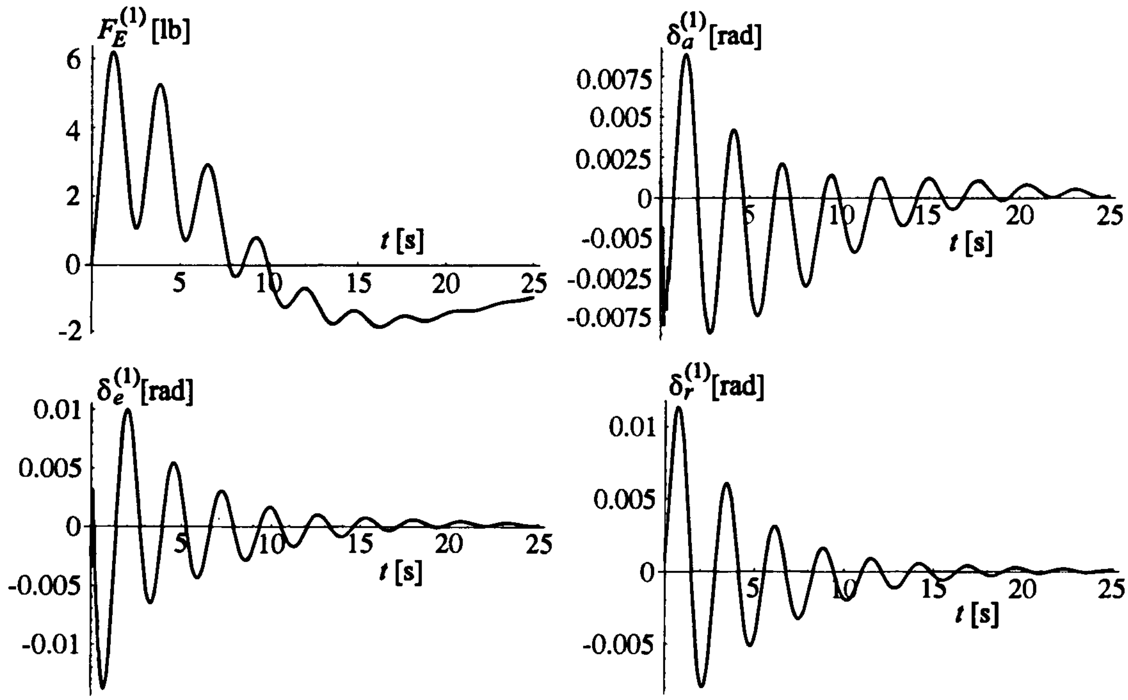

Figure 18. Control Inputs

9. Conclusions

A problem of increasing interest in aeronautics is the simulation of the flight of flexible aircraft on a computer. Note that on-line computer simulations can help expedite the design process, and possibly reduce the time devoted to flight testing. Moreover, the new class of autonomous aerial vehicles requires autopilots, which in turn requires real-time simulations. This points to the need for a new paradigm in the treatment of flying flexible aircraft, one using the system concept to produce a rigorous formulation of the dynamics and control problem and one using potent methodology permitting an efficient solution of the problem. This work develops such a paradigm in the form of an on-line formulation integrating pertinent material from the disciplines of analytical dynamics, structural dynamics, aerodynamics and controls. Moreover, the formulation is cast in a certain matrix form ideally suited for computer processing. A perturbation approach permits division of the problem into a nonlinear flight dynamics problem for maneuvering quasi-rigid aircraft and a linear "extended aeroservoelasticity" problem for the elastic deformations and small perturbations in the rigid body translations and rotations, where the solution of the first problem enters as an input into the second problem. As a result, there is a different extended aeroservoelasticity problem corresponding to each aircraft maneuver. The controls for the flight dynamics problem are obtained by an inverse process, which amounts to prescribing a given maneuver and determining the controls permitting realization of the given maneuver. On the other hand, the elastic deformations and perturbations in the rigid body motions characterizing the extended aeroservoelasticity problem are driven to zero by means of feedback controls designed using linear quadratic theory in conjunction with a stochastic observer, thus ensuring the stability of the aircraft maneuver. A numerical example presents a variety of time simulations of rigid body perturbations and elastic deformations about 1) a steady level flight and 2) a level steady turn maneuver.

The integration of the aerodynamics into the unified process is particularly challenging, and requires elaboration. For seamless integration, the aerodynamic forces must be referred to the same generally noninertial reference frame as that used for all other forces and they must be expressed in terms of variables compatible with the variables used throughout the entire formulation. Moreover, because the simulation of the system response on a computer is carried out in discrete time, the size of the time step is of vital importance. Indeed, on line and real time simulations require that the time step be quite small, the time step for the latter being of the order of a minute fraction of a second. The implication is that, to be ready to compute the state at the next sampling time, it is necessary to be able to compute the aerodynamic forces within the time step; the computation of the other forces within the same time step presents no problem. These two requirements are quite difficult to satisfy as most aerodynamic theories have been developed for purposes other than time response simulations, and the computation of the aerodynamic forces are notorious for consuming a great deal of time. In view of this, the development of a new aerodynamic method seems highly desirable. Such a method need not be unduly accurate, as robust feedback controls should be able to tolerate small errors in the aerodynamic forces. An aerodynamic theory satisfying the two requirements outlined above is strip theory. Even though strip theory may not be entirely satisfactory for describing the aerodynamic forces acting on whole aircraft, the method is often used in aircraft design. In fact it is being used by the same company that provided the data for the **Numerical Example**. The development of an aerodynamic technique suitable for on line, or real time response simulations is likely to require a great deal of time and effort. Although the use of a more suitable aerodynamic theory is desirable, it is not really necessary at this time. Indeed, at this time it is more important to demonstrate how the unified formulation works and how an eventual aerodynamic theory is to be integrated into the overall process. Certainly, such a demonstration can provide valuable guidance in the development of an appropriate aerodynamic method to be used in conjunction with aircraft time response simulations, thus helping reduce the time and effort required for the development in question.

Finally, it should be pointed out that, with appropriate modifications, the present formulation is eminently suited for UAVs, and in particular for autonomous UAVs. The fact that it was applied here to an executive jet is due entirely to the ready availability of data from an actual flying aircraft. It should also be pointed out that all the time response simulations presented here were carried out on a 1 GHz PC using MATHEMATICA. This is particularly important for autonomous UAVs, which must be controlled by autopilots, as the required onboard computer is likely to be much closer to a PC than to a multiprocessor supercomputer.

10. References

1. Collar, A. R., "The Expanding Domain of Aeroelasticity," *Journal of the Royal Aeronautical Society*, Vol. 50, 1946, p. 428.

2. J. B. Rea Co., "Aeroelasticity in Stability and Control," *Wright Air Development Center, Technical Report 55-173*, 1957.

3. Taylor, A. S., "The Present Status of Aircraft Stability Problems in the Aeroelastic Domain," *Journal of the Royal Aeronautical Society*, Vol. 63, 1959, p. 580.

4. Bisphinghoff, R. L. and Ashley, H., *Principles of Aeroelasticity* (Ch. 9), John Wiley & Sons, Inc., New York, 1962. (Reprinted by Dover Publications, Inc., New York, 1975).

5. Milne, R. D., "Dynamics of the Deformable Aeroplane, Parts I and II," *Her Majesty's Stationery Office, Reports and Memoranda No. 3345*, London, 1962.

6. Taylor, A. S. and Woodcock, D. L., "Mathematical Approaches to the Dynamics of Deformable Aircraft, Parts I and II, "*Her Majesty's Stationery Office*, Reports and Memoranda No. 3776, London, 1971.

7. Dusto, A.R. et al., "A Method for Predicting the Stability Characteristics of an Elastic Airplane, Vol. 1-FLEXSTAB Theoretical Description," *NASA CR-114712*, October 1974.

8. Roger, K. L., "Airplane Math Modeling Methods for Active Control Design," *Structural Aspects of Active Control, AGARD-CP-228*, 1977, pp. 4-1 – 4-11.

9. Schwanz, R. C., "Consistency in Aircraft Structural and Flight Control Analysis," *Structural Aspects of Active Control, AGARD-CP-228*, 1977, pp. 5-1 – 5-16.

10. Miller, G. D., Wykes, J.H. and Brosnan, M. J., "Rigid-Body Structural Mode Coupling on a Forward Swept Wing Aircraft," *Journal of Aircraft*, Vol. 20, No. 8, 1983, pp. 696-702.

11. Weisshaar, T. A. and Zeiler, T. A., "Dynamic Stability of Flexible Forward Swept Wing Aircraft," *Journal of Aircraft*, Vol. 20, No. 12, 1983, pp. 1014-1020.

12. Rodden, W. P. and Love, J. R., "Equations of Motion of a Quasi-Steady Flight Vehicle Utilizing Restrained Static Aeroelastic Characteristics," *Journal of Aircraft*, Vol. 22, No. 9, 1985, pp. 802-809.

13. Cerra, J. J.II, Calico, R. A. and Noll, T. E., "Modelling of Rigid-Body and Elastic Aircraft Dynamics for Flight Control Development," *Proceedings of the Atmospheric Flight Mechanics Conference*, Williamsburg, VA, Aug. 18-20, 1986, pp. 386-395.

14. Arbuckle, P. D., Buttrill, C.S. and Zeiler, T. A., "A New Simulation Model Building Process for Use in Dynamic Systems Integration Research," *Paper 87-2498, AIAA Flight Simulation Technologies Conference*, Monterey, CA, August 17-19, 1987.

15. Buttrill, C. S., Zeiler, T. A. and Arbuckle, P.D., "Nonlinear Simulation of a Flexible Aircraft in Maneuvering Flight, *Paper 87-2501-CP, AIAA Flight Simulation Technologies Conference*, Monterey, CA, Aug. 17-19, 1987.

16. Zeiler, T. A. and Butrill, C. S., "Dynamic Analysis of an Unrestrained, Rotating Structure Through Nonlinear Simulation," *Proceedings of the AIAA/ASME/ASCE/AHS 29th Structures, Structural Dynamics and Materials Conference*, Williamsburg, VA, April 18-20, 1988, pp. 167-177.

17. Waszak, M. R. and Schmidt, D. K., "Flight Dynamics of Aeroelastic Vehicles," *Journal of Aircraft*, Vol. 25, No. 6, 1988, pp. 563-571.

18. Sipcic, S. R. and Morino, L., "Dynamic Behavior of Fluttering Two-Dimensional Panels on an Airplane in Pull-Up Maneuver," *AIAA Journal*, Vol. 29, No. 8, 1991, pp. 1304-1312.

19. Waszak, M. R., Buttrill, C. S. and Schmidt, D. K., "Modeling and Model Simplification of Aeroelastic Vehicles: An Overview," *NASA TM 107691*, September 1992.

20. Bilimoria, K. D. and Schmidt, D. K., "Integrated Development of the Equations of Motion for Elastic Hypersonic Flight Vehicles," *Journal of Guidance, Control, and Dynamics*, Vol. 18, No. 1, 1995, pp. 73-81.

21. Olsen, J. J., "Unified Flight Mechanics and Aeroelasticity for Accelerating, Maneuvering, Flexible Aircraft," *RTO AVT Specialists' Meeting on "Structural Aspects of Flexible Aircraft Control"*, Ottawa, Canada, Oct. 18-20, 1999, pp. 6-1 – 6-12.

22. Teufel, P., Hanel, M. and Well, K. H., "Integrated Flight Mechanics and Aeroelastic Modelling and Control of a Flexible Aircraft Considering Multidimensional Gust Input," *RTO AVT Specialists' Meeting on "Structural Aspects of Flexible Aircraft Control"*, Ottawa, Canada, Oct. 18-20, 1999, 21, pp. 18-1 – 18-9.

23. König, K. and Schuler, J., "Integral Control of Large Flexible Aircraft," *RTO AVT Specialists' Meeting on "Structural Aspects of Flexible Aircraft Control"*, Ottawa, Canada, Oct. 18-20, 1999, 21, pp. 19-1 – 19-12.

24. Samareh, J. A. and Bhatia, K. G., "A Unified Approach to Modeling Multidisciplinary Interactions," *Paper 2000-4704, 8th AIAA/NASA/USAF/ISSMO Multidisciplinary Analysis and Optimization Symposium*, Long Beach, CA, September 6-8, 2000.

25. Schmidt, D. K. and Raney, D. L., "Modeling and Simulation of Flexible Flight Vehicles," *Journal of Guidance, Control, and Dynamics*, Vol. 24, No. 3, 2001, pp. 539-546.

26. Meirovitch, L., *Methods of Analytical Dynamics*, McGraw-Hill Book Co., New York, 1970. (A Dover Publications edition is to appear in 2003).

27. Meirovitch, L. and Nelson, H. D., "On the High-Spin Motion of a Satellite Containing Elastic Parts," *Journal of Spacecraft and Rockets*, Vol. 3, No. 11, 1966, pp. 1597-1602.

28. Meirovitch, L., "Hybrid State Equations of Motion for Flexible Bodies in Terms of Quasi-Coordinates," *Journal of Guidance, Control, and Dynamics*, Vol. 14, No. 5, 1991, pp. 1008-1013.

29. Platus, D. H., "Aeorelastic Stability of Slender, Spinning Missiles," *Journal of Guidance, Control, and Dynamics*, Vol. 15, No. 1, 1992, pp. 144-151.

30. Meirovitch, L., "Derivation of Equations for Flexible Multibody Systems in Terms of Quasi-Coordinates from the Extended Hamilton's Principle," *Journal of Shock and Vibration*, Vol. 1, Issue 2, 1993/94, pp. 107-119.

31. Meirovitch, L. and Stemple, T. J., "Hybrid Equations of Motion for Flexible Multibody Systems Using Quasi-Coordinates," *Journal of Guidance, Control, and Dynamics*, Vol. 18, No. 4, 1995, pp. 678-688.

32. Meirovitch, L., "A Unified Theory for the Flight Dynamics and Aeroelasticity of Whole Aircraft," *Proceedings of the Eleventh Symposium on Structural Dynamics and Control*, Blacksburg, VA, May 12-14, 1997, pp. 461-468.

33. Nydick, I. and Friedmann, P. P., "Aeroelastic Analysis of a Trimmed Generic Hypersonic Vehicle," *Proceedings of the CEAS/AIAA/ICASE/NASA International Forum on Aeroelasticity, and Structural Dynamics*, Langley Research Center, Hampton, VA, 1999, pp. 777-809.

34. Meirovitch, L. and Tuzcu, I., "Multidisciplinary Approach to the Modeling of Flexible Aircraft," *Proceedings of the CEAS/AIAA/AIAE International Forum on Aeroelasticity and Structural Dynamics*, Madrid, Spain, June 5-7, 2001, pp. 435-448.

35. Fornasier, L., Rieger, H. Tremel, U. and van der Weide, E., "Time-Dependent Aeroelastic Simulation of Rapid Manoeuvering Aircraft," Paper AIAA-2002-0949, *40th Aerospace Sciences Meeting and Exhibit*, Reno, NV, January 14-17, 2002.

36. Etkin, B., *Dynamics of Flight* (2nd Ed.), John Wiley & Sons, New York, 1982.

37. Meirovitch, L., *Principles and Techniques of Vibrations*, Prentice-Hall, Inc., Upper Saddle River, NJ, 1997.

38. Dowell, E. H. (Editor), *A Modern Course in Aeroelasticity* (3rd Ed.), Kluwer Academic Publishers, Dordrecht/Boston/London, 1995.

39. Meirovitch, L. and Seitz, T. J., "Structural Modeling for Optimization of Low-Aspect-Ratio Wings, " *Journal of Aircraft*, Vol. 32, No. 5, 1995, pp. 1114-1123.

40. Meirovitch, L., *Dynamics and Control of Structures*, John Wiley & Sons, New York, 1990.

41. Biezad, D. J., *Integrated Navigation and Guidance Systems*, AIAA Education Series, Reston, VA, 1999.

Appendix - Numerical Values of the Aircraft Parameters

The values of the pertinent aircraft parameters were provided by an aircraft manufacturer in lumped form, and the current formulation assumes distributed parameters. This presents no problem, however, as lumped parameters can always be treated as distributed by means of spatial Dirac delta functions.[37]

In the first place, we consider the aircraft geometry. To this end, we regard the fuselage as consisting of two cantilever beams, a fore part and an aft part, with the origin of both sets of body axes at point O_f and with axes x_f^F and x_f^A collinear (Fig. 2), where superscripts denote the fore part and aft part. The wing is also divided into two parts, the right half-wing and the left half-wing, both with the origin of the respective body axes at O_w^R and O_w^L and with the longitudinal axes coinciding with the respective elastic axes. Moreover, the empenage consists of the horizontal stabilizer, divided into a right half and a left half, both with the origin of the respective body axes at O_e^R and O_e^L, and a vertical stabilizer with the origin of the body axes at O_e^V. The radius vectors from O_f to the corresponding origins are

$$\begin{aligned} &\mathbf{r}_{fw}^R = \mathbf{r}_{fw}^L = [-5.04 \;\; 0 \;\; 38.33]^T \text{ in} \\ &\mathbf{r}_{fe}^R = \mathbf{r}_{fe}^L = [-244.75 \;\; 0 \;\; -43.13]^T \text{ in}, \;\; \mathbf{r}_{fe}^V = [-238.97 \;\; 0 \;\; -24.01]^T \text{ in} \end{aligned} \tag{A1}$$

The formulation calls for matrices of direction cosines between the various component body axes and the fuselage body axes, and in particular the body axes of the fore part of the fuselage denoted by $x_f y_f z_f$. The component body axes can be obtained from $x_f y_f z_f$ through a sequence of rotations. For example, axes $x_w^R y_w^R z_w^R$ for the right half-wing can be obtained through a rotation γ_1 about $x_f y_f z_f$ to an intermediate set of axes $x_w' y_w' z_w'$ and a rotation γ_2 about y_w' to $x_w^R y_w^R z_w^R$, where in the case of the wing γ_2 is known as the dihedral angle. Table 2 gives the rotation angles for the individual components.

Table 2 - Rotation Angles for Component Body Axes

Component Body Axes	Rotations		
	γ_1	γ_2	γ_3
$x_f^A y_f^A z_f^A$ Aft fuselage	180°	0	0
$x_w^R y_w^R z_w^R$ Right half-wing	90°	4°	0
$x_w^L y_w^L z_w^L$ Left half-wing	−90°	4°	0
$x_e^R y_e^R z_e^R$ Right horizontal stabilizer	94.30°	9°	0
$x_e^L y_e^L z_e^L$ Left horizontal stabilizer	−94.30°	9°	0
$x_e^V y_e^V z_e^V$ Vertical Stabilizer	0	118.74°	−90°

Using analogies with the first of Eqs. (2), the various matrices of direction cosines are as follows:

$$\begin{aligned} &C_f^A = \begin{bmatrix} -1 & 0 & 0 \\ 0 & -1 & 0 \\ 0 & 0 & 1 \end{bmatrix}, \quad C_w^R = \begin{bmatrix} 0 & 0.9976 & -0.0698 \\ -1 & 0 & 0 \\ 0 & 0.0698 & 0.9976 \end{bmatrix} \\ &C_w^L = \begin{bmatrix} 0 & -0.9976 & -0.0698 \\ 1 & 0 & 0 \\ 0 & -0.0698 & 0.9976 \end{bmatrix}, \quad C_e^R = \begin{bmatrix} -0.0750 & 0.9849 & -0.1560 \\ -0.9972 & -0.0741 & 0.0117 \\ 0 & 0.1564 & 0.9877 \end{bmatrix} \\ &C_e^L = \begin{bmatrix} -0.0750 & -0.9849 & -0.1560 \\ 0.9972 & -0.0741 & -0.0117 \\ 0 & -0.1564 & 0.9877 \end{bmatrix}, \quad C_e^V = \begin{bmatrix} -0.4808 & 0 & -0.8768 \\ -0.8768 & 0 & 0.4808 \\ 0 & 1 & 0 \end{bmatrix} \end{aligned} \tag{A2}$$

The inertia properties of the aircraft model are given in lumped form. To this end, the flexible components are divided into certain numbers of bays and the mass corresponding to each bay is lumped at the mass center of the bay. Moreover, the manner in which the mass is distributed over the associated cross-sectional area is represented by mass moments and mass products of inertia about axes with the origin at the mass center and parallel to the body axes of the respective component. Table 3 lists the coordinates of the mass centers, the mass values and the mass moments and mass products of inertia, in which the symmetry of the inertia matrices is implied. The masses have units $\text{lb} \cdot \text{s}^2/\text{in}$ and the mass moments and mass products of inertia have units $\text{lb} \cdot \text{s}^2 \cdot \text{in}$. The cantilever beams lengths are $L_f^F = 295.86$ in, $L_f^A = 279.79$ in, $L_w^R = L_w^L = 328.83$ in, $L_e^R = L_e^L = 127.46$ in, $L_e^V = 113.48$ in.

Table 3 - Inertia Properties

Fore Part of the Fuselage										
No.	x_f^F	y_f^F	z_f^F	m_f^F	J_{xxf}^F	J_{yyf}^F	J_{zzf}^F	J_{xyf}^F	J_{xzf}^F	J_{yzf}^F
1	7.41	0	5.20	0.7237	514.6542	230.8500	313.3728	−0.1010	−7.9229	0
2	24.74	0	1.98	0.2095	206.4986	115.1881	97.2035	−0.3495	1.4603	0
3	38.95	0	-1.54	0.3014	333.7084	182.4735	160.9599	0.1424	−1.9160	0
4	48.49	0	3.25	0.7558	354.9372	129.9051	251.8536	1.2350	−0.6913	0
5	55.08	0	8.60	0.3555	351.5220	181.4974	177.6291	1.3775	3.0682	0
6	69.88	0	7.88	0.5562	559.9651	274.9544	306.9516	−2.2111	2.9413	0
7	84.47	0	7.32	0.3167	298.6947	182.3156	124.5506	−0.3573	−2.2086	0
8	101.30	0	5.29	0.7053	501.1153	418.5278	480.2490	0.1657	5.3648	0
9	111.10	0	5.40	0.1546	137.1911	84.7780	54.2436	−0.1605	0.3754	0
10	129.67	0	1.62	1.0289	934.8339	556.8193	535.0830	−10.4733	1.2842	0
11	160.23	0	6.60	1.2664	919.9719	477.2896	595.6675	3.1044	17.3295	0
12	189.38	0	−0.30	1.0170	673.8353	340.9581	437.3046	2.3821	−20.5815	0
13	204.35	0	1.98	1.0789	623.3512	354.2640	386.3648	−0.4686	−1.1859	0
14	223.81	0	1.16	1.0497	394.7331	245.3210	192.5843	−0.8907	9.7354	0
15	237.71	0	6.55	0.2496	86.3807	41.6213	48.6587	−0.5308	0.0829	0
16	251.30	0	6.57	0.7234	135.0187	96.6805	69.4034	0.9425	−9.6525	0
17	266.50	0	14.02	0.4702	65.4238	49.4018	57.8918	1.1289	7.6562	0
18	281.47	0	17.71	0.0979	14.8309	8.2310	10.2739	−0.0104	−0.0647	0
19	292.08	0	17.66	0.0640	3.0164	2.1283	2.1801	−0.0673	0.0104	0
Aft Part of the Fuselage										
No.	x_f^A	y_f^A	z_f^A	m_f^A	J_{xxf}^A	J_{yyf}^A	J_{zzf}^A	J_{xyf}^A	J_{xzf}^A	J_{yzf}^A
1	1.67	0	0.81	0.1434	160.7476	76.2673	84.8272	−0.0052	0.1320	0
2	10.66	0	17.72	0.6147	2114.0956	253.7152	1887.3572	0.7172	8.8913	0
3	22.18	0	19.00	1.4282	3571.1313	848.8131	2879.2026	7.9514	−102.4285	0
4	40.41	0	2.00	0.1183	133.0820	72.5725	60.7063	0.0233	0.0777	0
5	46.82	0	8.04	0.5808	354.6912	221.2985	163.5387	-0.1709	-4.8263	0
6	66.11	0	9.51	0.2506	259.3829	186.0932	84.9230	0.4246	−0.7664	0
7	83.74	0	8.39	0.7843	900.7860	470.6690	478.1052	8.3087	−14.4348	0
8	98.21	0	3.87	0.5821	317.6683	222.4144	138.4934	−3.6275	2.4908	0
9	117.50	0	−8.33	0.5870	634.8913	217.1299	530.1143	−0.3728	11.5375	0
10	142.62	0	−6.45	0.6048	317.3757	146.8824	212.2078	0.5593	−4.3913	0
11	156.28	0	−10.77	0.4945	168.9475	127.7664	71.1511	3.7414	−6.0380	0
12	173.22	0	−11.04	0.1165	62.1588	48.9953	21.8166	0.4609	1.1496	0
13	189.26	0	−12.24	0.2131	49.4821	37.8178	19.5795	0.5644	1.3852	0
14	203.41	0	−6.82	0.1220	36.0701	28.0876	15.0225	−0.1605	−3.7207	0
15	218.31	0	−19.66	0.0880	40.5364	37.9395	11.4727	−0.0129	3.5368	0
16	238.30	0	−10.17	0.0585	14.7040	11.5064	5.9785	0.0078	−0.8596	0
17	253.16	0	−14.94	0.0580	6.6491	6.2555	3.7440	0.1036	−0.4220	0
18	278.12	0	−17.35	0.0098	0.4143	0.9580	0.8415	−0.0052	−0.1087	0

Table 3 - Continued

No.										
Wing										
No.	x_w^R	y_w^R	z_w^R	m_w^R	J_{xxw}^R	J_{yyw}^R	J_{zzw}^R	J_{xyw}^R	J_{xzw}^R	J_{yzw}^R
1	17.34	−5.67	−0.41	0.7932	592.7715	135.2155	675.5300	−11.4074	−20.6970	23.8870
2	41.44	−0.36	0.64	0.3380	259.1733	13.6761	253.5778	2.9790	0.1402	14.4486
3	55.80	7.21	0.72	0.5481	203.2508	22.5351	202.0929	−2.4412	−0.1781	16.5185
4	68.45	0.92	−1.55	0.2900	145.9962	10.7568	144.9995	1.1106	0.4620	4.8288
5	80.75	4.29	−0.63	0.3517	109.3290	19.5652	117.3550	0.4698	−1.1316	4.4349
6	95.11	2.34	−0.89	0.1960	87.6687	7.3973	86.7071	−3.5075	−0.1369	3.3911
7	109.21	5.70	−0.49	0.1405	68.3377	5.1512	67.9640	0.3682	−0.0707	3.2896
8	123.58	10.93	−0.20	0.2014	98.0351	8.6246	100.8629	−5.1787	−0.2981	4.7601
9	141.58	6.17	−0.36	0.1441	62.7718	6.3306	64.6489	−0.3631	−0.0224	2.5948
10	159.69	5.62	−0.59	0.1550	58.9409	7.3054	62.3486	−2.4040	−0.0168	1.5852
11	180.67	2.46	−0.60	0.1481	57.8061	6.8510	61.6321	−1.7038	0.0205	1.7613
12	199.99	5.62	−0.49	0.1504	44.7968	8.9780	51.3853	−4.0862	−0.1240	1.2184
13	223.12	3.28	−0.46	0.1146	26.2412	4.9868	29.6906	0.2463	0.0071	0.5415
14	242.88	1.87	−0.49	0.0825	16.9014	4.1168	19.9998	−0.2915	−0.0464	0.3456
15	260.53	−0.02	−0.71	0.0700	11.9896	2.0960	13.3314	0.1592	0.0681	0.3213
16	278.05	1.04	−0.46	0.0628	9.2044	1.9160	10.6262	0.1316	0.0019	0.0663
17	295.21	−0.06	−0.38	0.0471	6.9537	1.6338	8.2733	0.2092	−0.0066	−0.0035
18	311.97	−3.95	−0.38	0.0334	4.6844	0.6266	5.1908	0.1694	−0.0063	−0.0284
19	328.86	0.04	−0.40	0.0287	2.3874	0.7263	3.0305	−0.0109	−0.0045	−0.0293
Horizontal Stabilizer										
No.	x_e^R	y_e^R	z_e^R	m_e^R	J_{xxe}^R	J_{yye}^R	J_{zze}^R	J_{xye}^R	J_{xze}^R	J_{yze}^R
1	3.4154	−2.0199	4.8360	0.1298	152.7019	24.5226	24.9826	9.4614	−20.3966	0.6193
2	14.6498	4.1648	−0.0644	0.0618	13.3528	2.0288	14.9172	1.0676	−0.0060	0.0244
3	32.5615	6.2772	−0.0954	0.0625	12.1552	1.9324	13.7307	0.2775	0.0112	0.0409
4	50.7350	3.5463	−0.1694	0.0574	8.3296	2.7220	10.7676	0.5878	0.0612	−0.0078
5	66.0100	3.8814	−0.0389	0.0273	3.6287	0.3475	3.8652	0.2049	−0.0006	0.0143
6	76.5595	2.0048	0.0296	0.0173	2.3491	0.2014	2.4673	0.1894	0.0006	0.0055
7	88.2275	2.7918	−0.1213	0.0348	3.6527	0.9998	4.5598	0.3189	0.0164	0.0305
8	105.1312	2.4328	−0.0898	0.0259	2.2711	0.6068	2.8183	−0.0003	−0.0048	0.0187
9	121.3090	3.3819	−0.0468	0.0199	1.6192	0.4246	2.0069	0.1574	−0.0007	0.0040
10	128.5213	−2.0644	−0.0276	0.0135	0.3576	0.0114	0.3586	0.0197	−0.0001	−0.0010
Vertical Stabilizer										
No.	x_e^V	y_e^V	z_e^V	m_e^V	J_{xxe}^V	J_{yye}^V	J_{zze}^V	J_{xye}^V	J_{xze}^V	J_{yze}^V
1	−3.0130	−4.0388	0	0.0867	26.0215	26.8758	50.3184	18.1691	0.1131	0.1417
2	17.3464	−5.0753	0	0.0419	8.2448	2.9690	10.2273	3.9298	0.0052	0.0149
3	32.7117	−3.0312	0	0.0347	6.6885	2.6766	8.6842	3.2180	0.0097	0.0124
4	48.0499	−0.6415	0	0.0298	7.0021	2.2154	8.7929	3.2766	0.0395	0.0935
5	49.3577	25.8074	0	0.0741	5.0234	42.2968	46.9395	−2.2970	−0.0025	−0.0045
6	90.2614	−3.2365	0	0.0176	1.7168	1.1158	2.6177	1.0828	−0.1246	−0.1088
7	101.9491	19.9499	0	0.0062	0.2111	0.1462	0.3470	0.0991	0	0
8	103.6312	−3.8959	0	0.0150	1.3610	0.8632	2.1464	0.8286	−0.0010	0.0035
9	114.7248	−10.6405	0	0.0065	0.3567	0.2077	0.5619	0.2227	0	0
10	116.1657	2.4489	0	0.0523	4.5419	1.0689	5.5228	1.0377	0	0
Engine Pylon (Attached to the Aft Part of the Fuselage)										
No.	x_f^A	y_f^A	z_f^A	m_f^A	J_{xxf}^A	J_{yyf}^A	J_{zzf}^A	J_{xyf}^A	J_{xzf}^A	J_{yzf}^A
1	102.44	−64.05	−19.15	3.0115	347.7133	1947.0343	1872.5444	−18.0506	34.9386	4.6139
2	108.62	−37.00	−13.96	0.2647	35.2545	137.1807	162.3658	7.4957	11.3756	5.7131

The stiffness properties consist of the flexural rigidity and torsional rigidity of the cross-sectional area at certain locations of the elastic components. Both have units $\mathrm{lb} \cdot \mathrm{in}^2$. Table 4 gives the locations of the cross-sectional areas and the values of the corresponding rigidities.

Table 4 - Stiffness Properties

Fuselage

Fore Part

No.	x_f^F	EI_{fy}^F	EI_{fz}^F	GJ_f^F
1	0.00	1.10×10^{11}	7.40×10^{10}	4.07×10^{10}
2	10.21	1.10×10^{11}	7.44×10^{10}	4.10×10^{10}
3	25.21	1.10×10^{11}	7.47×10^{10}	4.12×10^{10}
4	38.21	1.10×10^{11}	7.47×10^{10}	4.12×10^{10}
5	47.21	1.10×10^{11}	7.47×10^{10}	4.12×10^{10}
6	55.21	1.10×10^{11}	7.47×10^{10}	4.12×10^{10}
7	70.21	1.10×10^{11}	7.45×10^{10}	4.12×10^{10}
8	84.71	1.10×10^{11}	7.36×10^{10}	4.12×10^{10}
9	99.71	1.10×10^{11}	7.20×10^{10}	4.12×10^{10}
10	111.21	1.10×10^{11}	7.03×10^{10}	4.12×10^{10}
11	129.21	1.08×10^{11}	6.80×10^{10}	4.11×10^{10}
12	144.21	1.02×10^{11}	6.54×10^{10}	3.87×10^{10}
13	160.21	9.06×10^{10}	6.14×10^{10}	3.14×10^{10}
14	185.71	6.5×10^{10}	5.25×10^{10}	1.71×10^{10}
15	205.71	4.37×10^{10}	4.23×10^{10}	8.67×10^{9}
16	224.71	2.68×10^{10}	3.97×10^{10}	2.98×10^{9}
17	238.11	1.76×10^{10}	2.04×10^{10}	2.19×10^{9}
18	251.11	1.11×10^{10}	1.28×10^{10}	1.27×10^{9}
19	267.06	6.01×10^{9}	6.42×10^{9}	6.43×10^{8}
20	282.06	3.13×10^{9}	2.87×10^{9}	3.05×10^{8}
21	295.86	1.16×10^{9}	6.15×10^{8}	7.72×10^{7}

Aft Part

No.	x_f^A	EI_{fy}^A	EI_{fz}^A	GJ_f^A
1	1.29	1.1×10^{11}	7.44×10^{10}	4.1×10^{10}
2	5.04	1.09×10^{11}	7.40×10^{10}	4.07×10^{10}
3	8.79	1.04×10^{11}	7.37×10^{10}	4.04×10^{10}
4	26.29	9.44×10^{10}	6.87×10^{10}	3.67×10^{10}
5	40.29	7.98×10^{10}	6.17×10^{10}	3.23×10^{10}
6	49.79	6.72×10^{10}	5.32×10^{10}	2.87×10^{10}
7	65.79	6.72×10^{10}	4.15×10^{10}	2.27×10^{10}
8	82.79	6.45×10^{10}	3.21×10^{10}	1.72×10^{10}
9	101.29	5.15×10^{10}	2.43×10^{10}	1.37×10^{10}
10	120.29	4.07×10^{10}	1.94×10^{10}	1.12×10^{10}
11	138.79	2.30×10^{10}	1.37×10^{10}	8.39×10^{9}
12	156.29	1.09×10^{10}	9.68×10^{9}	5.79×10^{9}
13	172.79	1.63×10^{10}	6.62×10^{9}	3.92×10^{9}
14	188.79	2.10×10^{10}	4.39×10^{9}	2.58×10^{9}
15	204.79	1.38×10^{10}	2.80×10^{9}	1.63×10^{9}
16	220.79	7.48×10^{9}	1.70×10^{9}	9.67×10^{8}
17	237.29	4.67×10^{9}	9.22×10^{8}	5.46×10^{8}
18	256.29	3.02×10^{9}	4.88×10^{8}	3.08×10^{8}
19	279.79	1.30×10^{9}	2.40×10^{8}	1.17×10^{8}

Wing

No.	x_w^R	EI_w^R	GJ_w^R
1	0.00	1.09×10^{10}	1.07×10^{10}
2	17.10	9.70×10^{9}	1.07×10^{10}
3	34.19	8.65×10^{9}	1.04×10^{10}
4	40.95	8.10×10^{9}	9.95×10^{9}
5	54.45	6.95×10^{9}	8.80×10^{9}
6	67.85	5.70×10^{9}	7.60×10^{9}
7	81.11	4.84×10^{9}	6.40×10^{9}
8	94.45	4.28×10^{9}	5.30×10^{9}
9	107.95	3.49×10^{9}	4.50×10^{9}
10	122.95	2.81×10^{9}	3.92×10^{9}
11	140.45	2.18×10^{9}	3.19×10^{9}
12	159.45	1.68×10^{9}	2.43×10^{9}
13	179.45	1.35×10^{9}	1.86×10^{9}
14	200.70	1.02×10^{9}	1.37×10^{9}
15	221.95	7.35×10^{8}	8.80×10^{8}
16	241.70	5.65×10^{8}	5.55×10^{8}
17	259.95	4.28×10^{8}	3.56×10^{8}
18	276.70	3.54×10^{8}	2.53×10^{8}
19	293.95	2.82×10^{8}	1.71×10^{8}
20	311.10	2.02×10^{8}	8.55×10^{7}
21	327.01	1.27×10^{8}	6.50×10^{6}

Horizontal Stabilizer

No.	x_e^R	EI_e^R	GJ_e^R
1	0.00	3.92×10^{8}	2.43×10^{8}
2	2.41	3.78×10^{8}	2.36×10^{8}
3	13.84	3.16×10^{8}	2.09×10^{8}
4	31.89	2.32×10^{8}	1.73×10^{8}
5	49.94	1.66×10^{8}	1.35×10^{8}
6	64.33	1.23×10^{8}	1.03×10^{8}
7	75.11	9.70×10^{7}	8.05×10^{7}
8	88.35	7.10×10^{7}	5.85×10^{7}
9	103.98	4.82×10^{7}	4.14×10^{7}
10	119.63	3.27×10^{7}	2.98×10^{7}
11	127.46	2.74×10^{7}	2.19×10^{7}

Vertical Stabilizer

No.	x_e^V	EI_e^V	GJ_e^V
1	0.00	1.56×10^{9}	7.30×10^{8}
2	7.40	1.33×10^{9}	6.70×10^{8}
3	21.15	9.66×10^{8}	5.57×10^{8}
4	34.90	6.86×10^{8}	4.45×10^{8}
5	49.73	4.61×10^{8}	3.55×10^{8}
6	63.98	3.06×10^{8}	2.41×10^{8}
7	77.63	2.01×10^{8}	1.38×10^{8}
8	91.31	1.26×10^{8}	8.69×10^{7}
9	105.82	6.88×10^{7}	3.56×10^{7}
10	113.48	4.25×10^{7}	8.51×10^{6}

The aerodynamic forces involve the slope $C_{L\alpha i}$ of the lift curve, the drag coefficient C_{Di0}, the slope $C_{s\beta i}$ of the lateral force curve and the control effectiveness coefficients $C_{L\delta a}$, $C_{s\delta e}$ and $C_{s\delta r}$. To determine the aerodynamic forces, the aircraft components are divided into a given number of sections and the coefficients are given for each of the sections. A typical section has a trapezoidal shape defined by two points $x_{ia}y_{ia}z_{ia}$ and $x_{ib}y_{ib}z_{ib}$ and by respective chords c_{ia} and c_{ib}, where the chords are parallel to the longitudinal axis x_f of the fuselage (Fig. A). For all

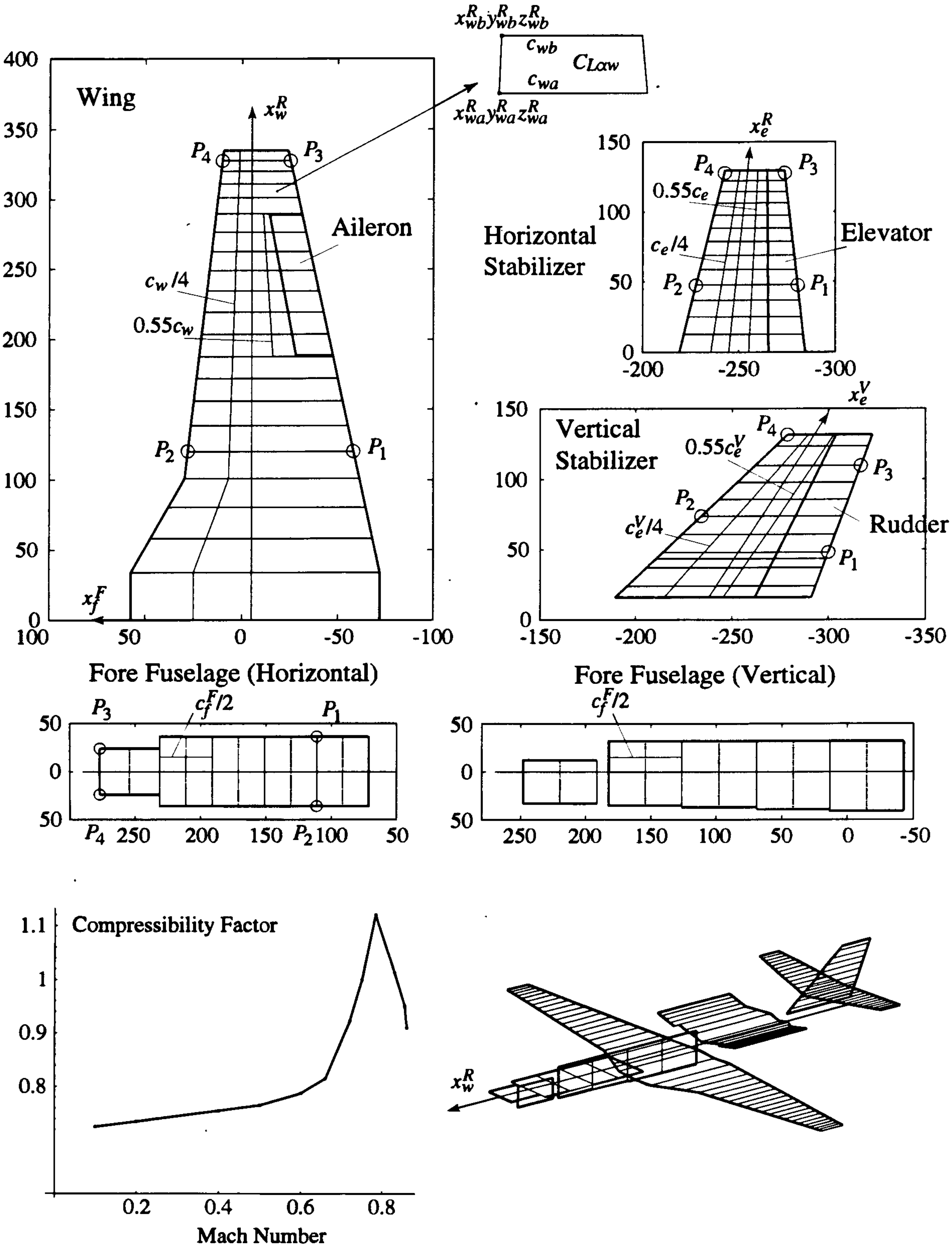

Figure A. Aerodynamic Sections for the Model sections, $C_{Df0} = C_{Dw0} = 0.016$ and $k_f = k_w = 0.04$. The lines of the aerodynamic centers are also shown in Fig. A; they are located at one quarter of the chord of the wing and horizontal and vertical stabilizers. The line of aerodynamic centers for the fuselage are located at one half of the chord of each aerodynamic section, as shown in Fig. A. The aerodynamic forces for the fore and aft parts of the fuselage are acting at the line of the aerodynamic centers. The control forces, on the other hand, are acting at 0.55 of the chord. The aerodynamic coefficients corresponding to the sections just mentioned are listed in Table 5. The slope of the lift coefficients and the control effectiveness for the aileron and the elevator listed in Table 5 are given for a single Mach number of 0.75. They must be corrected for different Mach numbers by the compressibility factor given in Fig. A. Note that there are only seven sections for the wing with control effectiveness coefficients; they correspond to the aileron.

Table 5

Fore Part of the Fuselage - Horizontal Lifting Surface									
x_{fa}^F	y_{fa}^F	z_{fa}^F	c_{fa}^F	x_{fb}^F	y_{fb}^F	z_{fb}^F	c_{fb}^F	$C_{L\alpha f}^F$	
111.21	−24.00	0.17	40.00	111.21	24.00	0.17	40.00	0.065	
151.21	−36.25	0.17	40.00	151.21	36.25	0.17	40.00	0.065	
191.21	−36.25	0.17	40.00	191.21	36.25	0.17	40.00	0.20	
231.21	−36.25	0.17	40.00	231.21	36.25	0.17	40.00	0.50	
277.21	−36.25	0.17	46.00	277.21	36.25	0.17	46.00	0.50	
Fore Part of the Fuselage - Vertical Lifting Surface									
x_{fa}^F	y_{fa}^F	z_{fa}^F	c_{fa}^F	x_{fb}^F	y_{fb}^F	z_{fb}^F	c_{fb}^F	$C_{L\beta f}^F$	
13.21	0	41.17	56.00	13.21	0	41.17	56.00	0.142	
69.21	0	39.17	56.00	69.21	0	39.17	56.00	0.142	
126.23	0	37.17	56.80	126.23	0	37.17	56.80	0.142	
182.21	0	35.17	55.98	182.21	0	35.17	55.98	0.242	
248.21	0	33.17	57.00	248.21	0	33.17	57.00	0.305	
Wing									
x_{wa}^R	y_{wa}^R	z_{wa}^R	c_{wa}^R	x_{wb}^R	y_{wb}^R	z_{wb}^R	c_{wb}	$C_{L\alpha w}$	$C_{L\delta a}$
0	−62.49	0	129.49	34.00	−62.49	0	129.49	4.9675	
34.00	−62.49	0	129.49	58.36	−52.40	0	115.51	6.1879	
58.36	−52.40	0	115.51	80.71	−43.15	0	102.68	6.5604	
80.71	−43.15	0	102.68	101.07	−34.72	0	90.99	6.7609	
101.07	−34.72	0	90.99	120.35	−33.06	0	86.25	6.9328	
120.35	−33.06	0	86.25	138.62	−31.49	0	81.75	7.1620	
138.62	−31.49	0	81.75	155.90	−30.00	0	77.50	7.4485	
155.90	−30.00	0	77.50	172.17	−28.60	0	73.50	7.7349	
172.17	−28.60	0	73.50	187.43	−27.29	0	69.75	7.9641	
187.43	−27.29	0	69.75	203.59	−25.89	0	65.77	8.1647	2.4494
203.59	−25.89	0	65.77	219.20	−24.55	0	61.93	8.2792	2.4838
219.20	−24.55	0	61.93	234.30	−23.25	0	58.21	8.3365	2.5010
234.30	−23.25	0	58.21	248.91	−21.99	0	54.62	8.3365	2.5010
248.91	−21.99	0	54.62	263.01	−20.78	0	51.15	8.2506	2.4752
263.01	−20.78	0	51.15	276.62	−19.61	0	47.80	8.0214	2.4064
276.62	−19.61	0	47.80	289.72	−18.48	0	44.58	7.7063	2.3119
289.72	−18.48	0	44.58	301.25	−17.49	0	41.74	7.2766	
301.25	−17.49	0	41.74	311.27	−16.62	0	39.28	6.6463	
311.27	−16.62	0	39.28	320.29	−15.85	0	37.06	5.7869	
320.29	−15.85	0	37.06	327.66	−15.21	0	35.25	4.5837	
327.66	−15.21	0	35.25	335.02	−14.58	0	33.43	2.5783	

Table 5 (Continued)

Horizontal Stabilizer									
x_{ea}^R	y_{ea}^R	z_{ea}^R	c_{ea}^R	x_{eb}^R	y_{eb}^R	z_{eb}^R	c_{eb}	$C_{L\alpha e}$	$C_{L\delta e}$
0	−25.40	0	65.31	10.98	−24.06	0	61.62	1.5783	0.7891
10.98	−24.06	0	61.92	23.37	−22.77	0	58.67	1.6844	0.8422
23.37	−22.77	0	58.67	35.24	−21.54	0	55.55	1.8104	0.9052
35.24	−21.54	0	55.55	46.60	−20.36	0	52.57	1.9828	0.9414
46.60	−20.36	0	52.57	57.44	−19.23	0	49.72	2.2282	1.1141
57.44	−19.23	0	49.72	67.88	−18.14	0	46.98	2.5398	1.2699
67.88	−18.14	0	46.98	77.91	−17.10	0	44.34	2.8913	1.4457
77.91	−17.10	0	44.34	87.53	−16.10	0	41.82	3.1632	1.5816
87.53	−16.10	0	41.82	96.74	−15.15	0	39.40	3.3025	1.6512
96.74	−15.15	0	39.40	105.54	−14.23	0	37.09	3.2958	1.6479
105.54	−14.23	0	37.09	113.93	−13.36	0	34.88	3.1300	1.5650
113.93	−13.36	0	34.88	121.91	−12.53	0	32.79	2.7454	1.3727
121.91	−12.53	0	32.79	129.08	−11.79	0	30.90	1.9828	0.9914
Vertical Stabilizer									
x_{ea}^V	y_{ea}^V	z_{ea}^V	c_{ea}^V	x_{eb}^V	y_{eb}^V	z_{eb}^V	c_{eb}^V	$C_{s\beta e}^V$	$C_{s\delta r}^V$
−31.15	−39.58	0	102.00	−20.81	−37.96	0	97.85	0.9482	0.4267
−20.81	−37.96	0	97.85	−4.81	−35.44	0	91.43	1.4740	0.6633
−4.81	−35.44	0	91.43	3.05	−34.20	0	88.28	1.7290	0.7781
3.05	−34.20	0	88.28	8.92	−33.28	0	85.92	2.6550	1.1948
8.92	−33.28	0	85.92	25.14	−30.73	0	79.42	2.8540	1.2843
25.14	−30.73	0	79.42	41.37	−28.18	0	72.91	3.1030	1.3964
41.37	−28.18	0	72.91	56.34	−25.82	0	66.90	3.3020	1.4859
56.34	−25.82	0	66.90	71.32	−23.47	0	60.89	3.4280	1.5426
71.32	−23.47	0	60.89	86.30	−21.11	0	54.88	3.4350	1.5458
86.30	−21.11	0	54.88	103.37	−18.43	0	48.03	3.2020	1.4409
103.37	−18.43	0	48.03	113.44	−16.84	0	43.99	2.3430	1.0544
Engine Pylon									
x_{fa}^A	y_{fa}^A	z_{fa}^A	c_{fa}^A	x_{fb}^A	y_{fb}^A	z_{fb}^A	c_{fb}^A	$C_{L\alpha f}^A$	
50.79	0.00	−5.13	126.00	50.79	20.00	−11.83	126.00	1.2376	
50.79	20.00	−11.83	126.00	50.79	33.00	−16.16	117.33	1.2892	
50.79	33.00	−16.16	117.33	50.79	47.00	−20.83	108.00	1.2900	
42.79	47.00	−20.83	116.00	42.79	56.00	−23.84	116.00	1.1250	
42.79	56.00	−23.84	116.00	42.79	65.00	−26.85	116.00	1.0500	
42.79	65.00	−26.85	116.00	42.79	74.00	−29.86	116.00	0.8500	
42.79	74.00	−29.86	116.00	42.79	82.00	−32.53	116.00	0.5500	

REPORT DOCUMENTATION PAGE

Form Approved

1. AGENCY USE ONLY *(Leave blank)*

2. REPORT DATE
July 2003

3. REPORT TYPE AND DATES COVERED
Contractor Report

4. TITLE AND SUBTITLE
Integrated Approach to the Dynamics and Control of Maneuvering Flexible Aircraft

5. FUNDING NUMBERS
NCC1-346

706-31-41-02

6. AUTHOR(S)
Leonard Meirovitch and Ilhan Tuzcu

7. PERFORMING ORGANIZATION NAME(S) AND ADDRESS(ES)

Virginia Polytechnic Institute and State University
Engineering Science and Mechanics Department, MC 0219
Blacksburg, VA 24061

8. PERFORMING ORGANIZATION REPORT NUMBER

9. SPONSORING/MONITORING AGENCY NAME(S) AND ADDRESS(ES)

National Aeronautics and Space Administration
Langley Research Center
Hampton, VA 23681-2199

10. SPONSORING/MONITORING AGENCY REPORT NUMBER
NASA/CR-2003-211748

11. SUPPLEMENTARY NOTES
An electronic version can be found at http://techreports.larc.nasa.gov/ltrs/ or http://ntrs.nasa.gov
Langley Technical Monitor: Martin R. Waszak

12a. DISTRIBUTION/AVAILABILITY STATEMENT
Unclassified-Unlimited
Subject Category 08 Distribution: Standard
Availability: NASA CASI (301) 621-0390

12b. DISTRIBUTION CODE

13. ABSTRACT *(Maximum 200 words)*
This work uses a fundamental approach to the problem of simulating the flight of flexible aircraft. To this end, it integrates into a single formulation the pertinent disciplines, namely, analytical dynamics, structural dynamics, aerodynamics and controls. It considers both the rigid body motions of the aircraft, three translations (forward motion, sideslip and plunge) and three rotations (roll, pitch and yaw), and the elastic deformations of every point of the aircraft, as well as the aerodynamic, propulsion, gravity and control forces. The equations of motion are expressed in a form ideally suited for computer processing. A perturbation approach yields a flight dynamics problem for the motions of a quasi-rigid aircraft and an "extended aeroservoelasticity" problem for the elastic deformations and perturbations in the rigid body motions, with the solution of the first problem entering as an input into the second problem. The control forces for the flight dynamics problem are obtained by an "inverse" process and the feedback controls for the extended aeroservoelasticity problem are determined by the LQG theory. A numerical example presents time simulations of rigid body perturbations and elastic deformations about 1) a steady level flight and 2) a level steady turn maneuver.

14. SUBJECT TERMS
Flexible Aircraft, Integrated Approach, Flight Dynamics, Extended Aeroservoelasticity, Time Simulations

15. NUMBER OF PAGES
76

16. PRICE CODE

17. SECURITY CLASSIFICATION OF REPORT	18. SECURITY CLASSIFICATION OF THIS PAGE	19. SECURITY CLASSIFICATION OF ABSTRACT	20. LIMITATION OF ABSTRACT
Unclassified	Unclassified	Unclassified	UL